DISS. ETH NO. 23266

Single cell analysis tools for gene expression by *Salmonella* Typhimurium

A thesis submitted to attain the degree of

DOCTOR OF SCIENCES of ETH ZURICH

(Dr. sc. ETH ZURICH)

presented by

ISMETA CURKIĆ

M.Sc., Veterinärmedizinische Universität Wien

born on 17.10.1987

citizen of Austria

accepted on the recommendation of

Prof. Wolf-Dietrich Hardt

Prof. Martin Ackermann

Prof. Manfred Claassen

Prof. Hans-Martin Fischer

2016

"You can`t think out of the box if you are always in the box."

Giampalmi J.

Table of Contents

Summary

Since its first description in 1885, *Salmonella enterica* has caused numerous cases of disease throughout the world. The non-typhoidal *Salmonella enterica* subspecies enterica serovar Typhimurium (*S*. Tm) is a major cause of foodborne disease worldwide and is mainly transmitted via contaminated food or water.

The pathogenicity of *Salmonella* spp. is based on the two type-three secretion systems, the type three secretion system 1 (TTSS-1 or T1) and the type three secretion system 2 (TTSS-2 or T2). Both TTSSs form needle-like structures. They contribute to different steps of the infection. The T1 is essential for invasion into host cells, whereas T2 allows intracellular survival and replication. The genes encoding a functional T1 needle are encoded on a 40 kb pathogenicity island, termed *Salmonella* pathogenicity island 1 (SPI-1). Its expression is highly regulated and its regulation includes core regulation factors as well as global regulators that are encoded outside of SPI-1. The core regulatory cascade that controls T1 expression is comprised of the transcription factors *hilD*, *hilA*, *hilC* and *rtsA*, which activate the expression of each other and display auto-regulatory feedback loops to amplify their own expression. The major known T1 repressor *hilE* is encoded outside SPI-1 and represses T1 by direct binding of the T1 master regulator HilD. This highly complex regulation cascade controls and fine-tunes T1 expression.

The expression of the T1 needle is very costly for *S*. Tm and causes a metabolic burden that is accompanied by a reduced growth rate of the T1 expressing ($T1^+$) cells. Because of the "cost" paid by T1 expressing cells, only a small subpopulation of the bacterial cells expresses this virulence factor in a given environment. Although the genes of the T1 regulation cascade are well established and the bistable behavior of T1 has been demonstrated in several earlier studies, the source of bistability has remained unclear. To clarify the roles of the different T1 regulators, it would be of interest to study the expression of all regulatory genes behind T1 simultaneously in single cells. This would allow identifying expression patterns before *t1* is expressed and might give insights into the generation of T1 bistability. Previous studies used fluorescent proteins coupled to single or more genes to analyze gene expression in single cells. However, when analyzing gene expression dynamics using different fluorescent proteins, variable maturation kinetics of the variable chromophores bias the gene expression analyses.

Gene expression reporter systems that allow the dynamic analysis of several genes in real time without introducing a folding kinetics-based bias are still missing.

In Chapter 2, I describe the establishment of an invasin-based reporter system, a novel gene expression reporter system in *S*. Tm that might be used as alternative for fluorescent proteins. We fused a hemagglutinin epitope-tagged invasin reporter (*invA*$_{HA}$) to different SPI-1 encoded genes, and benchmarked its expression using standard *gfp* reporter. We could demonstrate that the InvA$_{HA}$ reporter system performs at least as well as the fluorophore-based approach. This chapter provides important groundwork for the future establishment of a multidimensional *invA* reporter system using differentially epitope-tagged *invA* variants.

Chapter 3 describes the establishment of the microfluidics microscopy system, which allows the analysis of gene expression within single cells in a stable long-term incubation system. This setting provides a useful tool to assess the dynamics of the T1 regulatory genes, i.e. when combined with the epitope-tagged invasin reporters as described in Chapter 1.

Finally, we were analyzing the role of the RpoE-mediated membrane stress response during the expression of the T1 needle and cytoplasmic fluorophores. In particular, we addressed the role of the zinc-metalloprotease RseP, which is involved in the membrane stress response (Chapter 4).

Overall, this thesis provides important groundwork to demonstrate the suitability of the *invA*$_{HA}$ reporter system for gene expression analyses as alternative for fluorescent reporters in *S*. Tm. This reporter system could be applied in the microfluidics microscopy setup, described in this thesis. Furthermore, this thesis points out the still unresolved complexity of T1 regulation.

Zusammenfassung

Seit der Beschreibung im Jahre 1885, hat *Salmonella* enterica weltweit zahlreiche Krankheitsfälle ausgelöst. Der nicht-typhoide Salmonellenstamm *Salmonella enterica* Subspezies enterica Serovar Typhimurium (*S*. Tm) ist einer der bedeutendsten Erreger von Lebensmittelinfektionen weltweit und wird hauptsächlich durch kontaminierte Nahrung oder Wasser übertragen.

Die Pathogenität von Salmonellen basiert auf den zwei Typ-3 Sekretionssystemen, Typ-3 Sekretionssystem 1 (TTSS-1 oder T1) und Typ-3 Sekretionssystem 2 (TTSS-2 oder T2). Beide Typ-3 Sekretionssysteme bilden nadelähnliche Strukturen. Sie sind an verschiedenen Schritten der Infektion beteiligt. Das T1 ist für die Invasion in die Wirtszelle essenziell, wobei das T2 das intrazelluläre Überleben und Replikation gewährleistet. Die Gene, die für eine funktionelle T1-Nadel kodieren, sind auf einer 40 kB grossen Pathogenitätsinsel, die als Salmonellen Pathogenitätsinsel 1 (SPI-1) bezeichnet wird, kodiert. Dessen Expression ist höchst reguliert und ihre Regulation umfasst sowohl Kern-Regulationsfaktoren als auch globale Regulatoren, die ausserhalb von SPI-1 kodiert sind. Die Kern-Regulationskaskade, die die T1 Expression kontrolliert, besteht aus den Transkriptionsfaktoren *hilD*, *hilA*, *hilC* und *rtsA,* die sich gegenseitig aktivieren und über Auto-Feedback Mechanismen besitzen, die ihre eigene Expression amplifizieren. Der wichtigste bekannte Repressor *hilE* wird ausserhalb von SPI-1 kodiert und reprimiert T1 durch direktes Binden an HilD. Diese hochkomplexe Regulationskaskade kontrolliert und stimmt die T1 Expression ab.

Die Expression der T1-Nadel ist für *S*. Tm sehr aufwändig und bewirkt eine metabolische Belastung, die eine reduzierte Wachstumsrate von Zellen, die T1 exprimieren ($T1^+$ Zellen), mit sich zieht. Wegen des "Preises", den T1 exprimierende Zellen zahlen müssen, exprimiert nur eine kleine Subpopulation der genetisch identischen Population diesen Virulenzfaktor in der gegebenen Umwelt. Obwohl die Gene der T1 Regulationskaskade schon gut etabliert sind und das bistabile Verhalten von T1 schon in mehreren früheren Studien demonstriert wurde, ist der Ursprung der Bistabilität noch immer unbekannt. Um die Rollen der einzelnen T1 Regulatoren klarzustellen, wäre es interessant die Expression aller T1 Regulationsgene gleichzeitig in einzelnen Zellen zu bestimmen. Das würde erlauben, die Expressionsmuster

bevor *t1* exprimiert wird zu identifizieren, und könnte Hinweise zur Generation von T1 Bistabilität geben. Vorherige Studien verwendeten Fluoreszenzproteine, gekoppelt an einzelne oder mehrere Gene, um Geneexpression in einzelnen Zellen zu analysieren. Jedoch, wenn man Genexpressions-Dynamiken mit verschiedenen Fluoreszenzproteinen analysiert, können variable Reifungskinetiken der unterschiedlichen Chromophore die Geneexpressionsanalysen verfälschen. Genexpressions-Reportersysteme, die dynamische Analysen von mehreren Genen in Realzeit erlauben, ohne die Verfälschung durch verschiedene Faltungskinetiken, sind noch nicht entwickelt.

Im Kapitel 2 beschreibe ich die Etablierung eines neuen Geneexpressions-Systems für *S*. Tm, das Invasin-basierende Reportersystem, das als Alternative für Fluoreszenzprotein genutzt werden könnte. Wir haben einen Hämagglutinin-getaggten Invasin-Reporter (*invA*$_{HA}$) an verschiedene SPI-1 kodierte Gene fusioniert und bewerteten dessen Expression mit dem Standardreporter *gfp*. Wir konnten demonstrieren, dass das InvA$_{HA}$ Reportersystem zumindest genauso gut wie die Fluorophore-basierte Methode funktioniert. Dieses Kapitel stellt eine wichtige Grundlage für die zukünftige Etablierung eines multidimensionalen *invA* Reportersystemes dar, das auf verschieden getaggten *invA*-Varianten basiert.

Kapitel 3 beschreibt die Entwicklung eines Mikrofluidics-Mikroskopie Systems, das die Genexpressionsanalyse in einzelnen Zellen in einem stabilen Langzeit-Inkubationssystem erlaubt. Dieser Aufbau stellt ein nützliches Werkzeug dar, um dynamische Analysen von T1 Regulationsgenen, zu ermitteln, wenn es z.B. mit Epitop-getaggten Invasin-Reportern, wie im Kapitel 1 beschrieben, kombiniert wird.

Letztendlich analysierten wir die Rolle der RpoE-vermittelten Membranstress-Antwort während der T1-Nadel Expression während der Expression von cytoplasmischen Fluorophoren. Insbesondere, haben wir die Rolle der Zink-Metalloprotease RseP, die in der Membranstress-Antwort beteiligt ist, adressiert (Kapitel 4).

Insgesamt stellt diese Doktorarbeit wichtige Fundamente dar, um die Brauchbarkeit des *invA*$_{HA}$ Reportersystemes für Genexpressions-Analysen in *S*. Tm als Alternative zu Fluoreszenzreportern zu demonstrieren. Dieses Reportersystem könnte im Mikrofluidics-Mikroskopie Setup, das in dieser Arbeit beschrieben wird, verwendet werden. Weiterhin, zeigt diese Arbeit die noch immer ungelöste Komplexität der T1 Regulation auf.

1 General Introduction

1.1 *Salmonella* spp. and virulence

1.1.1 *Salmonella* spp. classification

Salmonella species (spp.) were first discovered by the American veterinarian Daniel Elmer Salmon and his assistant Theobald Smith in 1885 during their investigations of hog cholera (Fabrega and Vila, 2013). *Salmonella* spp. are Gram-negative, facultative anaerobic bacteria with peritrichous motility. The size ranges from 0.7-1.5 µm in diameter and 2-5 µm in length (Fabrega and Vila, 2013; Murray et al., 1999). The host range of *Salmonella* spp. includes humans as well as cold and warm-blooded animals (Brenner et al., 2000). Depending on the species, disease in humans ranges from life-threatening typhoid fever (typhoidal infection caused by *Salmonella* Typhi and Paratyphi) to a self-limiting gastroenteritis (salmonellosis; non-typhoidal infection) (Sanchez-Vargas et al., 2011).

The genus *Salmonella* is comprised of the species *Salmonella enterica* and *Salmonella bongori.* The recently discovered *Salmonella subterranea* is not classified as *Salmonella*, but might display a new species of *Enterobacter* or *Escherichia* (Canals et al., 2011; Centers for diesease control and prevention, 2011; Issenhuth-Jeanjean et al., 2014; Shelobolina et al., 2004). *Salmonella enterica* is further divided into the six subspecies *enterica* (I), *salamae* (II), *arizonae* (IIIa), *diarizonae* (IIIb), *houtenae* (IV) and *indica* (VI). For better differentiation of the subspecies, serotypes (serovars) have been defined based on different surface structures of the lipopolysaccharide (O-antigen) and flagella (flagellin, H-antigen). The huge variability in *Salmonella* serovars is reflected in the existence of more than 2500 serotypes. While *Salmonella bongori* and the subspecies II, IIIa, IIIb, IV, VI are mainly isolated from cold-blooded animals and the environment, 99% of all infections in humans and warm-blooded animals are attributable to *Salmonella enterica* subspecies enterica serotypes (Brenner et al., 2000; Centers for diesease control and prevention, 2011; Fabrega and Vila, 2013; Heyndrickx et al., 2005; Hurley et al., 2014).

The majority of infections in the United States is caused by the serotypes Typhimurium, Enteritidis, Newport and Heidelberg. The non-typhoidal serotypes Enteritidis and

Typhimurium (full name *Salmonella enterica* subspecies enterica serovar Typhimurium) display a broad host range including humans and animals, in contrast to "specialist" serovars, such as *Salmonella* Typhi and Paratyphi (human-restricted). For the serotype Typhimurium, the abbreviation *Salmonella* Typhimurium (*S.* Tm) is commonly used (Brenner et al., 2000; Canals et al., 2011; Hurley et al., 2014).

1.1.2 Relevance of *Salmonella* spp. - *Salmonella* Typhimurium infection

Infections with *Salmonella* spp. are a major cause of food-borne disease and pose serious health problems throughout the world (Galanis et al., 2006). The major sources of infection are contaminated water and food, such as eggs and meat (Food and Agriculture Organization of the United Nations, 2002; Humphrey, 2004). Infections with the typhoidal serotypes *S*. Typhi or Paratyphi can cause severe systemic bacteraemia and fever, resulting in a fatal outcome when untreated (Gordon, 2008). In contrast, non-typhoidal *Salmonella* spp. such as *Salmonella* Enteritidis or Typhimurium, lead to salmonellosis (symptoms: diarrhea, vomiting, abdominal pain), which is self-limiting within 5-7 days in healthy adults, but can be life threatening to children, elderly or immunocompromised individuals (Gordon, 2008). The infectious dose is estimated at 10^3-10^5 cells (Public Health Agency of Canada, 2011).

The majority of studies of the invasion process were done using *S*. Tm infections, as its systemic spread in mice is thought to resemble typhoid fever in humans (Brumell et al., 1999). The invasion by *S*. Tm is marked by various challenges, before successful infection can take place. Upon ingestion and passage through the acidic milieu of the stomach (Audia et al., 2001), *S*. Tm has to compete with the commensal population of the intestinal lumen to ensure survival. The human intestine is colonized by 10^{14} bacteria, which are comprised of 500-1000 different bacterial species and play an important role in preventing pathogen colonization of the intestine (Hurley et al., 2014). Furthermore, host factors such as antimicrobial peptides provide additional barriers blocking colonization by pathogenic bacteria (Hornef et al., 2004; Salzman et al., 2003). However, *S*. Tm has evolved different strategies to survive in hostile environments and competition with commensals. During the initial stages of infection in the absence of inflammation, *S*. Tm exploits the metabolism of the gut microbiota by using microbiota-derived hydrogen for its own growth (Maier et al., 2014a; Maier et al., 2013).

By triggering inflammation, *S*. Tm provides itself a competitive advantage over the commensal microbiota by changing the microbiota composition and preventing their growth (Stecher et al., 2007). Opportunities to take up iron from the environment during inflammation (Raffatellu et al., 2009) or to use tetrathionate (Winter et al., 2010) and nitrate (Lopez et al., 2012) as electron acceptors for anaerobic respiration provide *S*. Tm an additional advantage (LaRock et al., 2015).

For a successful infection, bacteria have to reach the lamina propria by invasion through the intestinal epithelium. One major route of invasion is through M cells (Jones et al., 1994) of the Peyer`s Patches. However, intestinal enterocytes also represent an important route of infection (Barthel et al., 2003; Hapfelmeier et al., 2005; Müller et al., 2012; Takeuchi and Sprinz, 1967). *S*. Tm can also be transported precisely across the gut epithelium via dendritic cells that can take up bacteria directly from the lumen by their dendrites (Rescigno et al., 2001; Santos and Baumler, 2004). For enterocyte invasion, *S*. Tm has evolved specific virulence determinants (see section "*Salmonella* Typhimurium virulence factors").

1.1.3 *Salmonella* Typhimurium virulence factors

For a successful infection, *S*. Tm has to use a variety of virulence factors, which are encoded by ~4% of the genome (Bowe et al., 1998). Most of the virulence genes are encoded on different genomic islands, termed *Salmonella* pathogenicity islands (SPIs) that were evolutionary acquired by horizontal gene transfer from phages or plasmids. SPI-s are distinct regions that exhibit a lower GC content (37-47%) that the residual chromosome of *Salmonella* spp. (~52%) and are often inserted into tRNA genes (Marcus et al., 2000). The different *Salmonella* serotypes harbor up to 12 known SPIs (Barlag and Hensel, 2015; Hensel, 2004; Marcus et al., 2000), from which SPI-1 and SPI-2 have been investigated with highest intensity (Fabrega and Vila, 2013).

***Salmonella* Pathogenicity island 1**

For a successful infection by *Salmonella* spp. invasion into host cells is crucial. This step is mediated by virulence genes encoded on a 40 kb island, located on centisome 63 of the *S*. Tm chromosome (Galan, 1996; Mills et al., 1995). This genomic region distinguishes itself from the residual chromosome by harboring a lower GC content of 42% (Hensel, 2004; Marcus et al.,

2000). The composition of genes on SPI-1 encodes for a fully functional type three secretion system 1 (T1) (Kubori et al., 1998). SPI-1 harbors three major operons (*prg-org*, *inv-spa* and *sic-sip)* that are interspersed with genes encoding transcriptional regulators. One subset of genes encodes for structural proteins, required for the assembly of the T1 needle, whereas the other subset of proteins function as effectors, chaperones and transcriptional activators (Figure 1.1). Secreted effectors, such as SipA, SopE and SopE2 (SopE and SopE2 are not encoded on SPI-1), re-arrange the structure of the host cytoskeleton to allow engulfment of the bacteria (Friebel and Hardt, 2000; Hardt et al., 1998a; Hardt et al., 1998b; Stender et al., 2000; Zhou et al., 1999). Transcriptional activators, such as HilD, regulate and fine-tune the expression of the T1 needle complex (Schechter et al., 1999; Schechter and Lee, 2001). Chaperones (e.g. SicA) stabilize effector proteins to allow efficient translocation through the needle (Tucker and Galan, 2000). The ATPase InvC is associated with the T1 complex, recognizes effector/chaperone complexes and mediates the release of effectors from the respective chaperone in an ATP-dependent manner (Akeda and Galan, 2005).

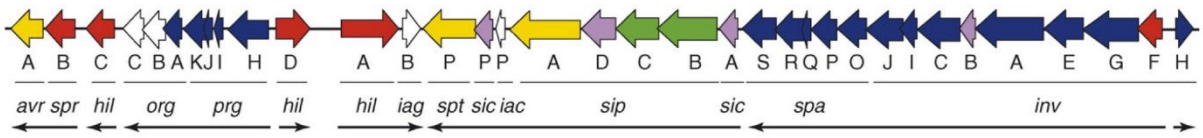

Figure 1.1. *Salmonella* Pathogenicity Island 1 (SPI-1).
SPI-1 is a 40 kb island within the *Salmonella* chromosome. It encodes virulence genes, including structural (blue), translocon (green), effector (yellow), chaperone (purple), regulatory (red) genes and genes of unknown function (white). The three biggest operons are the *inv-spa, sic-sip* and *prg-org* operons. Figure adopted from (Ellermeier and Slauch, 2007).

The T1 needle

The T1 needle is a multimeric complex, which is present in 10 to 100 copies per cell and reaches out 80 nm from the bacterial surface (Kubori et al., 1998). The T1 shares protein similarities with the flagellum, as phylogenetic studies demonstrate that both are derived from the same ancestor (Gophna et al., 2003).

One major function of the T1 needle is to translocate proteins directly into the host cell cytosol. The needle complex is formed by a basal body structure with an inner and outer rod that is connected to the needle. The inner ring is formed by PrgH and PrgK. Together with the outer ring, the neck of the basal body is composed of InvG. The needle consists of PrgI proteins

and is connected to the inner rod, composed of PrgJ, which controls the length of the needle. The needle terminates with the translocon, a pore that translocates bacterial proteins into the host cell. It is formed by SipB, SipC and SipD (Cornelis, 2010; Moest and Meresse, 2013) (Figure 1.2).

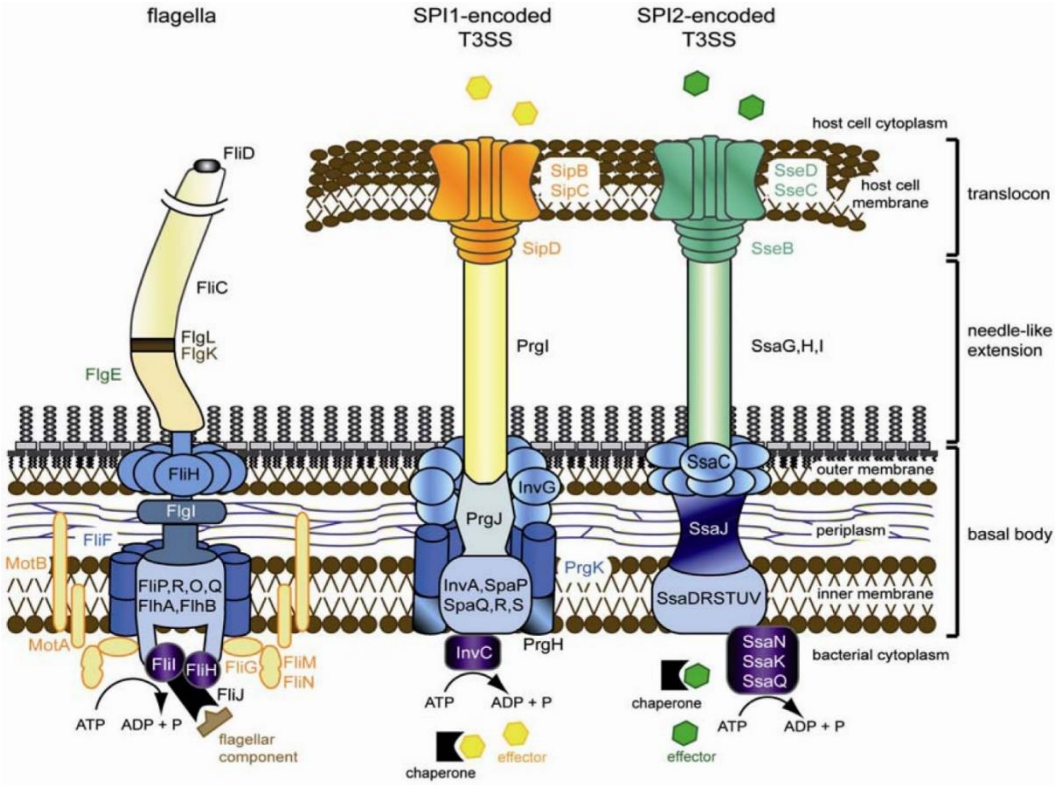

Figure 1.2. The type three secretion systems in *Salmonella* enterica.
The flagella (left), T1 (middle) and T2 (right) are illustrated in this scheme. Structural homologies of the different type three secretion systems (TTSSs) are indicated by the same color. All TTSSs are composed of basal structures and needle like extensions to the extracellular space. The T1 and T2 additionally harbor a translocon, which engages with the host cell membrane for virulence factor translocation. Figure adopted from (Hoelzer, 2010).

Other virulence factors

SPI-2 is a 40 kb region that encodes the type three secretion system 2 (T2) (Hensel, 2004). The T2 is essential for intracellular survival and replication, as deletion of SPI-2 reduces intracellular replication and systemic dissemination (Cirillo et al., 1998). The T2 encodes four types of virulence genes, including *ssa* (T2 apparatus), *ssr* (T2 regulators), *ssc* (T2 chaperones), *sse* (T2 effectors) (Marcus et al., 2000).

The two type three secretion systems (TTSSs) are required during different stages of the infection. Whereas the T1 governs the invasion into epithelial cells (Galan and Curtiss, 1989), the T2 ensures survival and replication in an intracellular environment (Cirillo et al., 1998).

However, recent evidence demonstrates an overlapping period of expression, during which both secretion systems are active (Hautefort et al., 2008; Laughlin et al., 2014).

Other virulence factors include adhesins, which are structures on the surface of the cells. *Salmonella enterica* displays a large number of adhesins, including type I fimbriae, Curli, autotransported adhesins, such as MisL and ShdA and adhesins that are secreted via the type one secretion system, such as BapA and SiiE (reviewed in (Barlag and Hensel, 2015)). The giant adhesin SiiE is encoded on SPI-4 and is required for a successful invasion of polarized cells. During the first steps of invasion, SiiE initiates contact with host cells by binding to glycostructures and thereby enhances translocation of bacterial proteins by the T1 into polarized cells (Barlag and Hensel, 2015; Gerlach et al., 2008).

A second type of surface organelles that are required for virulence are flagella. Flagella are filaments that enable bacteria to swim. Flagella-mediated virulence is promoted by sensing environmental cues via the chemotaxis machinery and subsequent swimming towards the target stimulus (Macnab, 2003; Macnab and Koshland, 1972). Via counterclockwise rotation of the flagellar filaments, *Salmonella enterica* swims ("runs"), while tumbling is caused by clockwise rotation of one or more flagella (Ramos et al., 2004). Furthermore, the main constituent of the flagella filament, flagellin, is a potent inducer of the host immune response and thereby increases the pathogenicity of the bacteria (Franchi et al., 2006).

Furthermore, *Salmonella enterica* expresses a strong immunogen, the lipopolysaccharide (LPS), which induces a strong innate immune response that can lead to septic shock in infected patients (Bone, 1991). The LPS O-side chain structure varies in different species and elicits pronounced antibody responses (Trent et al., 2006). While *S.* Tm displays a LPS structure consisting of lipid A (also known as endotoxin), a core oligosaccharide and an O-antigen polysaccharide (=smooth LPS, Figure 1.3), *Escherichia coli* (*E. coli*) K12 lacks the O-antigen and harbors a rough LPS layer (=lipid A and core) (Liu and Reeves, 1994; Ruiz et al., 2009).

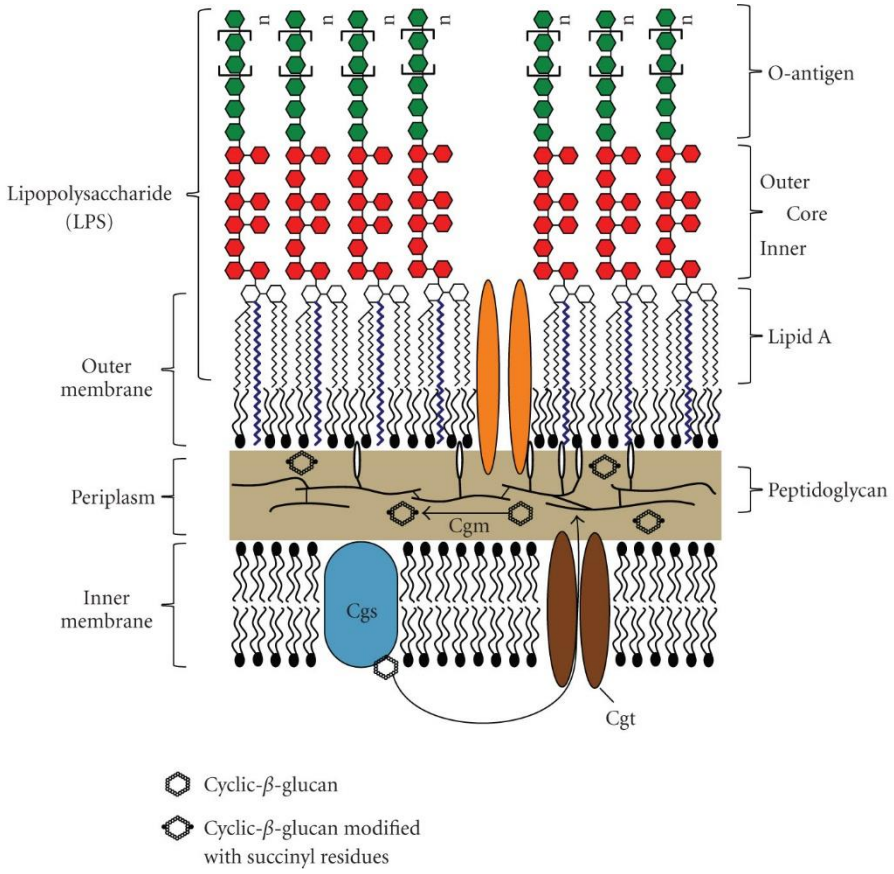

Figure 1.3. The composition of the lipopolysaccharide.
The cell envelope, including inner membrane, periplasm, outer membrane and the LPS structure of Gram-negative *Brucella* spp. is illustrated. LPS is comprised of three parts, namely lipid A, the core structure (inner and outer core) and an O-antigen. Lipid A anchors the LPS to the outer membrane and is connected to the core structure, which in turn connects the O-antigen polysaccharide chain with lipid A. Figure modified from (Haag et al., 2010).

1.1.4 Regulation of T1

During its life, *S.* Tm has to overcome various potentially detrimental environments, which require differential gene expression depending on individual situations. After having crossed the acidic milieu of the stomach, the intestinal environment provides an optimal site for invasion (Altier, 2005). Consequently, the expression of the T1 needle is required to invade epithelial cells and reach the underlying phagocytic cells (Moest and Meresse, 2013). However, the pathogenicity of *S.* Tm is dependent on the timing and location of T1 expression, as the regulation of SPI-1 has been incorporated into global regulatory pathways. *S*. Tm is supposed to trigger the expression of the T1 when the organism reaches its preferred invasion site (intestinal epithelium) by sensing external stimuli and subsequently intitiating the corresponding internal global regulatory cascades (Altier, 2005).

One example for integration of the virulence expression into global regulatory networks is the regulation by the two-component regulatory systems PhoQ/PhoP (Groisman et al., 1989; Miller et al., 1989), BarA/SirA, EnvZ/OmpR and PhoR/PhoB. Two-component regulatory systems are comprised of two parts: a membrane-bound histidine kinase, which is in charge of sensing environmental signals, and a response regulator that initiates differential gene expression corresponding to the incoming signal (Fabrega and Vila, 2013). The sensor kinase PhoQ is activated upon low pH and low Mg^{2+} concentrations and subsequently initiates a PhoP-mediated response (Alpuche Aranda et al., 1992; Garcia Vescovi et al., 1996). The PhoQ/PhoP system represses T1 expression by repressing *prg* (PhoP-repressed genes) genes and *hilA* (Bajaj et al., 1996; Behlau and Miller, 1993; Pegues et al., 1995). However, PhoQ/PhoP is required for survival within macrophages and induces SPI-2 expression (Belden and Miller, 1994; Miller et al., 1989). The BarA/SirA system controls genes in carbohydrate metabolism, motility, biofilm formation and invasion. Unknown environmental signals activate the sensor kinase BarA, which in turn activates T1 expression by inhibiting the mRNA destabilizing actions of the RNA binding protein CsrA on *hilD* mRNA (Martinez et al., 2011). This is done by activating the expression of the small RNAs *csrB* and *csrC*, which bind CsrA and thereby prevent its actions (Romeo, 1998). However, bile represses invasion, acting via BarA/SirA or an above regulating system (Prouty and Gunn, 2000). The EnvZ sensor kinase is activated upon increase of extracellular osmolarity and mediates OmpR-mediated activation of SPI-1 gene expression via HilD (Ellermeier et al., 2005). The PhoR kinase senses low levels of extracellular inorganic phosphate and initiates a PhoB response that activates the two regulators of type 1 fimbriae expression, FimZ and FimY. The *fimZY* genes trigger *hilE* expression and thereby repress SPI-1 induction (Baxter and Jones, 2005).

In addition to the above examples, nucleoid-associated proteins (NAPs) modulate SPI-1 expression. NAPs bind their target DNA and change the supercoiling structures of the DNA, which in turn may influence gene expression of the respective gene (Dillon and Dorman, 2010). H-NS has silencing effects on both SPI-1 (Schechter et al., 2003b) and SPI-2 (Navarre et al., 2006).

Other regulators, affecting SPI-1 expression include iron regulatory protein Fur and the global regulator Fis, activating SPI-1 (Ellermeier and Slauch, 2008; Schechter et al., 2003b). SPI-1 is repressed by the global regulator of metabolism Lrp, which also represses SPI-2 (Baek et al.,

2009). The Lon protease is activated during stress situations and also represses SPI-1 expression (Takaya et al., 2002).

1.1.5 Core regulators of SPI-1

The induction of T1 is highly controlled by a set of internal regulatory genes (Figure 1.4). The coordination of expression of the T1 needle is very complex as it fine-tunes the switch-like induction (Ellermeier and Slauch, 2007; Moest and Meresse, 2013) after having reached an activation threshold for expression (Saini et al., 2010a).

The core regulators of the T1 are HilD (hyperinvasion locus D), HilA, HilC (SirC or SprA), RtsA and the inhibitor HilE. All transcriptional regulators are encoded on SPI-1, except *rtsA*, which is encoded in an operon with *rtsB* on a 15 kb genomic region close to the $tRNA^{PheU}$ (Ellermeier and Slauch, 2003). HilD is at the top of the regulatory cascade and together with HilC and RtsA, it belongs to the AraC/XylS family of transcriptional activators (Schechter et al., 1999). HilD is essential for invasion and is necessary for HilA expression, as in the absence of *hilD*, *hilA* expression is highly reduced (Ellermeier et al., 2005; Schechter et al., 1999). Furthermore, the promoter of *hilC* (P*hilC*) is only expressed weakly and P*rtsA* expression is absent upon deletion of *hilD* (Saini et al., 2010a). HilD, HilC and RtsA interact with each other and can trigger the expression of their "own" genes (auto-regulation) and control *hilA* expression in a complex feed-forward loop (Ellermeier et al., 2005; Ellermeier and Slauch, 2007). *hilC* and *rtsA* amplify T1 expression (Saini et al., 2010a), but cannot induce *hilA* expression in the absence of *hilD* (Ellermeier et al., 2005). The activation of *hilA* by *hilD* and *hilC* is mediated by countering the silencing of the nucleoid protein H-NS and thereby de-repressing the *hilA* promoter rather than by direct activation (Olekhnovich and Kadner, 2006; Schechter et al., 2003b). The negative regulator HilE represses T1 expression by directly binding to HilD (Baxter et al., 2003). The transcriptional activator HilA is a member of the OmpR/ToxR family (Lee et al., 1992). It directly activates the three major operons encoding a functional T1 by binding to the promoter regions of *prg-org*, *inv-spa* and by activating *sic-sip* via read through from *inv-spa* (Darwin and Miller, 2000; Lostroh et al., 2000; Moest and Meresse, 2013). It was shown that HilC, HilD and RtsA bind to overlapping binding sites within the promoter region of *hilA (Ellermeier and Slauch, 2003; Olekhnovich and Kadner, 2002)*, which suggested the existence dimers binding to the promoter (Ellermeier et al., 2005). InvF is an additional transcription factor of the AraC

family (Martin and Rosner, 2001) that is encoded in the *inv-spa* operon. Together with the chaperone SicA, InvF is capable of inducing virulence genes inside and outside of SPI-1 (Darwin and Miller, 2000; Darwin and Miller, 2001) (Figure 1.4).

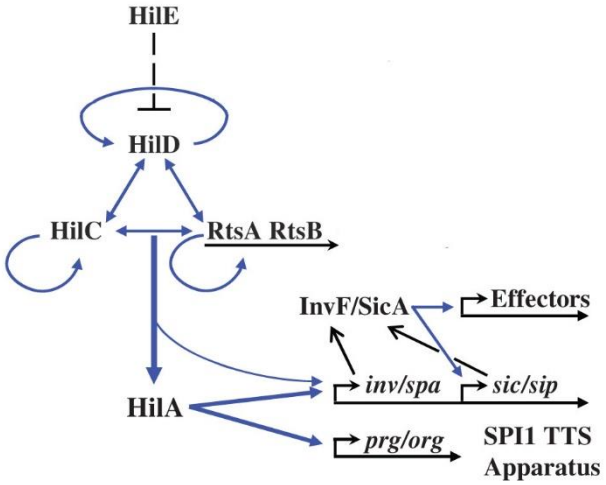

Figure 1.4. Core regulatory cascade of SPI-1.
Transcriptional regulation of the core transcriptional regulators *hilD*, *hilC*, *rtsA* and *hilA* is indicated by the arrows. Activation is indicated by blue arrowheads, whereas repression is illustrated by blunt ends. All core regulators act as transcription factors, except for HilE, which represses HilD at the protein level. The activation of *hilA* results in the expression of downstream genes, required for a functional T1 needle apparatus. Figure modified from (Ellermeier et al., 2005).

1.1.6 Cross talk of SPI-1 with other virulence factors

To coordinate the expression of the corresponding virulence factors for the appropriate time points and locations, *S.* Tm applies complex gene regulatory networks. The coordination of the different virulence factors requires cross talk and co-regulation of the different SPI-s. The expression of the different pathogenic traits seems to follow a hierarchical and temporal order, depending on the roles during pathogenesis (Fabrega and Vila, 2013; Saini et al., 2010b). Figure 1.5 illustrates the dynamic expression of flagella, the T1 and type I fimbriae in the course of a time course experiment, during which flagellar genes are expressed during early exponential growth (Saini et al., 2010b). Furthermore, the flagellar protein FliZ was shown to stimulate T1 expression by activating HilD, but at the same time, represses the expression of type I fimbrial genes by repressing *fimZ* (Chubiz et al., 2010; Saini et al., 2010b). According to the hierarchy model of Saini and colleagues, the T1 is expressed during late logarithmic growth (Saini et al., 2010b). During this growth phase, Gerlach and colleagues demonstrated a co-regulation of the SPI-4 encoded SiiE and the T1 that is dependent on HilA

and the global regulator SirA (Gerlach et al., 2007). In experiments with polarized cells, they showed that SiiE-mediated adhesion is required to initiate intimate contact and thereby allow T1-mediated effector protein translocation (Gerlach et al., 2008). During this phase motility is repressed by HilA and RtsB-mediated actions on the *flhDC* flagellar operon (Ellermeier and Slauch, 2003; Thijs et al., 2007). The T1 master regulator HilD mediates then the switch to the intracellular phenotype by activating the SPI-2 encoded T2, which is required for intracellular growth and survival (Bustamante et al., 2008; Ochman et al., 1996). At the same time, T1 and flagellar expression are repressed through FimZ-mediated action on the major negative regulator HilE and the flagellar genes *flhDC*, respectively (Saini et al., 2010b) (Figure 1.5).

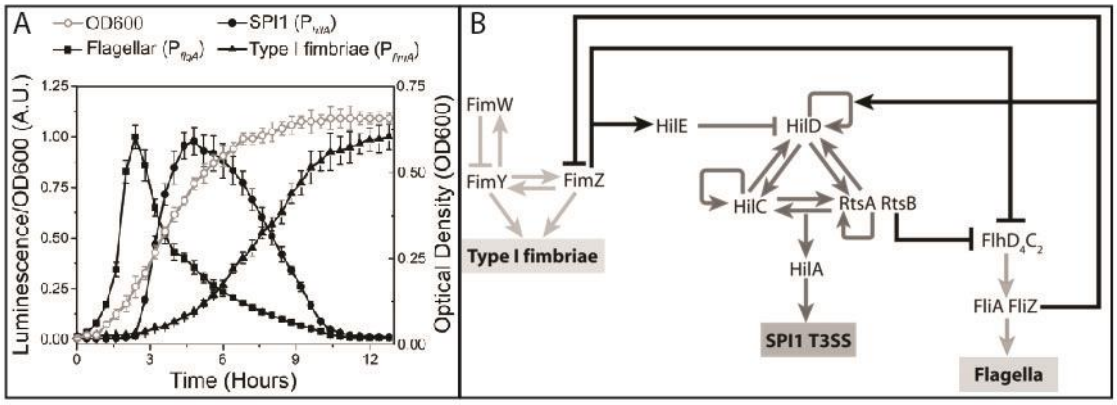

Figure 1.5. Different dynamics of the flagella, the SPI-1-mediated T1 expression and type-1 fimbriae during bacterial culture and cross regulation between these virulence factors.
A) Time course dynamic expression of the flagella (P*flgA*), the T1 (P*hilA*) and the type 1 fimbriae (P*fimA*) promoters. The optical density is illustrated as reference for the different growth phases. Whereas the flagella is expressed during early exponential phase, SPI-1 encoded T1 is most active during late exponential phase, followed by expression of the type I fimbriae during stationary phase. B) The cross talk between the flagella, T1 and type-1 fimbriae is indicated. Arrowheads and blunt ends indicate activation or repression, respectively. Figure modified from(Saini et al., 2010b).

1.1.7 Membrane stress response regulation by RpoE/RseP

During its life cycle inside and outside the host, *S.* Tm needs to react to different environmental stimuli and respond through different transcriptional networks to induce rapid adaptation and protection mechanisms. Common stresses include thermal, osmotic or oxidative stress as well as starvation (for detailed information on the reaction to the different stresses see (Runkel et al., 2013)). The envelope stress responses (ESR or membrane stress responses) play an important role in encountering stress factors that induce damage to the cell envelope. Gram-negative bacteria harbor an envelope that consists of an inner membrane (IM) and an outer membrane (OM). The two membranes are separated by the periplasmic space, which displays

a peptidoglycan layer that maintains structural integrity (Brass et al., 1986). ESRs include the alternative sigma factor RpoE ($\sigma^{E/24}$) pathway (Duguay and Silhavy, 2004; Erickson and Gross, 1989), the CpxAR two-component system (Cosma et al., 1995; Duguay and Silhavy, 2004), the phage shock protein (PSP) system (Brissette et al., 1990), the RcsCDB phosphorelay system (Majdalani et al., 2005), the Bae pathway (Leblanc et al., 2011) and additional membrane stress response mechanisms that release misfolded periplasmic proteins via outer membrane vesicles (McBroom and Kuehn, 2007). The different stress response systems react to different kinds of stress (e.g., Cpx and σ^E are induced in response to the increase of misfolded proteins in the periplasm). However, as several inducing factors are shared by different ESRs, interaction and cross talk between the stress response systems has been suggested (McBroom and Kuehn, 2007; Runkel et al., 2013). The RpoE system has been first described in 1989 in *E. coli* (Erickson and Gross, 1989). One of the main inducers of RpoE are unfolded or misfolded OM proteins that accumulate in the periplasm (Runkel et al., 2013). This ESR is activated upon stresses, including temperature changes (Erickson and Gross, 1989), ethanol, antimicrobial peptides, pH changes, osmotic (McMeechan et al., 2007), oxidative stress (Bang et al., 2005), shift to different carbon sources and the resulting adaptation to new environments (Kenyon et al., 2005) and accumulation of misfolded and proteins (Mecsas et al., 1993).

In the absence of stress, RpoE is sequestered to the membrane by RseA (Missiakas et al., 1997). Stress that leads to the accumulation of misfolded proteins in the periplasm activates the membrane anchored serine protease DegS, which subsequently induces the stress response pathway to release RpoE. Upon DegS activation, it cleaves RseA in the periplasmic space (cleavage site 1, Figure 1.6), which is followed by a second cleavage step (cleavage site 2, Figure 1.6) by the metalloprotease RseP (YaeL) within its inner membrane spanning region (Li et al., 2009). The RpoE-RseA complex is then released into the cytoplasm where the residual part of RseA is degraded by the cytosolic ClpXP protease (Figure 1.6) (Flynn et al., 2004). RpoE is released and binds to the RNA polymerase (RNAP), thereby inducing the expression of the RpoE-regulated genes to cope with envelope stress. The RpoE regulon includes genes from the primary metabolism and sensory function, chaperones and protein folding, outer membrane protein assembly and LPS biogenesis (Rowley et al., 2006; Skovierova et al., 2006).

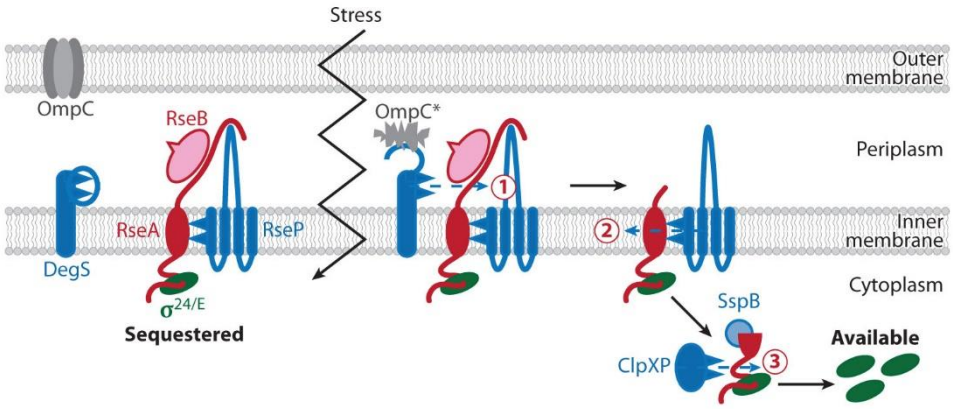

Figure 1.6. RpoE-mediated stress response.
In a non-stress situation, RseA sequesters the sigma factor RpoE (σ24/E) to the membrane. Upon stress induction by misfolded proteins in the periplasm (e.g. OmpC*), DegS mediates the first cleavage of RseA, followed by a second cleavage step by RseP. The released RseA/RpoE complex is mediated by SspB to the cytosolic protease ClpXP, where RpoE is released and induces expression of its target genes. Figure adopted from (Osterberg et al., 2011).

In *E. coli*, RpoE is required for survival (De Las Penas et al., 1997). In *S.* Tm, RpoE is not essential. However, deleting *rpoE* results increased sensitivity to different stresses, attenuation in infection capabilities and bacteria cannot survive in macrophages (Humphreys et al., 1999).

1.1.8 Autotransporters

Gram-negative bacteria harbor numerous proteins on their surface, including flagella, adhesins and specialized protein secretion systems. The secretion systems include seven known protein secretion systems (type I secretion system through to type VII secretion system) and a chaperone-usher (CU) system, which is essential for pilus assembly (Barnhart and Chapman, 2006; Bonemann et al., 2010; Coburn et al., 2007; Delepelaire, 2004; Desvaux et al., 2009; Johnson et al., 2006; Simeone et al., 2009; Wallden et al., 2010). The autotransporters belong to the type V secretion system and are most abundantly used by Gram-negative bacteria to secrete proteins to the surface (Leyton et al., 2012). Interestingly, Meyer and colleagues mentioned this name for this group of proteins during their studies of the IgA protease of *Neisseria gonorrhoeae*. The name referred to the model of outer membrane translocation of the immunoglobulin A1 (IgA1) protease, which at that time point did not include any auxiliary factors. Therefore the translocation was believed to be autonomous, which is misleading by the current state of knowledge, as it is known by now that other proteins are involved in the process of translocation (Klauser et al., 1993; Pohlner

et al., 1987). Today, five known types of type V secretion systems have been described (type Va - Ve) (for a review on the different types see (Leo et al., 2012)). The type Ve autotransporter family or inverse autotransporter (IAT) family is an inverted type of the classical type Va translocation mechanism and is mainly represented by intimin and invasin. However, other IATs have been described, including the antivirulence modulator system ZirTS in *S*. Tm, which shares similarities with the type Vb and Ve adhesin families and plays important roles in fine-tuning the degree of pathogenesis in the host (Gal-Mor et al., 2008). Intimin mediates attachment to host cells, thereby causing lesions and is present in numerous bacterial species, including *E. coli* and *Citrobacter rodentium* (Schmidt, 2010). Invasin is expressed by the enteropathogenic *Yersinia* species, *Y. enterocolitica* and *Y. pseudotuberculosis*. It is encoded by the *invA* gene and binds to β1 integrins of the host cell (Isberg et al., 1987).

The IAT is comprised of three functional domains: i. the N-terminal signal peptide (SP, in yellow), ii. the translocation unit, which is divided into a linker and β-barrel, iii. the C-terminal surface localized passenger domain consisting of immunoglobulin-like domains (Hamburger et al., 1999) (Figure 1.7). The signal peptide mediates the translocation from the cytoplasm through the IM via the general secretion (Sec) (Tsai et al., 2010) machinery and is cleaved during translocation. The function of the periplasmic domain (Figure 1.7) remains unknown. In the periplasm, the unfolded autotransporter is maintained in an unfolded state by the periplasmic chaperones SurA, Skp and the protease DegS, which degrades misfolded proteins (Bodelon et al., 2009). The translocation through the OM is mediated by the BAM complex, which integrates the β-barrel into the OM (Ieva and Bernstein, 2009; Knowles et al., 2009). The linker region forms a hairpin and initiates the translocation trough the previously formed β-barrel. The detailed mechanism for the translocation of the passenger domain remains unknown. Translocation is thought to occur by the formation of a hairpin intermediate formed by the passenger domain and the linker region. However, an alternative model exists, in which the BAM complex assists during passenger domain translocation (Leyton et al., 2012). The energy source for OM translocation is ATP-independent and not known. However, it is hypothesized that the initiation of protein folding of the passenger domain provides the energy for continuation of the translocation (Henderson et al., 2004; Thanassi et al., 2005).

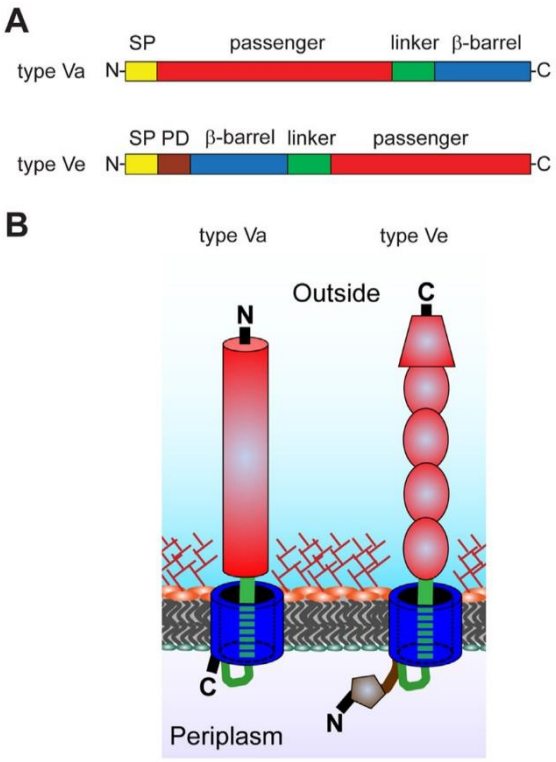

Figure 1.7. Classical and inverted autotransporters.
A) Schematic representation of the structures of classical autotransporters (Type Va) and inverted autotransporters (IAT, type Ve). Both types are comprised of a signal peptide (SP, yellow), passenger domain (red) and a translocation unit, which is divided into linker (green) and β-barrel (blue). The translocation unit anchors the complex into the outer membrane and secretes the passenger domain into extracellular space. The IAT has an N-terminal periplasmic domain (PD, brown), which is absent in the classical autotransporter. The passenger domain in the IAT is C-terminally located, in contrast to the classical autotransporter. **B)** Topological structure of the classical and inversed autotransporter. The colors of the domains are described in A. The IAT passenger domain is comprised of four immunoglobulin like domains. Figure adopted from (Leo et al., 2015).

1.2 Phenotypic diversity

1.2.1 Phenotypic diversity

Phenotypic diversity (or phenotypic heterogeneity) among bacteria describes a state where different phenotypes co-exist in an environment. This diversity naturally occurs in microbial communities as a result of genetic or environmental variations. However, phenotypic diversity can also occur in bacterial communities of the same genetic background when sharing the same environment (Ackermann, 2015; Sturm et al., 2011). In the past, classical microbiological studies primarily focused on the averaged traits of cell populations and neglected individuality among bacterial cells, thereby excluding different behavior of subpopulations from analyses (Dubnau and Losick, 2006; Kreibich and Hardt, 2015). However, individuality was already observed in the 1940s, when Delbruck observed different burst sizes of bacteriophages within

a similar number of bacteria. He found that the number of bacteriophages per burst ranged from 50 to over 1000 particles (Figure 1.8) (Delbruck, 1945b). Furthermore, in 1957 Novick and Weiner demonstrated phenotypic diversity in the regulatory program controlling lactose utilization in an isogenic *E*. *coli* population. They analyzed the β-galactosidase induction in bacteria that were re-cultured upon induction with low concentrations of inducer. They described a so-called "all-or-none phenomenon", where bacteria that were re-cultured upon induction displayed either a full β-galactosidase ("on") or no ("off") induction (Novick and Weiner, 1957; Smits et al., 2006a).

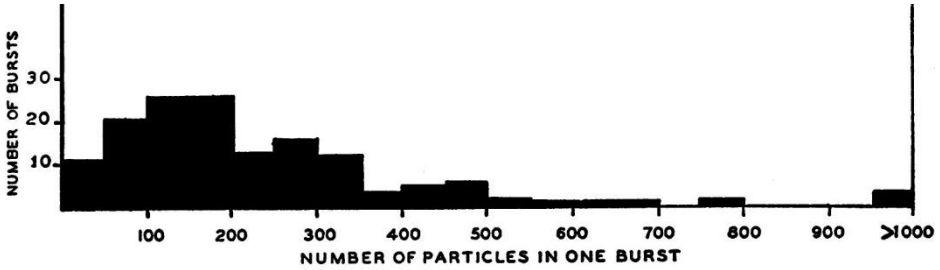

Figure 1.8. Different burst sizes of phage particles derived from individual *E. coli* cells.
Figure adopted from (Delbruck, 1945a).

These phenomena clearly demonstrate the existence of phenotypic diversity between isogenic populations already in early studies. However, the lack of proficient single cell studies prevented detailed analysis of these phenotypes (Kreibich and Hardt, 2015; Raj and van Oudenaarden, 2008). With the advent of techniques, such as flow cytometry and microscopy in combination with fluorescent protein reporters or antibody staining, visualization of single cells and subpopulations was possible (Smits et al., 2006a; Smits et al., 2006b).

One of the first studies looking at the origins of phenotypic diversity were from Elowitz and Ozbudak. Elowitz and colleagues demonstrated that noisy gene expression was responsible for different expression levels of two fluorescent reporters that were driven by the same promoter. They introduced two copies of the same promoter into E. *coli*, driving the expression of the genes, encoding either cyan fluorescent protein (*cfp*) yellow fluorescent protein (*yfp*) (Figure 1.9). To distinguish between intrinsic and extrinsic noise, they developed the following concept: If only extrinsic noise was present (i.e. variations in the number of specific molecules present in the cell that affect both fluorophores), the cells react similarly as both reporters would be affected equally in one cell (Figure 1.9B, upper graph). However, when the intrinsic noise is high, because of variations during transcription or translation, the

reporter genes should be affected independently from each other. Thus, the cell harbors different levels of CFP and YFP (Figure 1.9B, lower graph). Elowitz and colleagues found that both intrinsic and extrinsic noise contribute to formation of phenotypically different cells (Figure 1.9) (Elowitz et al., 2002). The study by Ozbudak and colleagues found that the level of phenotypic noise could be modified by changing the levels of transcription and translation. They used an inducible promoter system in *Bacillus subtilis* that controlled the expression of *gfp*. Transcription rates were controlled by varying the degree of induction, whereas translation rates were varied by modifying the ribosomal binding site sequence. They found that genes with low transcription but high translation rates showed high fluctuations in protein number, whereas high transcription and low translation rates displayed low variations, resulting in lower phenotypic diversity. Afterwards, groups succeeded in visualizing single mRNA molecules (Golding et al., 2005), but also single proteins (Cai et al., 2006; Choi et al., 2008; Yu et al., 2006).

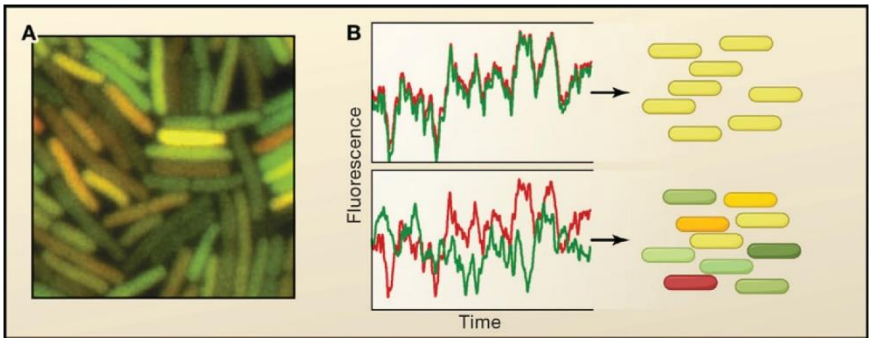

Figure 1.9. Phenotypic diversity in isogenic bacterial population.
A) Phenotypic diversity within an isogenic population is visualized in single cells by the expression of the two reporter genes *cfp* and *yfp*, which are under the control of the same promoter sequence. **B)** Intrinsic and extrinsic noise were measured by using two different reporters within one cell (*cfp* in green and *yfp* in red). Figure adopted from (Elowitz et al., 2002; Raj and van Oudenaarden, 2008).

1.2.2 Bistability and noisy gene expression

Phenotypic diversity has important implications for the survival of an isogenic bacterial population within a changing environment. Bacteria can react to different environmental conditions (e.g. temperature changes, nutrient limitation, antibiotics) by activating different stress response genes to survive (Dubnau and Losick, 2006). An isogenic bacterial population within a given environment can increase its chance of surviving future changes by expressing different phenotypes (Ackermann et al., 2008; Diard et al., 2013). The existence of two subpopulations within an isogenic population in a given environment is called bistability. In a

bistable system, two stable states exist and can switch from one state to the other. Figure 1.10A depicts a culture harboring two subpopulations, with only one expressing GFP, yielding a bimodal fluorescence distribution on the histogram (Figure 1.10B, C) (Dubnau and Losick, 2006; Kaern et al., 2005; Smits et al., 2006b).

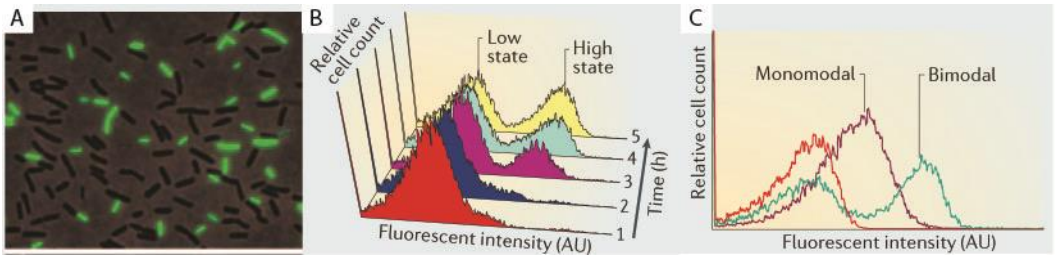

Figure 1.10. Bistability in single isogenic cells.
A) Fluorescent microscopic analysis of a population displaying bistable behavior in expressing GFP. **B)** Flow cytometric analysis of a bistable population in the course of time. **C)** Histogram displaying bimodal (green) and monomodal (red) distribution. The red curve represents background fluorescence by a non-fluorescent culture. Figure modified from (Smits et al., 2006a).

Bistability is generated by stochastic events (or noise) during gene expression, when random events are amplified by positive feedback and result in a nonlinear response. The level of the molecule of interest has to reach a certain threshold concentration, before the positive auto-stimulatory feedback reinforces its activation that leads to the second steady state (Figure 1.11B) (Dubnau and Losick, 2006; Smits et al., 2006a; Veening et al., 2008). A non-linear response can be induced by multimerization or cooperativity in DNA binding (Smits et al., 2006a; Smits et al., 2006b) and a positive feedback stimulation, e.g. by auto-stimulation. Due to noisy gene expression, some cells reach the threshold activation required to induce auto-stimulation of the gene of interest, that enables the cells to switch from a low to a high expressing state (Figure 1.11B). The switch to the second steady state can also be enforced by two other types of positive feedback. A double positive loop allows two regulators to trigger the expression of each other. Furthermore, a system response is also reinforced when two regulators repress each other, thereby allowing the action of one the two repressors at a time (Figure 1.11) (Smits et al., 2006a; Veening et al., 2008).

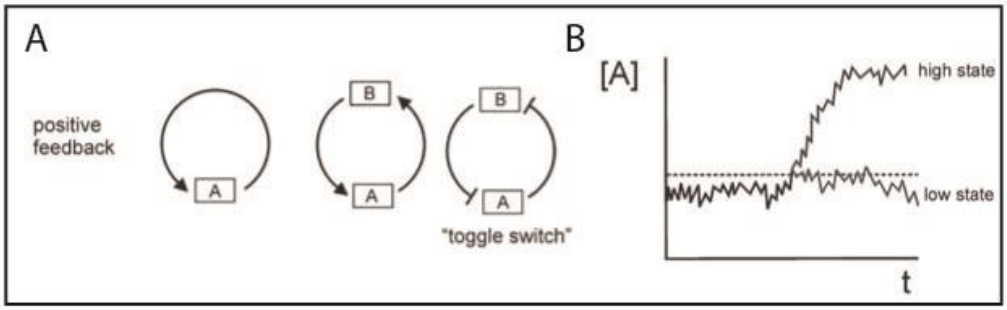

Figure 1.11. Positive feedback mechanisms enforcing bifurcation of a bistable population into high and low expressing states.
A) Bistable behavior of a population is enforced by positive feedback mechanisms that include one-component (left) or two-component systems (middle and right) systems**. B)** Protein levels of a population expressing low and high amounts of a certain regulator. The high state is induced by positive feedback as soon as a threshold level of protein is achieved, whereas noisy gene expression without feedback enforcement results in a low state of protein. Figure modified from (Smits et al., 2006b).

The noise in prokaryotic gene expression originates from the digital nature of transcription, which results in translational bursts (Ozbudak et al., 2002). Noisy gene expression is higher if low numbers of molecules are involved in the rate-limiting steps (finite number effect) (Kaern et al., 2005) (Figure 1.12). Noise can be classified into intrinsic (inherent cellular processes, e.g. transcription, translation) and extrinsic (other cellular components influencing these processes) (Kaern et al., 2005; Swain et al., 2002) and has already been quantified by Elowitz and colleagues (Figure 1.9) (Elowitz et al., 2002).

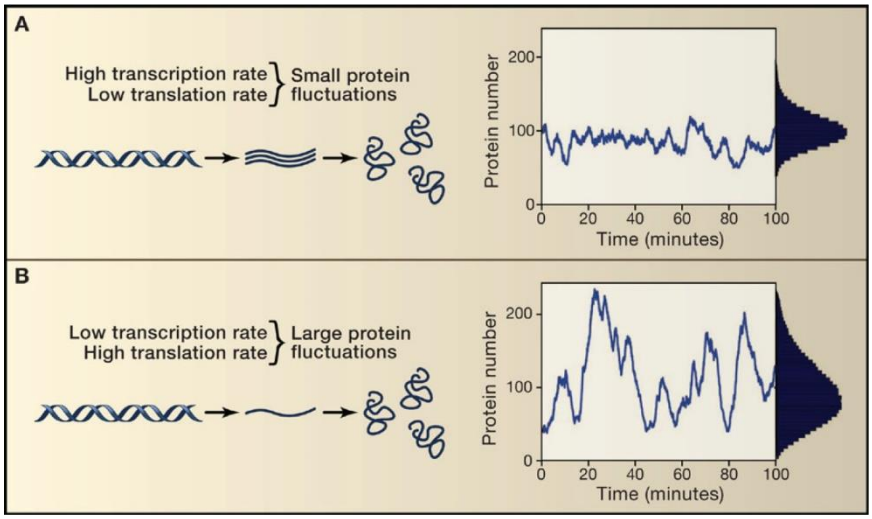

Figure 1.12. Origins of noise in gene expression.
Noisy gene expression in prokaryotic cells is caused by low transcription rates, resulting in low mRNA levels from which large protein amounts are translated (B). In contrast, high transcription rates in combination with low translation rates reduces noise in gene expression (A). Figure adopted from (Raj and van Oudenaarden, 2008).

As noise in gene expression systems can have detrimental effects, biological systems tend to reduce the noise in expression of essential genes (Fraser et al., 2004; Raser and O'Shea, 2005). A system can be stabilized by noise reduction measurements, such as negative feedback loops (Becskei and Serrano, 2000). However, noisy gene expression resulting in bistable populations can be beneficial and result in increased fitness of the whole population (Diard et al., 2013). Furthermore, it is an important contributor for the generation of phenotypic diversity (Raj and van Oudenaarden, 2008).

1.2.3 SPI-1 as an example for bistable gene expression

Bistable gene expression represents a strategy for bacteria to increase their fitness and thereby increase the survival chances of the genotype. *S.* Tm has exploited this mechanism to maximize the infection chances by expressing T1 by only a subpopulation of cells, leading to the co-existence of T1 expressing ($T1^+$) and not expressing ($T1^-$) cells. Hautefort and colleagues already described the existence of two populations within an isogenic population. They used a chromosomally integrated *gfp* reporter to analyze the expression of the *prgH* promoter (P*prgH*) which encodes a structural protein of the T1 needle, to analyze P*prgH* expression using a flow cytometry-based assay (Hautefort et al., 2008). Bistable T1 expression was also reported during mouse infections with *S*. Tm, where Ackermann and colleagues found 15% of $T1^+$ cells in the gut lumen (Ackermann et al., 2008). By analyzing the role of the feedback circuits of T1, Saini and colleagues demonstrated bistability of the transcription factor *hilD*. Using plasmid-based *gfp* reporters fused to the promoters of interest, they showed that the *hilD* promoter (P*hilD*) mediates the switch-like transition from the $T1^-$ off to $T1^+$ state, as exchanging P*hilD* with the weaker *hilC* promoter, converted the switch like P*hilA* response to a continuous and rheostatic response (Figure 1.13) (Saini et al., 2010a).

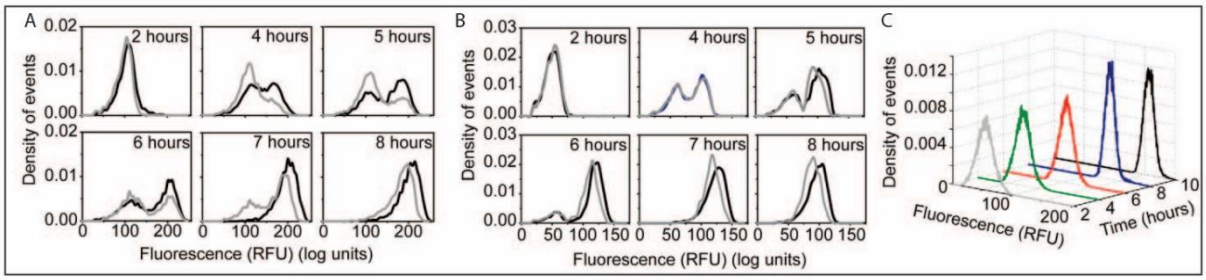

Figure 1.13. Bistable gene expression of the *S*. Tm T1.
Flow cytometric analysis of a culture harboring *gfp* expression under the control of the *hilD* (P*hilD*, black curve, **A**) or *hilA* (P*hilA*, black curve, **B**) promoter at the indicated time points. Deletion of *hilC* and *rtsA* does not change the switch-like behavior of the promoters (grey curves in A, B). **C)** Exchange of P*hilD* with the weaker promoter P*hilC* diminishes the switch-like behavior of p*hilA* and results in rheostatic expression. Figure modified from (Saini et al., 2010a).

By analyzing the phenotype of the T1 expressing subpopulation, Sturm and colleagues found that the T1 expressing cells displayed a reduced growth phenotype, thereby paying a cost for virulence factor expression (Sturm et al., 2011). However, for a successful infection *S*. Tm requires both T1 subpopulations (Ackermann et al., 2008; Diard et al., 2013; Stecher et al., 2007).

1.2.4 Bet hedging and division of labor

Phenotypic diversity and the resulting subpopulations have important functional implications for the survival of bacterial populations. It lies in the nature of microorganisms to endure different environments during the process of infection or when living in natural ecosystems. Bacteria have to survive in extreme conditions, including changes in temperature, pH and nutrient availability or exposure to antibiotics or other toxins (Dubnau and Losick, 2006). In fast-changing environments, the existence of different phenotypes can provide significant advantages for the propagation of the population`s genotype, if a subset of cells expresses a set of genes that guarantees its survival (bet hedging). Furthermore, the evolution of different phenotypes within an isogenic population provides a second advantage, which allows bacteria to specialize in expressing one particular phenotype and benefit from other existing phenotypes (division of labor, Figure 1.14) (Ackermann, 2013; Ackermann, 2015).

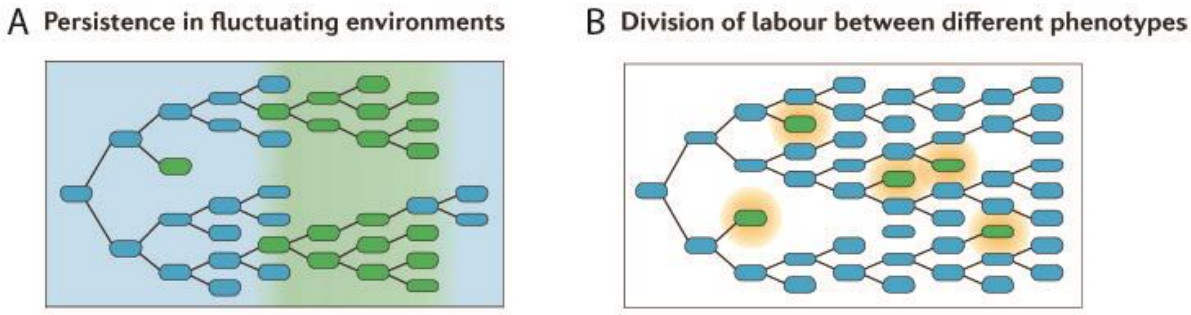

Figure 1.14. Bet hedging versus division of labor.
A) Bet hedging among isogenic bacteria allows persistence of one of the two phenotypes (blue and green) to survive in fluctuating environments (light green and light blue). **B)** Two phenotypes (blue, green) can emerge within an isogenic population that complement each other in function. E.g., the green phenotype produces a substrate, which the blue phenotype uses for survival. Figure adopted from (Ackermann, 2015).

Bet hedging is a good strategy for bacteria to increase their competitive advantage in fluctuating environments. While the majority of the bacterial population is adapted to the present growth conditions, another subpopulation expresses genes that would allow its survival after a future sudden environmental shift. However, these phenotypic traits might fit to a given environment, but be disadvantageous in the current growth conditions (e.g. by inferring a growth disadvantage) (Acar et al., 2008; Sturm et al., 2011). This theory complements the conventional idea that bacteria first sense stimuli and then respond accordingly by respective gene expression. In some cases, environmental changes might be too fast for bacteria to adapt or bacteria are not able to respond because they lack the cellular resources (Kashiwagi et al., 2006). The bet hedging strategy is exemplified by a recent study in *S*. Tm that observed a small subpopulation of cells to survive antibiotic treatment upon expression of the T1. By expressing the virulence factor cells are affected by metabolic costs. These slow down growth and thereby increase survival when the population is exposed to high antibiotic concentrations (Arnoldini et al., 2014).

Division of labor does not require fluctuating environments and provides benefits to subpopulations by the interaction with other specialized phenotypes within an isogenic population. Physical contact between bacteria is not required. However, they have to be in proximity (Ackermann, 2013; Ackermann, 2015). This strategy has been observed in biofilms, where bacteria live together in spatially structured organizations and produce compounds from which other bacteria can potentially benefit (Stewart and Franklin, 2008). Another example for division of labor is provided by *S*. Tm during infection between $T1^+$ and $T1^-$

bacterial cells. The two subpopulations complement each other during infection. While the $T1^+$ subpopulation invades the intestinal epithelium and thereby triggers inflammation, the $T1^-$ subpopulation remains in the lumen and takes advantage of the inflammation to outcompete the gut microbiota (Ackermann et al., 2008; Stecher et al., 2007). As described with the previous examples during *S*. Tm infection, the two adaptive functions bet hedging and division of labor are not exclusive to each other and provide particular advantages at different situations. Division of labor between the $T1^+$ and $T1^-$ subpopulations is required for the invasion process of *S*. Tm (Ackermann et al., 2008; Stecher et al., 2007). However, phenotypic diversity provided by the bet hedging mechanism can provide competitive advantage during antibiotic treatment by the expression of the T1 by a subpopulation (Arnoldini et al., 2014).

The outcome of phenotypic diversity within bacterial populations also poses major challenges to medicine. The emergence of bacteria that persist antibiotic treatment is a well-known phenomenon (Arnoldini et al., 2014; Bigger, 1944). Furthermore, experimental data from bulk assays should be analyzed with care, considering the potential presence of different subpopulations (Veening et al., 2008).

1.2.5 Single cell analysis using microfluidics

The importance of phenotypic diversity and the resulting emergence of subpopulations has been recognized as essential for understanding the host-pathogen interactions (Kreibich and Hardt, 2015). The behavior of *S*. Tm during the infection process provides a good example, as understanding the bistability of T1 virulence factor expression during the interaction with the host requires the analysis of the two subpopulations ($T1^+$ and $T1^-$) driving the invasion process. One of the most common techniques for studying single cells are fluorescence microscopy-based assays (Smits et al., 2006a), which enable the analysis of phenotypic diversity within clonal populations (Choi et al., 2008; Sturm et al., 2011; Yu et al., 2006). Flow cytometry studies enable the analysis of large numbers of cells within short time and have been applied to study T1 bistability (Hautefort et al., 2003; Saini et al., 2010a; Temme et al., 2008).

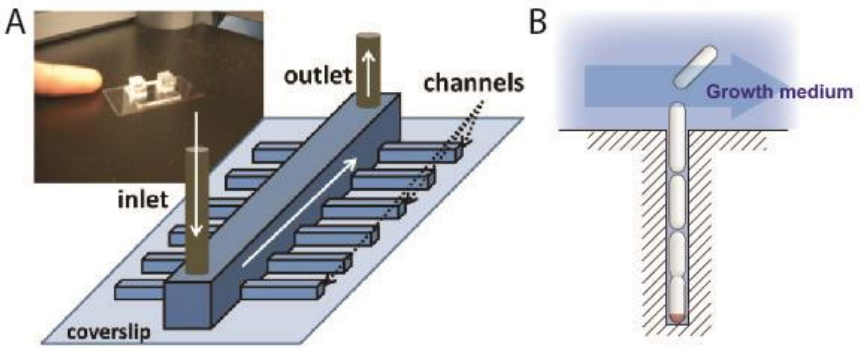

Figure 1.15. "Mother machine" design.
A) Design of the microfluidic device ("mother machine"), displaying the main trench with the inlet and outlet as well as the growth channels. The growth medium is applied through the main trench and allows controlled growth observation of bacteria growing in the growth channels. **B)** Schematic illustration of bacterial growth within one single growth channel. Figure modified from (Wang et al., 2010).

During the last decade, another useful tool has been introduced to study individual bacteria. Microbial studies have been combined with microfluidic systems to provide a powerful tool to study bacteria at single cell level (Hol and Dekker, 2014). This tool allows long-term monitoring of single bacteria in controlled environmental settings and precise manipulation of the microenvironment. This setup allows the analysis of fundamental questions about growth and death and bacterial shape. Using a microfluidic setup that allows monitoring of one bacterial cell ("mother machine", Figure 1.15), Wang and colleagues monitored growth and death of *E. coli* over 200 generations. Previous setups using agar pads for monitoring of cell growth allowed the observation of ~10 generations (Stewart et al., 2005). With their results, they could demonstrate that growth in *E. coli* is uncoupled from death, which was possible due to the microfluidic setup (Wang et al., 2010). This design was used by other groups that started analyzing effects of antibiotics on particular persisting cells (Arnoldini et al., 2014; Kiviet et al., 2014).

1.3 Aim of the thesis

At the beginning of this thesis, the bistable behavior of T1 expression of *S*. Tm was known and the core regulators governing the expression of the T1 virulence factor of *S*. Tm were well established. However, mechanistic studies to unravel the dynamic interactions of these regulators were missing. Previous studies analyzing gene expression of multiple genes within

one cell used different fluorophores for visualization of gene expression. The drawback of this approach is that different folding and maturation properties of the individual fluorophores do not allow precise dynamics assessment. Therefore, we sought to establish a transcriptional reporter system that sets ground for a future analysis of several genes within one cell and allows precise analysis of gene expression.

First, we established a reporter system that is based on the autotransporter invasin (encoded by the *invA* gene) that is epitope-tagged with a hemagglutinin (HA) epitope (*invA*$_{HA}$). We aimed to investigate its suitability as alternative gene expression reporter system to the standard *gfp* reporter. In particular, I wanted to focus on T1 expression and explain T1 expression patterns at the single cell level. Therefore, I chose genes encoding for *t1* expression to evaluate the expression of *invA*$_{HA}$. We sought to analyze the expression of the surface exposed HA epitope by antibody-staining using flow cytometry and microscopy. Second, we aimed to set up a microfluidics-based microscopy technique, an alternative single cell analysis method that would allow gene expression analysis at single cell level. Third, we addressed the role of the T1 and cytoplasmic fluorophores in the RpoE-mediated membrane stress response. In particular, we focused on the zinc-metalloprotease RseP that activates RpoE.

1.4 References

Acar, M., J.T. Mettetal, and A. van Oudenaarden. 2008. Stochastic switching as a survival strategy in fluctuating environments. *Nature genetics* 40:471-475.

Ackermann, M. 2013. Microbial individuality in the natural environment. *The ISME journal* 7:465-467.

Ackermann, M. 2015. A functional perspective on phenotypic heterogeneity in microorganisms. *Nature reviews Microbiology* 13:497-508.

Ackermann, M., B. Stecher, N.E. Freed, P. Songhet, W.D. Hardt, and M. Doebeli. 2008. Self-destructive cooperation mediated by phenotypic noise. *Nature* 454:987-990.

Akeda, Y., and J.E. Galan. 2005. Chaperone release and unfolding of substrates in type III secretion. *Nature* 437:911-915.

Alpuche Aranda, C.M., J.A. Swanson, W.P. Loomis, and S.I. Miller. 1992. Salmonella typhimurium activates virulence gene transcription within acidified macrophage phagosomes. *Proceedings of the National Academy of Sciences of the United States of America* 89:10079-10083.

Altier, C. 2005. Genetic and environmental control of salmonella invasion. *Journal of microbiology* 43 Spec No:85-92.

Arnoldini, M., I.A. Vizcarra, R. Pena-Miller, N. Stocker, M. Diard, V. Vogel, R.E. Beardmore, W.D. Hardt, and M. Ackermann. 2014. Bistable expression of virulence genes in salmonella leads to the formation of an antibiotic-tolerant subpopulation. *PLoS biology* 12:e1001928.

Audia, J.P., C.C. Webb, and J.W. Foster. 2001. Breaking through the acid barrier: an orchestrated response to proton stress by enteric bacteria. *International journal of medical microbiology : IJMM* 291:97-106.

Baek, C.H., S. Wang, K.L. Roland, and R. Curtiss, 3rd. 2009. Leucine-responsive regulatory protein (Lrp) acts as a virulence repressor in Salmonella enterica serovar Typhimurium. *Journal of bacteriology* 191:1278-1292.

Bajaj, V., R.L. Lucas, C. Hwang, and C.A. Lee. 1996. Co-ordinate regulation of Salmonella typhimurium invasion genes by environmental and regulatory factors is mediated by control of hilA expression. *Molecular microbiology* 22:703-714.

Bang, I.S., J.G. Frye, M. McClelland, J. Velayudhan, and F.C. Fang. 2005. Alternative sigma factor interactions in Salmonella: sigma and sigma promote antioxidant defences by enhancing sigma levels. *Molecular microbiology* 56:811-823.

Barlag, B., and M. Hensel. 2015. The giant adhesin SiiE of Salmonella enterica. *Molecules* 20:1134-1150.

Barnhart, M.M., and M.R. Chapman. 2006. Curli biogenesis and function. *Annual review of microbiology* 60:131-147.

Barthel, M., S. Hapfelmeier, L. Quintanilla-Martinez, M. Kremer, M. Rohde, M. Hogardt, K. Pfeffer, H. Russmann, and W.D. Hardt. 2003. Pretreatment of mice with streptomycin provides a Salmonella enterica serovar Typhimurium colitis model that allows analysis of both pathogen and host. *Infection and Immunity* 71:2839-2858.

Baxter, M.A., T.F. Fahlen, R.L. Wilson, and B.D. Jones. 2003. HilE Interacts with HilD and Negatively Regulates hilA Transcription and Expression of the Salmonella enterica Serovar Typhimurium Invasive Phenotype. *Infection and Immunity* 71:1295-1305.

Baxter, M.A., and B.D. Jones. 2005. The fimYZ genes regulate Salmonella enterica Serovar Typhimurium invasion in addition to type 1 fimbrial expression and bacterial motility. *Infection and Immunity* 73:1377-1385.

Becskei, A., and L. Serrano. 2000. Engineering stability in gene networks by autoregulation. *Nature* 405:590-593.

Behlau, I., and S.I. Miller. 1993. A PhoP-repressed gene promotes Salmonella typhimurium invasion of epithelial cells. *Journal of bacteriology* 175:4475-4484.

Belden, W.J., and S.I. Miller. 1994. Further characterization of the PhoP regulon: identification of new PhoP-activated virulence loci. *Infection and Immunity* 62:5095-5101.

Bigger, B.W. 1944. Treatment of staphylococcal infecitons with penicillin. *The Lancet* 244:497-500.

Bodelon, G., E. Marin, and L.A. Fernandez. 2009. Role of periplasmic chaperones and BamA (YaeT/Omp85) in folding and secretion of intimin from enteropathogenic Escherichia coli strains. *Journal of bacteriology* 191:5169-5179.

Bone, R.C. 1991. Gram-negative sepsis. Background, clinical features, and intervention. *Chest* 100:802-808.

Bonemann, G., A. Pietrosiuk, and A. Mogk. 2010. Tubules and donuts: a type VI secretion story. *Molecular microbiology* 76:815-821.

Bowe, F., C.J. Lipps, R.M. Tsolis, E. Groisman, F. Heffron, and J.G. Kusters. 1998. At least four percent of the Salmonella typhimurium genome is required for fatal infection of mice. *Infection and Immun* 66:3372-3377.

Brass, J.M., C.F. Higgins, M. Foley, P.A. Rugman, J. Birmingham, and P.B. Garland. 1986. Lateral diffusion of proteins in the periplasm of Escherichia coli. *Journal of bacteriology* 165:787-795.

Brenner, F.W., R.G. Villar, F.J. Angulo, R. Tauxe, and B. Swaminathan. 2000. Salmonella nomenclature. *Journal of clinical microbiology* 38:2465-2467.

Brissette, J.L., M. Russel, L. Weiner, and P. Model. 1990. Phage shock protein, a stress protein of Escherichia coli. *Proceedings of the National Academy of Sciences of the United States of America* 87:862-866.

Brumell, J.H., O. Steele-Mortimer, and B.B. Finlay. 1999. Bacterial invasion: Force feeding by Salmonella. *Current Biology* 9:R277-R280.

Bustamante, V.H., L.C. Martinez, F.J. Santana, L.A. Knodler, O. Steele-Mortimer, and J.L. Puente. 2008. HilD-mediated transcriptional cross-talk between SPI-1 and SPI-2. *Proceedings of the National Academy of Sciences of the United States of America* 105:14591-14596.

Cai, L., N. Friedman, and X.S. Xie. 2006. Stochastic protein expression in individual cells at the single molecule level. *Nature* 440:358-362.

Canals, R., M. McClelland, C.A. Santiviago, and H. Andrews-Polymenis. 2011. Genomics of Salmonella Species. 171-235.

Centers for diesease control and prevention. 2011. National enteric surveillance: *Salmonella* surveillance overview.

Choi, P.J., L. Cai, K. Frieda, and X.S. Xie. 2008. A stochastic single-molecule event triggers phenotype switching of a bacterial cell. *Science* 322:442-446.

Chubiz, J.E., Y.A. Golubeva, D. Lin, L.D. Miller, and J.M. Slauch. 2010. FliZ regulates expression of the Salmonella pathogenicity island 1 invasion locus by controlling HilD protein activity in Salmonella enterica serovar typhimurium. *Journal of bacteriology* 192:6261-6270.

Cirillo, D.M., R.H. Valdivia, D.M. Monack, and S. Falkow. 1998. Macrophage-dependent induction of the Salmonella pathogenicity island 2 type III secretion system and its role in intracellular survival. *Molecular microbiology* 30:175-188.

Coburn, B., I. Sekirov, and B.B. Finlay. 2007. Type III secretion systems and disease. *Clinical microbiology reviews* 20:535-549.

Cornelis, G.R. 2010. The type III secretion injectisome, a complex nanomachine for intracellular 'toxin' delivery. *Biological chemistry* 391:745-751.

Cosma, C.L., P.N. Danese, J.H. Carlson, T.J. Silhavy, and W.B. Snyder. 1995. Mutational activation of the Cpx signal transduction pathway of Escherichia coli suppresses the toxicity conferred by certain envelope-associated stresses. *Molecular microbiology* 18:491-505.

Darwin, K.H., and V.L. Miller. 2000. The putative invasion protein chaperone SicA acts together with InvF to activate the expression of Salmonella typhimurium virulence genes. *Molecular microbiology* 35:949-960.

Darwin, K.H., and V.L. Miller. 2001. Type III secretion chaperone-dependent regulation: activation of virulence genes by SicA and InvF in Salmonella typhimurium. *The EMBO journal* 20:1850-1862.

De Las Penas, A., L. Connolly, and C.A. Gross. 1997. SigmaE is an essential sigma factor in Escherichia coli. *Journal of bacteriology* 179:6862-6864.

Delbruck, M. 1945a. The burst size distribution in the growth of bacterial viruses (bacteriophages). *Journal of bacteriology* 50:131-135.

Delbruck, M. 1945b. The Burst Size Distribution in the Growth of Bacterial Viruses (Bacteriophages). *Journal of bacteriology* 50:131-135.

Delepelaire, P. 2004. Type I secretion in gram-negative bacteria. *Biochimica et biophysica acta* 1694:149-161.

Desvaux, M., M. Hebraud, R. Talon, and I.R. Henderson. 2009. Secretion and subcellular localizations of bacterial proteins: a semantic awareness issue. *Trends in microbiology* 17:139-145.

Diard, M., V. Garcia, L. Maier, M.N. Remus-Emsermann, R.R. Regoes, M. Ackermann, and W.D. Hardt. 2013. Stabilization of cooperative virulence by the expression of an avirulent phenotype. *Nature* 494:353-356.

Dillon, S.C., and C.J. Dorman. 2010. Bacterial nucleoid-associated proteins, nucleoid structure and gene expression. *Nature reviews. Microbiology* 8:185-195.

Dubnau, D., and R. Losick. 2006. Bistability in bacteria. *Molecular microbiology* 61:564-572.

Duguay, A.R., and T.J. Silhavy. 2004. Quality control in the bacterial periplasm. *Biochimica et biophysica acta* 1694:121-134.

Ellermeier, C.D., J.R. Ellermeier, and J.M. Slauch. 2005. HilD, HilC and RtsA constitute a feed forward loop that controls expression of the SPI1 type three secretion system regulator hilA in Salmonella enterica serovar Typhimurium. *Molecular microbiology* 57:691-705.

Ellermeier, C.D., and J.M. Slauch. 2003. RtsA and RtsB Coordinately Regulate Expression of the Invasion and Flagellar Genes in Salmonella enterica Serovar Typhimurium. *Journal of bacteriology* 185:5096-5108.

Ellermeier, J.R., and J.M. Slauch. 2007. Adaptation to the host environment: regulation of the SPI1 type III secretion system in Salmonella enterica serovar Typhimurium. *Current opinion in microbiology* 10:24-29.

Ellermeier, J.R., and J.M. Slauch. 2008. Fur regulates expression of the Salmonella pathogenicity island 1 type III secretion system through HilD. *Journal of bacteriology* 190:476-486.

Elowitz, M.B., A.J. Levine, E.D. Siggia, and P.S. Swain. 2002. Stochastic gene expression in a single cell. *Science* 297:1183-1186.

Erickson, J.W., and C.A. Gross. 1989. Identification of the sigma E subunit of Escherichia coli RNA polymerase: a second alternate sigma factor involved in high-temperature gene expression. *Genes & development* 3:1462-1471.

Fabrega, A., and J. Vila. 2013. Salmonella enterica serovar Typhimurium skills to succeed in the host: virulence and regulation. *Clinical microbiology reviews* 26:308-341.

Flynn, J.M., I. Levchenko, R.T. Sauer, and T.A. Baker. 2004. Modulating substrate choice: the SspB adaptor delivers a regulator of the extracytoplasmic-stress response to the AAA+ protease ClpXP for degradation. *Genes & development* 18:2292-2301.

Food and Agriculture Organization of the United Nations. 2002. W.H.O (Risk assessment of *Salmonella* in eggs and broiler chickens). In.

Franchi, L., A. Amer, M. Body-Malapel, T.D. Kanneganti, N. Ozoren, R. Jagirdar, N. Inohara, P. Vandenabeele, J. Bertin, A. Coyle, E.P. Grant, and G. Nunez. 2006. Cytosolic flagellin requires Ipaf for activation of caspase-1 and interleukin 1beta in salmonella-infected macrophages. *Nature immunology* 7:576-582.

Fraser, H.B., A.E. Hirsh, G. Giaever, J. Kumm, and M.B. Eisen. 2004. Noise minimization in eukaryotic gene expression. *PLoS biology* 2:e137.

Friebel, A., and W.D. Hardt. 2000. Purification and biochemical activity of Salmonella exchange factor SopE. *Methods in enzymology* 325:82-91.

Gal-Mor, O., D.L. Gibson, D. Baluta, B.A. Vallance, and B.B. Finlay. 2008. A novel secretion pathway of Salmonella enterica acts as an antivirulence modulator during salmonellosis. *PLoS pathogens* 4:e1000036.

Galan, J.E. 1996. Molecular genetic bases of Salmonella entry into host cells. *Molecular microbiology* 20:263-271.

Galan, J.E., and R. Curtiss, 3rd. 1989. Cloning and molecular characterization of genes whose products allow Salmonella typhimurium to penetrate tissue culture cells. *Proceedings of the National Academy of Sciences of the United States of America* 86:6383-6387.

Galanis, E., D.M. Lo Fo Wong, M.E. Patrick, N. Binsztein, A. Cieslik, T. Chalermchikit, A. Aidara-Kane, A. Ellis, F.J. Angulo, H.C. Wegener, and S.-S. World Health Organization Global. 2006. Web-based surveillance and global Salmonella distribution, 2000-2002. *Emerging infectious diseases* 12:381-388.

Garcia Vescovi, E., F.C. Soncini, and E.A. Groisman. 1996. Mg2+ as an extracellular signal: environmental regulation of Salmonella virulence. *Cell* 84:165-174.

Gerlach, R.G., N. Claudio, M. Rohde, D. Jackel, C. Wagner, and M. Hensel. 2008. Cooperation of Salmonella pathogenicity islands 1 and 4 is required to breach epithelial barriers. *Cellular microbiology* 10:2364-2376.

Gerlach, R.G., D. Jackel, N. Geymeier, and M. Hensel. 2007. Salmonella pathogenicity island 4-mediated adhesion is coregulated with invasion genes in Salmonella enterica. *Infect Immun* 75:4697-4709.

Golding, I., J. Paulsson, S.M. Zawilski, and E.C. Cox. 2005. Real-time kinetics of gene activity in individual bacteria. *Cell* 123:1025-1036.

Gophna, U., E.Z. Ron, and D. Graur. 2003. Bacterial type III secretion systems are ancient and evolved by multiple horizontal-transfer events. *Gene* 312:151-163.

Gordon, M.A. 2008. Salmonella infections in immunocompromised adults. *The Journal of infection* 56:413-422.

Groisman, E.A., E. Chiao, C.J. Lipps, and F. Heffron. 1989. Salmonella typhimurium phoP virulence gene is a transcriptional regulator. *Proceedings of the National Academy of Sciences of the United States of America* 86:7077-7081.

Haag, A.F., K.K. Myka, M.F. Arnold, P. Caro-Hernandez, and G.P. Ferguson. 2010. Importance of Lipopolysaccharide and Cyclic beta-1,2-Glucans in Brucella-Mammalian Infections. *International journal of microbiology* 2010:124509.

Hamburger, Z.A., M.S. Brown, R.R. Isberg, and P.J. Bjorkman. 1999. Crystal structure of invasin: a bacterial integrin-binding protein. *Science* 286:291-295.

Hapfelmeier, S., B. Stecher, M. Barthel, M. Kremer, A.J. Muller, M. Heikenwalder, T. Stallmach, M. Hensel, K. Pfeffer, S. Akira, and W.D. Hardt. 2005. The Salmonella pathogenicity island (SPI)-2 and SPI-1 type III secretion systems allow Salmonella serovar typhimurium to trigger colitis via MyD88-dependent and MyD88-independent mechanisms. *Journal of immunology* 174:1675-1685.

Hardt, W.D., L.M. Chen, K.E. Schuebel, X.R. Bustelo, and J.E. Galan. 1998a. S. typhimurium encodes an activator of Rho GTPases that induces membrane ruffling and nuclear responses in host cells. *Cell* 93:815-826.

Hardt, W.D., H. Urlaub, and J.E. Galan. 1998b. A substrate of the centisome 63 type III protein secretion system of Salmonella typhimurium is encoded by a cryptic bacteriophage. *Proceedings of the National Academy of Sciences of the United States of America* 95:2574-2579.

Hautefort, I., M.J. Proenca, and J.C.D. Hinton. 2003. Single-Copy Green Fluorescent Protein Gene Fusions Allow Accurate Measurement of Salmonella Gene Expression In Vitro and during Infection of Mammalian Cells. *Applied and environmental microbiology* 69:7480-7491.

Hautefort, I., A. Thompson, S. Eriksson-Ygberg, M.L. Parker, S. Lucchini, V. Danino, R.J. Bongaerts, N. Ahmad, M. Rhen, and J.C. Hinton. 2008. During infection of epithelial cells Salmonella enterica serovar Typhimurium undergoes a time-dependent transcriptional adaptation that results in simultaneous expression of three type 3 secretion systems. *Cellular microbiology* 10:958-984.

Henderson, I.R., F. Navarro-Garcia, M. Desvaux, R.C. Fernandez, and D. Ala'Aldeen. 2004. Type V protein secretion pathway: the autotransporter story. *Microbiology and molecular biology reviews : MMBR* 68:692-744.

Hensel, M. 2004. Evolution of pathogenicity islands of Salmonella enterica. *International journal of medical microbiology : IJMM* 294:95-102.

Heyndrickx, M., F. Pasmans, R. Ducatelle, A. Decostere, and F. Haesebrouck. 2005. Recent changes in Salmonella nomenclature: the need for clarification. *Veterinary journal* 170:275-277.

Hoelzer, S. 2010. Functional analysis of the type III secretion systems in Salmonella enterica. In Naturwissenschaftliche Fakultät. Friedrich-Alexander-Universität Erlangen-Nürnberg (FAU), Nürnberg.

Hol, F.J., and C. Dekker. 2014. Zooming in to see the bigger picture: microfluidic and nanofabrication tools to study bacteria. *Science* 346:1251821.

Hornef, M.W., K. Putsep, J. Karlsson, E. Refai, and M. Andersson. 2004. Increased diversity of intestinal antimicrobial peptides by covalent dimer formation. *Nature immunology* 5:836-843.

Humphrey, T. 2004. Salmonella, stress responses and food safety. *Nature reviews. Microbiology* 2:504-509.

Humphreys, S., A. Stevenson, A. Bacon, A.B. Weinhardt, and M. Roberts. 1999. The alternative sigma factor, sigmaE, is critically important for the virulence of Salmonella typhimurium. *Infect Immun* 67:1560-1568.

Hurley, D., M.P. McCusker, S. Fanning, and M. Martins. 2014. Salmonella-host interactions - modulation of the host innate immune system. *Frontiers in immunology* 5:481.

Ieva, R., and H.D. Bernstein. 2009. Interaction of an autotransporter passenger domain with BamA during its translocation across the bacterial outer membrane. *Proceedings of the National Academy of Sciences of the United States of America* 106:19120-19125.

Isberg, R.R., D.L. Voorhis, and S. Falkow. 1987. Identification of invasin: a protein that allows enteric bacteria to penetrate cultured mammalian cells. *Cell* 50:769-778.

Issenhuth-Jeanjean, S., P. Roggentin, M. Mikoleit, M. Guibourdenche, E. de Pinna, S. Nair, P.I. Fields, and F.X. Weill. 2014. Supplement 2008-2010 (no. 48) to the White-Kauffmann-Le Minor scheme. *Research in microbiology* 165:526-530.

Johnson, T.L., J. Abendroth, W.G. Hol, and M. Sandkvist. 2006. Type II secretion: from structure to function. *FEMS microbiology letters* 255:175-186.

Jones, B.D., N. Ghori, and S. Falkow. 1994. Salmonella typhimurium initiates murine infection by penetrating and destroying the specialized epithelial M cells of the Peyer's patches. *The Journal of experimental medicine* 180:15-23.

Kaern, M., T.C. Elston, W.J. Blake, and J.J. Collins. 2005. Stochasticity in gene expression: from theories to phenotypes. *Nature reviews. Genetics* 6:451-464.

Kashiwagi, A., I. Urabe, K. Kaneko, and T. Yomo. 2006. Adaptive response of a gene network to environmental changes by fitness-induced attractor selection. *PloS one* 1:e49.

Kenyon, W.J., S.M. Thomas, E. Johnson, M.J. Pallen, and M.P. Spector. 2005. Shifts from glucose to certain secondary carbon-sources result in activation of the extracytoplasmic function sigma factor sigmaE in Salmonella enterica serovar Typhimurium. *Microbiology* 151:2373-2383.

Kiviet, D.J., P. Nghe, N. Walker, S. Boulineau, V. Sunderlikova, and S.J. Tans. 2014. Stochasticity of metabolism and growth at the single-cell level. *Nature* 514:376-379.

Klauser, T., J. Pohlner, and T.F. Meyer. 1993. The secretion pathway of IgA protease-type proteins in gram-negative bacteria. *BioEssays : news and reviews in molecular, cellular and developmental biology* 15:799-805.

Knowles, T.J., A. Scott-Tucker, M. Overduin, and I.R. Henderson. 2009. Membrane protein architects: the role of the BAM complex in outer membrane protein assembly. *Nature reviews. Microbiology* 7:206-214.

Kreibich, S., and W.D. Hardt. 2015. Experimental approaches to phenotypic diversity in infection. *Current opinion in microbiology* 27:25-36.

Kubori, T., Y. Matsushima, D. Nakamura, J. Uralil, M. Lara-Tejero, A. Sukhan, J.E. Galan, and S.I. Aizawa. 1998. Supramolecular structure of the Salmonella typhimurium type III protein secretion system. *Science* 280:602-605.

LaRock, D.L., A. Chaudhary, and S.I. Miller. 2015. Salmonellae interactions with host processes. *Nature reviews. Microbiology* 13:191-205.

Laughlin, R.C., L.A. Knodler, R. Barhoumi, H.R. Payne, J. Wu, G. Gomez, R. Pugh, S.D. Lawhon, A.J. Baumler, O. Steele-Mortimer, and L.G. Adams. 2014. Spatial segregation of virulence gene expression during acute enteric infection with Salmonella enterica serovar Typhimurium. *mBio* 5:e00946-00913.

Leblanc, S.K., C.W. Oates, and T.L. Raivio. 2011. Characterization of the induction and cellular role of the BaeSR two-component envelope stress response of Escherichia coli. *Journal of bacteriology* 193:3367-3375.

Lee, C.A., B.D. Jones, and S. Falkow. 1992. Identification of a Salmonella typhimurium invasion locus by selection for hyperinvasive mutants. *Proceedings of the National Academy of Sciences of the United States of America* 89:1847-1851.

Leo, J.C., I. Grin, and D. Linke. 2012. Type V secretion: mechanism(s) of autotransport through the bacterial outer membrane. *Philosophical transactions of the Royal Society of London. Series B, Biological sciences* 367:1088-1101.

Leo, J.C., P. Oberhettinger, M. Schütz, and D. Linke. 2015. The inverse autotransporter family: intimin, invasin and related proteins. *International journal of medical microbiology : IJMM* 305:276-282.

Leyton, D.L., A.E. Rossiter, and I.R. Henderson. 2012. From self sufficiency to dependence: mechanisms and factors important for autotransporter biogenesis. *Nature reviews. Microbiology* 10:213-225.

Li, X., B. Wang, L. Feng, H. Kang, Y. Qi, J. Wang, and Y. Shi. 2009. Cleavage of RseA by RseP requires a carboxyl-terminal hydrophobic amino acid following DegS cleavage. *Proceedings of the National Academy of Sciences of the United States of America* 106:14837-14842.

Liu, D., and P.R. Reeves. 1994. Escherichia coli K12 regains its O antigen. *Microbiology* 140 (Pt 1):49-57.

Lopez, C.A., S.E. Winter, F. Rivera-Chavez, M.N. Xavier, V. Poon, S.P. Nuccio, R.M. Tsolis, and A.J. Baumler. 2012. Phage-mediated acquisition of a type III secreted effector protein boosts growth of salmonella by nitrate respiration. *mBio* 3:

Lostroh, C.P., V. Bajaj, and C.A. Lee. 2000. The cis requirements for transcriptional activation by HilA, a virulence determinant encoded on SPI-1. *Molecular microbiology* 37:300-315.

Macnab, R.M. 2003. How bacteria assemble flagella. *Annual review of microbiology* 57:77-100.

Macnab, R.M., and D.E. Koshland, Jr. 1972. The gradient-sensing mechanism in bacterial chemotaxis. *Proceedings of the National Academy of Sciences of the United States of America* 69:2509-2512.

Maier, L., M. Barthel, B. Stecher, R.J. Maier, J.S. Gunn, and W.D. Hardt. 2014. Salmonella Typhimurium strain ATCC14028 requires H2-hydrogenases for growth in the gut, but not at systemic sites. *PloS one* 9:e110187.

Maier, L., R. Vyas, C.D. Cordova, H. Lindsay, T.S. Schmidt, S. Brugiroux, B. Periaswamy, R. Bauer, A. Sturm, F. Schreiber, C. von Mering, M.D. Robinson, B. Stecher, and W.D. Hardt. 2013. Microbiota-derived hydrogen fuels Salmonella typhimurium invasion of the gut ecosystem. *Cell host & microbe* 14:641-651.

Majdalani, N., M. Heck, V. Stout, and S. Gottesman. 2005. Role of RcsF in signaling to the Rcs phosphorelay pathway in Escherichia coli. *Journal of bacteriology* 187:6770-6778.

Marcus, S.L., J.H. Brumell, C.G. Pfeifer, and B.B. Finlay. 2000. Salmonella pathogenicity islands: big virulence in small packages. *Microbes and infection / Institut Pasteur* 2:145-156.

Martin, R.G., and J.L. Rosner. 2001. The AraC transcriptional activators. *Current opinion in microbiology* 4:132-137.

Martinez, L.C., H. Yakhnin, M.I. Camacho, D. Georgellis, P. Babitzke, J.L. Puente, and V.H. Bustamante. 2011. Integration of a complex regulatory cascade involving the SirA/BarA and Csr global regulatory systems that controls expression of the Salmonella SPI-1 and SPI-2 virulence regulons through HilD. *Molecular microbiology* 80:1637-1656.

McBroom, A.J., and M.J. Kuehn. 2007. Release of outer membrane vesicles by Gram-negative bacteria is a novel envelope stress response. *Molecular microbiology* 63:545-558.

McMeechan, A., M. Roberts, T.A. Cogan, F. Jorgensen, A. Stevenson, C. Lewis, G. Rowley, and T.J. Humphrey. 2007. Role of the alternative sigma factors sigmaE and sigmaS in survival of Salmonella enterica serovar Typhimurium during starvation, refrigeration and osmotic shock. *Microbiology* 153:263-269.

Mecsas, J., P.E. Rouviere, J.W. Erickson, T.J. Donohue, and C.A. Gross. 1993. The activity of sigma E, an Escherichia coli heat-inducible sigma-factor, is modulated by expression of outer membrane proteins. *Genes & development* 7:2618-2628.

Miller, S.I., A.M. Kukral, and J.J. Mekalanos. 1989. A two-component regulatory system (phoP phoQ) controls Salmonella typhimurium virulence. *Proceedings of the National Academy of Sciences of the United States of America* 86:5054-5058.

Mills, D.M., V. Bajaj, and C.A. Lee. 1995. A 40 kb chromosomal fragment encoding Salmonella typhimurium invasion genes is absent from the corresponding region of the Escherichia coli K-12 chromosome. *Molecular microbiology* 15:749-759.

Missiakas, D., M.P. Mayer, M. Lemaire, C. Georgopoulos, and S. Raina. 1997. Modulation of the Escherichia coli sigmaE (RpoE) heat-shock transcription-factor activity by the RseA, RseB and RseC proteins. *Molecular microbiology* 24:355-371.

Moest, T.P., and S. Meresse. 2013. Salmonella T3SSs: successful mission of the secret(ion) agents. *Current opinion in microbiology* 16:38-44.

Müller, Andreas J., P. Kaiser, Kurt E.J. Dittmar, Thomas C. Weber, S. Haueter, K. Endt, P. Songhet, C. Zellweger, M. Kremer, H.-J. Fehling, and W.-D. Hardt. 2012. Salmonella Gut Invasion Involves TTSS-2-Dependent Epithelial Traversal, Basolateral Exit, and Uptake by Epithelium-Sampling Lamina Propria Phagocytes. *Cell host & microbe* 11:19-32.

Murray, P.R., E.J. Baron, P.M. A., F.C. Tenover, and R.H. Yolken. 1999. Manual of clinical microbiology. ASM Press, Washington, DC.,

Navarre, W.W., S. Porwollik, Y. Wang, M. McClelland, H. Rosen, S.J. Libby, and F.C. Fang. 2006. Selective silencing of foreign DNA with low GC content by the H-NS protein in Salmonella. *Science* 313:236-238.

Novick, A., and M. Weiner. 1957. Enzyme Induction as an All-or-None Phenomenon. *Proceedings of the National Academy of Sciences of the United States of America* 43:553-566.

Ochman, H., F.C. Soncini, F. Solomon, and E.A. Groisman. 1996. Identification of a pathogenicity island required for Salmonella survival in host cells. *Proceedings of the National Academy of Sciences of the United States of America* 93:7800-7804.

Olekhnovich, I.N., and R.J. Kadner. 2002. DNA-Binding Activities of the HilC and HilD Virulence Regulatory Proteins of Salmonella enterica Serovar Typhimurium. *Journal of bacteriology* 184:4148-4160.

Olekhnovich, I.N., and R.J. Kadner. 2006. Crucial roles of both flanking sequences in silencing of the hilA promoter in Salmonella enterica. *Journal of molecular biology* 357:373-386.

Osterberg, S., T. del Peso-Santos, and V. Shingler. 2011. Regulation of alternative sigma factor use. *Annual review of microbiology* 65:37-55.

Ozbudak, E.M., M. Thattai, I. Kurtser, A.D. Grossman, and A. van Oudenaarden. 2002. Regulation of noise in the expression of a single gene. *Nature genetics* 31:69-73.

Pegues, D.A., M.J. Hantman, I. Behlau, and S.I. Miller. 1995. PhoP/PhoQ transcriptional repression of Salmonella typhimurium invasion genes: evidence for a role in protein secretion. *Molecular microbiology* 17:169-181.

Pohlner, J., R. Halter, K. Beyreuther, and T.F. Meyer. 1987. Gene structure and extracellular secretion of Neisseria gonorrhoeae IgA protease. *Nature* 325:458-462.

Prouty, A.M., and J.S. Gunn. 2000. Salmonella enterica serovar typhimurium invasion is repressed in the presence of bile. *Infect Immun* 68:6763-6769.

Public Health Agency of Canada. 2011. Salmonella enterica spp. Pathogen safety data sheet - infectiuos substances.

Raffatellu, M., M.D. George, Y. Akiyama, M.J. Hornsby, S.P. Nuccio, T.A. Paixao, B.P. Butler, H. Chu, R.L. Santos, T. Berger, T.W. Mak, R.M. Tsolis, C.L. Bevins, J.V. Solnick, S. Dandekar, and A.J. Baumler. 2009. Lipocalin-2 resistance confers an advantage to Salmonella enterica serotype Typhimurium for growth and survival in the inflamed intestine. *Cell host & microbe* 5:476-486.

Raj, A., and A. van Oudenaarden. 2008. Nature, nurture, or chance: stochastic gene expression and its consequences. *Cell* 135:216-226.

Ramos, H.C., M. Rumbo, and J.C. Sirard. 2004. Bacterial flagellins: mediators of pathogenicity and host immune responses in mucosa. *Trends in microbiology* 12:509-517.

Raser, J.M., and E.K. O'Shea. 2005. Noise in gene expression: origins, consequences, and control. *Science* 309:2010-2013.

Rescigno, M., M. Urbano, B. Valzasina, M. Francolini, G. Rotta, R. Bonasio, F. Granucci, J.P. Kraehenbuhl, and P. Ricciardi-Castagnoli. 2001. Dendritic cells express tight junction proteins and penetrate gut epithelial monolayers to sample bacteria. *Nature immunology* 2:361-367.

Romeo, T. 1998. Global regulation by the small RNA-binding protein CsrA and the non-coding RNA molecule CsrB. *Molecular microbiology* 29:1321-1330.

Rowley, G., M. Spector, J. Kormanec, and M. Roberts. 2006. Pushing the envelope: extracytoplasmic stress responses in bacterial pathogens. *Nature reviews. Microbiology* 4:383-394.

Ruiz, N., D. Kahne, and T.J. Silhavy. 2009. Transport of lipopolysaccharide across the cell envelope: the long road of discovery. *Nature reviews. Microbiology* 7:677-683.

Runkel, S., H.C. Wells, and G. Rowley. 2013. Living with Stress: A Lesson from the Enteric Pathogen Salmonella enterica. *Advances in applied microbiology* 83:87-144.

Saini, S., J.R. Ellermeier, J.M. Slauch, and C.V. Rao. 2010a. The role of coupled positive feedback in the expression of the SPI1 type three secretion system in Salmonella. *PLoS pathogens* 6:e1001025.

Saini, S., J.M. Slauch, P.D. Aldridge, and C.V. Rao. 2010b. Role of cross talk in regulating the dynamic expression of the flagellar Salmonella pathogenicity island 1 and type 1 fimbrial genes. *Journal of bacteriology* 192:5767-5777.

Salzman, N.H., D. Ghosh, K.M. Huttner, Y. Paterson, and C.L. Bevins. 2003. Protection against enteric salmonellosis in transgenic mice expressing a human intestinal defensin. *Nature* 422:522-526.

Sanchez-Vargas, F.M., M.A. Abu-El-Haija, and O.G. Gomez-Duarte. 2011. Salmonella infections: an update on epidemiology, management, and prevention. *Travel medicine and infectious disease* 9:263-277.

Santos, R.L., and A.J. Baumler. 2004. Cell tropism of Salmonella enterica. *International journal of medical microbiology : IJMM* 294:225-233.

Schechter, L.M., S.M. Damrauer, and C.A. Lee. 1999. Two AraC/XylS family members can independently counteract the effect of repressing sequences upstream of the hilA promoter. *Molecular microbiology* 32:629-642.

Schechter, L.M., S. Jain, S. Akbar, and C.A. Lee. 2003. The Small Nucleoid-Binding Proteins H-NS, HU, and Fis Affect hilA Expression in Salmonella enterica Serovar Typhimurium. *Infection and Immunity* 71:5432-5435.

Schechter, L.M., and C.A. Lee. 2001. AraC/XylS family members, HilC and HilD, directly bind and derepress the Salmonella typhimurium hilA promoter. *Molecular microbiology* 40:1289-1299.

Schmidt, M.A. 2010. LEEways: tales of EPEC, ATEC and EHEC. *Cellular microbiology* 12:1544-1552.

Shelobolina, E.S., S.A. Sullivan, K.R. O'Neill, K.P. Nevin, and D.R. Lovley. 2004. Isolation, Characterization, and U(VI)-Reducing Potential of a Facultatively Anaerobic, Acid-Resistant Bacterium from Low-pH, Nitrate- and U(VI)-Contaminated Subsurface Sediment and Description of Salmonella subterranea sp. nov. *Applied and environmental microbiology* 70:2959-2965.

Simeone, R., D. Bottai, and R. Brosch. 2009. ESX/type VII secretion systems and their role in host-pathogen interaction. *Current opinion in microbiology* 12:4-10.

Skovierova, H., G. Rowley, B. Rezuchova, D. Homerova, C. Lewis, M. Roberts, and J. Kormanec. 2006. Identification of the sigmaE regulon of Salmonella enterica serovar Typhimurium. *Microbiology* 152:1347-1359.

Smits, W.K., O.P. Kuipers, and J.W. Veening. 2006a. Phenotypic variation in bacteria: the role of feedback regulation. *Nature reviews. Microbiology* 4:259-271.

Smits, W.K., J.W. Veening, and O.P. Kuipers. 2006b. Phenotypic variation and bistable switching in bacteria. Springer Berlin Heidelberg,

Stecher, B., R. Robbiani, A.W. Walker, A.M. Westendorf, M. Barthel, M. Kremer, S. Chaffron, A.J. Macpherson, J. Buer, J. Parkhill, G. Dougan, C. von Mering, and W.D. Hardt. 2007. Salmonella enterica serovar typhimurium exploits inflammation to compete with the intestinal microbiota. *PLoS biology* 5:2177-2189.

Stender, S., A. Friebel, S. Linder, M. Rohde, S. Mirold, and W.D. Hardt. 2000. Identification of SopE2 from Salmonella typhimurium, a conserved guanine nucleotide exchange factor for Cdc42 of the host cell. *Molecular microbiology* 36:1206-1221.

Stewart, E.J., R. Madden, G. Paul, and F. Taddei. 2005. Aging and death in an organism that reproduces by morphologically symmetric division. *PLoS biology* 3:e45.

Stewart, P.S., and M.J. Franklin. 2008. Physiological heterogeneity in biofilms. *Nature reviews. Microbiology* 6:199-210.

Sturm, A., M. Heinemann, M. Arnoldini, A. Benecke, M. Ackermann, M. Benz, J. Dormann, and W.D. Hardt. 2011. The cost of virulence: retarded growth of Salmonella Typhimurium cells expressing type III secretion system 1. *PLoS pathogens* 7:e1002143.

Swain, P.S., M.B. Elowitz, and E.D. Siggia. 2002. Intrinsic and extrinsic contributions to stochasticity in gene expression. *Proceedings of the National Academy of Sciences of the United States of America* 99:12795-12800.

Takaya, A., T. Tomoyasu, A. Tokumitsu, M. Morioka, and T. Yamamoto. 2002. The ATP-Dependent Lon Protease of Salmonella enterica Serovar Typhimurium Regulates Invasion and Expression of Genes Carried on Salmonella Pathogenicity Island 1. *Journal of bacteriology* 184:224-232.

Takeuchi, A., and H. Sprinz. 1967. Electron-Microscope Studies of Experimental Salmonella Infection in the Preconditioned Guinea Pig: II. Response of the Intestinal Mucosa to the Invasion by Salmonella typhimurium. *The American journal of pathology* 51:137-161.

Temme, K., H. Salis, D. Tullman-Ercek, A. Levskaya, S.H. Hong, and C.A. Voigt. 2008. Induction and relaxation dynamics of the regulatory network controlling the type III secretion system encoded within Salmonella pathogenicity island 1. *Journal of molecular biology* 377:47-61.

Thanassi, D.G., C. Stathopoulos, A. Karkal, and H. Li. 2005. Protein secretion in the absence of ATP: the autotransporter, two-partner secretion and chaperone/usher pathways of gram-negative bacteria (review). *Molecular membrane biology* 22:63-72.

Thijs, I.M., S.C. De Keersmaecker, A. Fadda, K. Engelen, H. Zhao, M. McClelland, K. Marchal, and J. Vanderleyden. 2007. Delineation of the Salmonella enterica serovar Typhimurium HilA regulon through genome-wide location and transcript analysis. *Journal of bacteriology* 189:4587-4596.

Trent, M.S., C.M. Stead, A.X. Tran, and J.V. Hankins. 2006. Diversity of endotoxin and its impact on pathogenesis. *Journal of endotoxin research* 12:205-223.

Tsai, J.C., M.R. Yen, R. Castillo, D.L. Leyton, I.R. Henderson, and M.H. Saier, Jr. 2010. The bacterial intimins and invasins: a large and novel family of secreted proteins. *PloS one* 5:e14403.

Tucker, S.C., and J.E. Galan. 2000. Complex function for SicA, a Salmonella enterica serovar typhimurium type III secretion-associated chaperone. *Journal of bacteriology* 182:2262-2268.

Veening, J.W., W.K. Smits, and O.P. Kuipers. 2008. Bistability, epigenetics, and bet-hedging in bacteria. *Annual review of microbiology* 62:193-210.

Wallden, K., A. Rivera-Calzada, and G. Waksman. 2010. Type IV secretion systems: versatility and diversity in function. *Cellular microbiology* 12:1203-1212.

Wang, P., L. Robert, J. Pelletier, W.L. Dang, F. Taddei, A. Wright, and S. Jun. 2010. Robust growth of Escherichia coli. *Current biology : CB* 20:1099-1103.

Winter, S.E., P. Thiennimitr, M.G. Winter, B.P. Butler, D.L. Huseby, R.W. Crawford, J.M. Russell, C.L. Bevins, L.G. Adams, R.M. Tsolis, J.R. Roth, and A.J. Baumler. 2010. Gut inflammation provides a respiratory electron acceptor for Salmonella. *Nature* 467:426-429.

Yu, J., J. Xiao, X. Ren, K. Lao, and X.S. Xie. 2006. Probing gene expression in live cells, one protein molecule at a time. *Science* 311:1600-1603.

Zhou, D., M.S. Mooseker, and J.E. Galan. 1999. Role of the S. typhimurium actin-binding protein SipA in bacterial internalization. *Science* 283:2092-2095.

2 Chapter 2 - Epitope-tagged autotransporters as single cell reporters for gene expression by *Salmonella* Typhimurium

Ismeta Curkić[1], Monika Schütz[2], Médéric Diard[1], Dirk Linke[2], Wolf-Dietrich Hardt[1]

[1]Institute of Microbiology, Department of Biology, ETH Zurich, Zurich, Switzerland

[2]Institute of Microbiology and Hygiene, University of Tübingen, Tübingen, Germany

Author contributions: I performed all experiments and strain constructions for this chapter. The epitope-tagged autotransporter was received from Monika Schütz and Dirk Linke. One strain was constructed by Médéric Diard.

2.1 Abstract

Phenotypic diversity is an important trait of bacterial populations and enhances fitness of the existing genotype in a given environment. To characterize different subpopulations, several studies have analyzed differential gene expression using fluorescent reporters. These studies visualized either single or multiple genes within single cells using different fluorescent proteins. However, variable maturation and folding kinetics of different fluorophores complicate the study of dynamics of gene expression. Here, we present a proof-of-principle study for an alternative gene expression system in *Salmonella* Typhimurium (*S*. Tm) that harbors the potential to standardize the maturation kinetics. We employed the hemagglutinin- (HA) tagged autotransporter invasin ($invA_{HA}$) as gene expression reporter for the expression of the type three secretion system 1 (T1) in *S.* Tm. Using a two-reporter approach with GFP and the $InvA_{HA}$ in single cells, we demonstrate that this reporter system can be used for T1 gene expression analysis. When we placed the two reporters *gfp* and $invA_{HA}$ under the control of either one or two different promoters of the T1 regulon, we were able to show correlative expression of both reporters. We conclude that the $invA_{HA}$ reporter system is a suitable tool to analyze *t1* gene expression in *S*. Tm and propose its applicability as molecular tool for gene expression studies within single cells.

2.2 Introduction

Most bacteria in the environment live in communities (e.g. biofilms). A characteristic of these communities is the presence of microorganisms expressing different phenotypes and taking over different roles within these communities (Stewart and Franklin, 2008). However, different phenotypes have increasingly been recognized within bacterial cultures that harbor the same genotype and share the same microenvironment. This phenotypic diversity (heterogeneity) within isogenic bacteria has been recognized as common trait among bacterial species and has recently developed into an important research field (Cummings et al., 2006; Elowitz et al., 2002; Sturm et al., 2011; Suel et al., 2006). The functional importance of such phenotypic heterogeneity has remained poorly understood. Phenotypic diversity within isogenic bacterial populations is caused by stochastic (random) events during gene

expression, molecular segregation during cell division and/or metabolic activity. In a given system (e.g. a virulence regulatory system), this stochastic behavior, combined with a threshold requirement and a subsequent positive feedback reinforcement that results in a non-linear response can lead to the formation of two (or more) stable phenotypes (=bistable or multistable states (for detailed information on the causes of phenotypic diversity see (Kaern et al., 2005; Raj and van Oudenaarden, 2008; Smits et al., 2006a)). Phenotypic diversity is thought to have important implications, i.e. in situations of bet hedging and division of labor (Ackermann, 2013; Ackermann, 2015).

In traditional microbial research, bacterial cultures were assumed to be homogenous as they were derived from genetically identical cells. Therefore, outcomes from experiments were usually averaged and researchers completely neglected the influence of different subpopulations in the obtained results. Since the awareness about phenotypic diversity within isogenic bacterial cultures increased, microscopy and flow cytometric analysis in combination with fluorescently labeled molecules of interest, has improved the knowledge of single cell behavior (Choi et al., 2008; Golding et al., 2005; Maamar and Dubnau, 2005; Sturm et al., 2011; Yu et al., 2006).

For *Salmonella enterica* subspecies enterica serovar Typhimurium (*S*. Tm), both bet hedging and division of labor have been discussed in the context of the expression of the type three secretion system 1 (T1) virulence factor (Ackermann et al., 2008; Arnoldini et al., 2014). *S*. Tm is an enteropathogenic, Gram-negative pathogen that causes self-limiting gastroenteritis (Sanchez-Vargas et al., 2011). For successful infection, *S*. Tm requires the T1 apparatus, which is encoded on the *Salmonella* pathogenicity island 1 (SPI-1) at centisome 63 of the chromosome (Mills et al., 1995). T1 is a key virulence factor for invasion and is expressed in a bistable fashion. Thus, even under inducing conditions *in vitro* and in the host`s intestine only a minority of cells are expressing T1 ($T1^+$ cells) (Ackermann et al., 2008; Diard et al., 2013; Sturm et al., 2011). The regulation of T1 has been the subject of numerous studies and the key regulatory factors controlling its expression are well established (for detailed information see (Ellermeier and Slauch, 2007; Moest and Meresse, 2013)). However, the detailed mechanism that leads to bistable expression is still not completely understood. To gain mechanistic insights into the T1 regulation, single cell studies analyzing multiple genes simultaneously would be of interest. Previous studies have used fluorescent protein reporters for analyzing

gene expression of one or two genes of interest (Elowitz et al., 2002; Saini et al., 2010a; Suel et al., 2006). Mechanistic analysis would benefit from expanding the number of genes measured in the individual cell. Also, the different maturation and folding properties of different fluorophores have complicated the study of dynamics of gene expression. Thus, new reporter systems with uniform maturation kinetics and the potential to analyze more than two genes per cell would be of significant interest.

Autotransporters are classified as a family of virulence factors that employ a type V secretion system and are capable of transporting their own extracellular passenger domain through the outer membrane. The type V secretion system is comprised of five classes, type Va through to Ve. The Type Ve autotransporter subfamily is characterized by an inverted topology and was only recently described as own class (Leo et al., 2012; Leo et al., 2015; Oberhettinger et al., 2012). Oberhettinger and colleagues demonstrated the inverted topology of this family using epitope-tagged intimin and invasin (Oberhettinger et al., 2012). The adhesins intimin and invasin, found in enteropathogenic *E. coli* and *Yersinia* species (spp.), respectively, represent two members of the type Ve autotransporter subfamily (Frankel et al., 1998; Grassl et al., 2003).

Here, we performed a proof-of-concept study to assess if autotransporters may be used as reporters for gene expression in Gram-negative bacteria. In particular, we tested the hemagglutinin (HA)-tagged autotransporter invasin to assess gene expression by *S*. Tm. To establish this system, we chose a two-reporter approach using the fluorophore GFP and the epitope-tagged invasin. Both reporters were placed under the control of promoters present on SPI-1 and thus under the control of the T1 regulon. We demonstrate here that both reporters can be successfully used in one single cell. We show correlative expression of both reporters when driven under the control of one or two different promoters of the T1 regulon. This expands the molecular toolbox for future studies of gene expression within a single bacterial cell.

2.3 Results

Analysis of a plasmid-based *invA*$_{HA}$ expression construct

An HA-tagged invasin (*invA*$_{HA}$) reporter plasmid had previously been designed for topological studies of the type Ve autotransporters in *E. coli* (Oberhettinger et al., 2012). The *invA*$_{HA}$ fusion gene harbored a double HA tag linked by the amino acid triplet GSG (GSG-HA-GSG-HA-GSG) within loop 4 of the invasin`s β-barrel at the position A204. The double HA tag is referred to as HA tag throughout the paper and its location is illustrated in Figure 2.1A. The fusion gene was located on a pASK-IBA2 plasmid backbone and its expression was controlled by a tetracycline-regulated promoter. This promoter can be induced using anhydrotetracycline (ATc), a tetracycline derivative, which lacks antibiotic activity. To verify the expression of the HA epitope tag in *Salmonella* spp., we transformed the *invA*$_{HA}$-harboring plasmid into the SL1344 *S*. Tm derivative SB300 (Hoiseth and Stocker, 1981). Indeed, Western blots of bacterial lysates verified the expression of InvA$_{HA}$ in SB300. However, when we stained the intact bacteria with anti-HA antibodies, we did not detect any HA-specific signal (Figure 2.1C). As the HA tag was located at the extracellular loop of the invasin`s β-barrel, we reasoned that the absence of anti-HA antibody staining might be attributable to shielding by the lipopolysaccharide (LPS) layer that prevented antibody access to the HA epitope.

We therefore decided to test for HA staining using *S*. Tm SKI-12, an isogenic mutant that was lacking the O-antigen polysaccharide moiety of LPS. The expression of the O-antigen was ablated due to the deletion of *wbaP*, which encodes a phosphogalactosyltransferase, essential for the initiation of the O-antigen biosynthesis (Ilg et al., 2009). Indeed, SKI-12 pInvA$_{HA}$ expressed the InvA$_{HA}$ protein upon induction with ATc, as shown by surface staining of induced bacterial cells and Western blot (Figure 2.1B, C). In conclusion, these data suggested that the O-antigen layer of the SB300 strain prevented antibody staining of the β-barrel-positioned HA epitope of invasin. Therefore, we have chosen SKI-12 as the background strain for the following experiments.

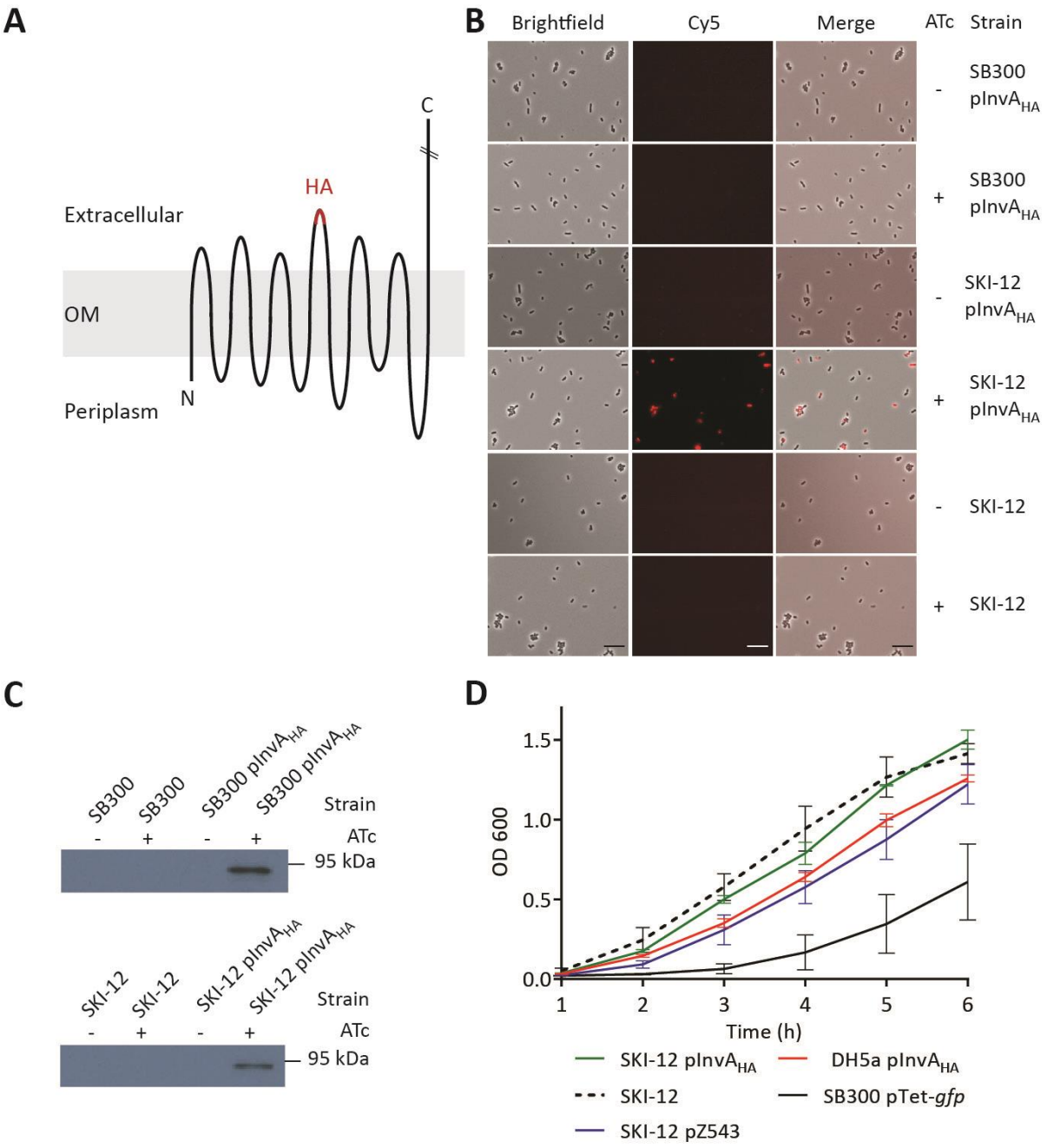

Figure 2.1. Scheme of HA epitope topology on invasin and characterization of plasmid based InvA$_{HA}$ expression. **A)** Schematic drawing of the HA epitope tag position within the β-barrel of invasin. Six extracellular loops extrude to the extracellular space, with loop 4 displaying the HA epitope tag. The C-terminal part of the passenger domain reaches out into extracellular space. Figure adapted from (Oberhettinger et al., 2012). **B)** Microscopic analysis of HA-specific staining in SB300 and SKI-12 (Δ*wbaP;* O-antigen-deficient strain, (Ilg et al., 2009)). The indicated strains harboring the pInvA$_{HA}$ plasmid were stained using the quick staining protocol described in the material and methods section. The scale bar represents 10 µm. **C)** Western blot analysis of HA protein levels upon induction of expression in SB300 and the O-antigen-deficient SKI-12. HA size ~94 kDa. **D)** Growth curves upon induction with 200 ng/ml ATc. pZ543 is the "empty" control vector and lacks *invA*$_{HA}$. pTet-*gfp* is a control plasmid expressing GFP from the tetracycline promoter. Mean and standard deviation are plotted. OM= outer membrane; +/- indicates presence or absence of 200 ng/ml ATc.

The expression of some proteins, including the expression of the T1 apparatus or even GFP can impose a significant burden upon the bacterial cell (Sturm et al., 2011; Wendland and Bumann, 2002). This can affect bacterial physiology as indicated by reduced growth rates or reduced colonization. To investigate whether the expression of the *invA*$_{HA}$ reporter had an influence on the growth of the bacterial cells, we performed a growth experiment and measured the growth of the cells upon induction of InvA$_{HA}$ expression. As shown in Figure 2.1D, the induction of InvA$_{HA}$ in the SKI-12 background did not significantly affect growth. *E. coli* DH5α and SKI-12 harboring an empty control vector served as additional controls. In contrast, a tetracycline-inducible *gfp*-expressing plasmid, which was known to inflict a burden to *S*. Tm, showed a much lower growth rate.

Comparison of InvA$_{HA}$ induction at the single cell level by tetracycline- and arabinose-inducible plasmids

In Figure 2.1B, we observed that induced cultures still harbored some cells not expressing InvA$_{HA}$ on their surface. It remained unclear if this was attributable to the expression construct. We therefore sought to compare the induction efficiency of the tetracycline-inducible promoter system with a construct driving *invA*$_{HA}$ expression from an arabinose-inducible pBAD promoter. For this purpose, the *invA*$_{HA}$ cassette was cloned into the pBAD24 backbone. The induction efficiency of both induction systems was analyzed using a concentration series of the appropriate inducers (Figure 2.2).

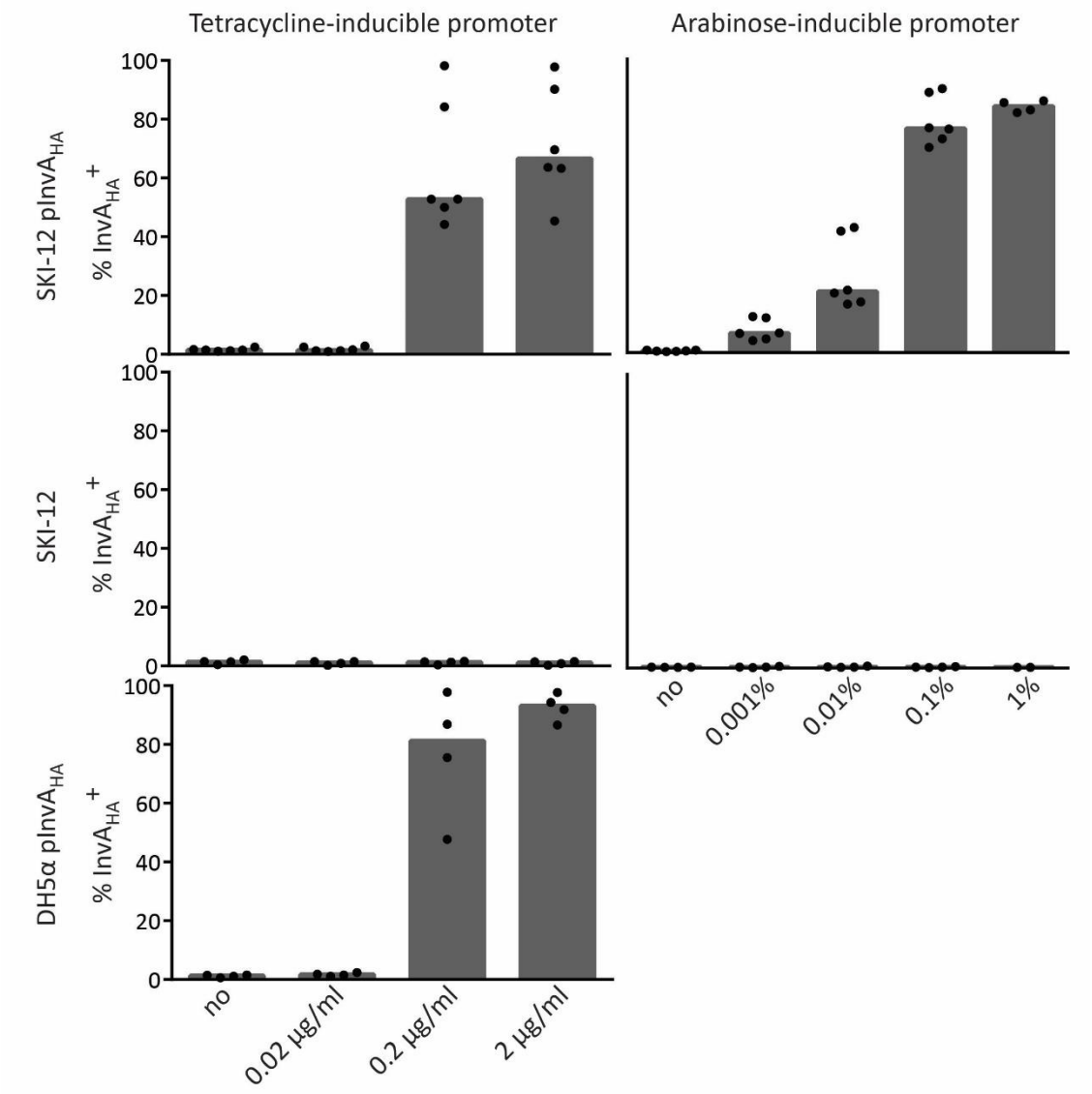

Figure 2.2. Comparison of induction efficiency of tetracycline- and arabinose-inducible plasmids.
The indicated strains were cultured for 4h and living cells were stained using a HA-specific antibody, before they were analyzed by flow cytometry. Induction of $InvA_{HA}$ expression was performed either by ATc or by arabinose in the indicated concentrations. DH5α p$InvA_{HA}$ was used as positive control for $InvA_{HA}$ induction. Four to six measurements were performed in two independent experiments.

The ATc-induced plasmid system exhibited a median of ~50-70% $InvA_{HA}$ expressing SKI-12 cells. The arabinose-inducible system displayed a median of ~80% $InvA_{HA}$ positive cells, suggesting a slightly better induction frequency. Furthermore, in both *S*. Tm SKI-12 and *E. coli* DH5α background, the ATc induction was more variable between the different experiments than the arabinose-inducible system, suggesting that the reduced staining is due to the variable induction of the tetracycline promoter. Figure 2.2 indicates that the arabinose-inducible plasmid system has a higher induction efficiency than the ATc-inducible plasmid. However, these data should be further confirmed by microscopic analysis.

Deletion of *wbaP* has a slight effect on T1 expression

In order to probe the suitability of *invA*$_{HA}$ as a transcriptional reporter, we wanted to compare it to the well-established *gfp* reporter. In particular, we wanted to assess SPI-1 expression. In the past, the expression of the T1 was mostly analyzed in the *S*. Tm background with O-antigen-proficient LPS (smooth LPS, SB300) (Diard et al., 2013; Sturm et al., 2011). In order to use the T1-*gfp* reporter in an O-antigen-deficient *wbaP* background, we first had to establish SPI-1 expression and monitor T1-*gfp* in this strain. To this end, we used the plasmid-based T1 reporter, expressing *gfp* under the promoter control of the SPI-1-encoded chaperone SicA (Sturm et al., 2011). The *sicA* promoter controls the expression of the operon, encoding *sicAsipBCDA* (Ellermeier and Slauch, 2007). Flow cytometric analysis revealed that T1 expression was reduced (from ~55% to ~45%) in the absence of the O-antigen polysaccharide Figure 2.3). Nevertheless, T1 is expressed at appreciable levels. Therefore, the Δ*wbaP* strain could be used for our proof-of-concept work to test if autotransporters can be used in principle as transcriptional gene expression reporters. The use of the Δ*wbaP* strain of InvA$_{HA}$ was of advantage, as the HA epitope could be stained in the O-antigen-deficient strain, in contrast to the SB300 strain harboring a smooth LPS layer Figure 2.1B).

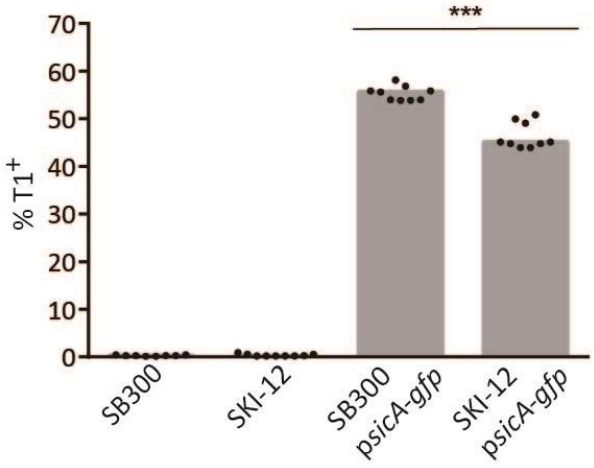

Figure 2.3. Effect of *wbaP* deletion on T1 expression.
SB300 or SKI-12 (Δ*wbaP*) were analyzed for T1 expression using the T1 reporter plasmid p*sicA-gfp* (pM972, (Sturm et al., 2011). T1 expression was assessed by flow cytometric analysis. The data were derived from three independent experiments. Statistical significance was assessed using the Mann-Whitney test.

Chromosomal *invA*$_{HA}$ as reporter for the expression of the SPI-1 promoters P*prgH* and P*sicA*

To assess the suitability of the autotransporter approach, we generated strains carrying the *invA*$_{HA}$ reporter in the chromosome. For this purpose, we focused on T1. First, we intended to verify that the T1 expression displayed by the *invA*$_{HA}$ reporter is comparable to the *gfp*-based T1 reporter system used in previous studies (Arnoldini et al., 2014; Diard et al., 2013; Hautefort et al., 2003; Sturm et al., 2011). We therefore used the previously published *prgH* promoter-driven *gfp* (P*prgH-gfp*) reporter strain JH3010 used by the Hinton laboratory to visualize T1 expression (Hautefort et al., 2003). PrgH is a structural protein of the T1 needle and is encoded on one of the three large operons of SPI-1. To allow future single cell analysis of these strains in a microfluidic setup (described in Chapter 3), we constructed all strains in a non-motile phenotype (Curtiss and Kang, 2004). By P22 transduction we introduced the P*prgH-gfp* allele of the JH3010 strain into the flagella-mutated background strain (χ8602), before we introduced the *invA*$_{HA}$ reporter downstream of the SPI-1 encoded effector *sipA* (Zhou et al., 1999). SipA is the last gene of the *sicAsipBCDA* operon and expressed under the control of the *sicA* promoter. Hence, both reporters, P*prgH*-driven *gfp* and P*sicA*-driven *invA*$_{HA}$, were under the control of the T1 regulon and should be expressed by the same cells. Finally, to allow HA-specific staining, we introduced *wbaP* deletions into all strains used for the following experiments (see Supplementary Table S2.1).

In this way, we obtained a non-motile strain in an O-antigen-deficient background (*wbaP* deletion), harboring P*prgH*-driven *gfp* and P*sicA*-driven *invA*$_{HA}$ expression (Z536, Figure 2.4A). Furthermore, we constructed two control strains (Z537 and Z555, respectively; Figure 2.4A), harboring either the P*sicA*-driven *invA*$_{HA}$ or the P*prgH*-driven *gfp* reporter. These latter strains should allow us to control for potential effects caused by the expression of two reporters within the same cell. The cells were grown in LB medium and life bacteria were stained for the HA epitope tag. The GFP levels could be measured without any additional staining. Analysis of the stained cells was done by microscopy and by flow cytometry. Microscopic analysis of Z536 verified that the *gfp* and *invA*$_{HA}$ reporters are indeed co-expressed ($r=0.651$, $p<0.0001$). As expected, the control strains Z537 and Z555 displayed either the InvA$_{HA}$ or the GFP-specific signal, respectively (Figure 2.4B). Quantification of the GFP signal revealed that the expression of both reporters within the same cell (i.e. in Z536) was virtually equivalent to that observed

in the strains expressing just one reporter at a time (i.e. Z537 and Z555). Only the P*prgH-gfp* reporter showed a slight reduction in strain Z536 (Figure 2.4C).

To obtain further evidence, we also performed FACS analysis of the same samples that had been used for microscopy. Again, we observed strong co-expression of P*prgH-gfp* and of P*sicA-invA*$_{HA}$ and a slight reduction of P*prgH-gfp* expression in Z536 (compare to Z555, Figure 2.4D). This indicated that the *invA*$_{HA}$ reporter is indeed suitable for monitoring T1 expression.

Next, we analyzed whether the integration of the different reporters resulted in negative effects on the growth of cells at the population level. We did not observe any adverse effects on growth of the new reporter strains (Figure 2.4E). However, as only a subpopulation of cells expresses T1 (Sturm et al., 2011), the absence of a growth phenotype in this bulk analysis does not reflect the single cell situation of cells harboring the newly introduced reporters. Single cell analysis e.g. by using agar pads (Sturm et al., 2011) or by using microfluidics (Wang et al., 2010) may help to further back this up.

In conclusion, these experiments showed that *invA*$_{HA}$ reporters are suitable for monitoring gene expression and suggested that this construct can be combined with established *gfp* reporters to monitor two different promoters in the same bacterial cell.

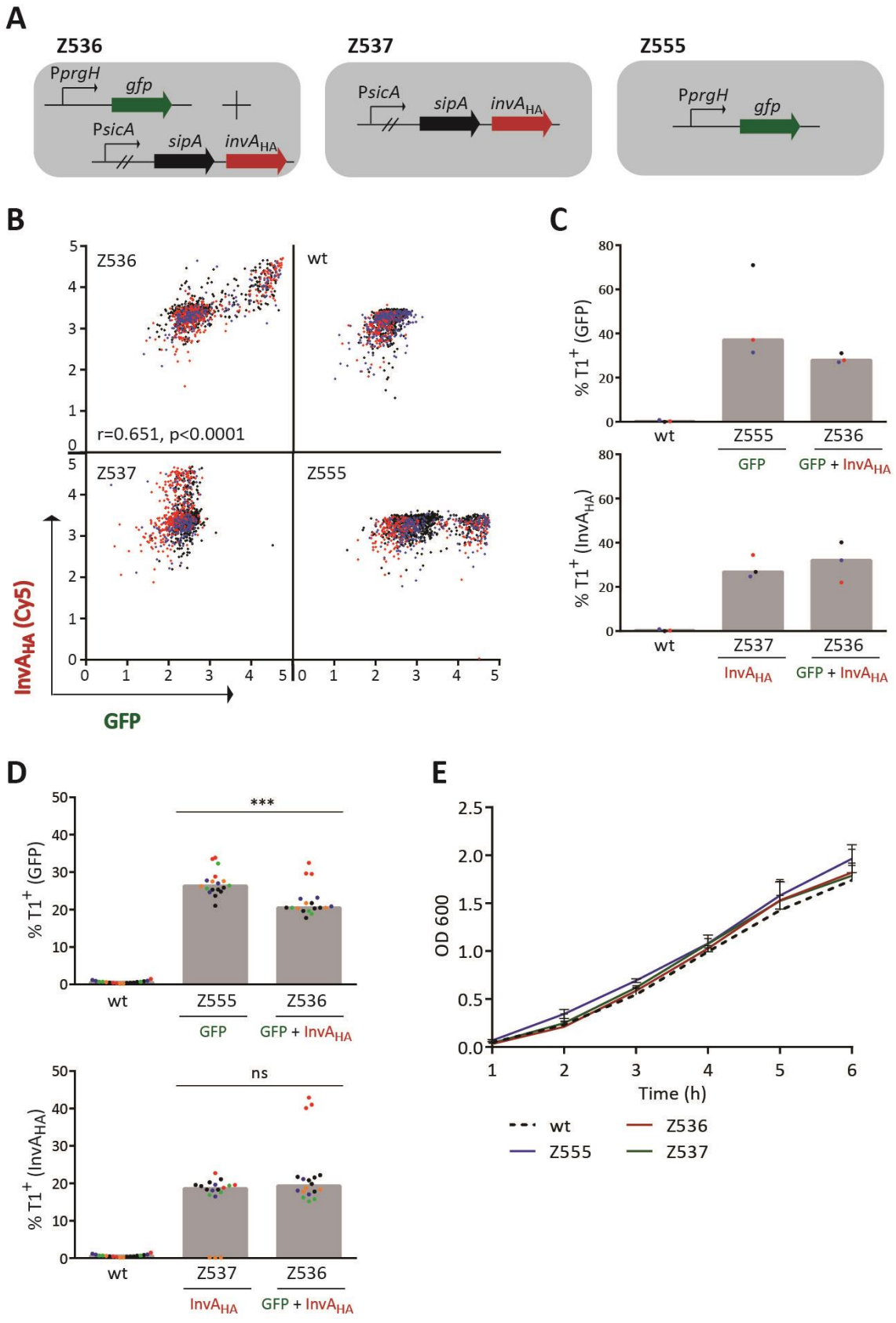

Figure 2.4. Scheme of chromosomal constructs of Z536, Z537 and Z555, expressing the *gfp* and *invA*$_{HA}$ reporters under the control of two SPI-1 encoded promoters and analysis of the constructs.

A) Schematic drawing of the chromosomal transcriptional fusions in the indicated strains. The reporters were under the control of either the *prgH* promoter (P*prgH*; Z555) or the *sicA* promoter (P*sicA*; Z537) or both (Z536).

The cells were stained as described in the material methods section. We used cells from the same preparation for either microscopic **(B, C)** or flow cytometric **(D)** analysis. Triplicates were measured by flow cytometry **(D),** whereas these samples were combined for microscopic analysis **(B, C). B)** Analysis of *gfp* and *invA*$_{HA}$ expression by the indicated strains, as measured by microscopy. The *invA*$_{HA}$ staining was measured by the Cy5 exciting laser for microscopy. The three colors indicate the different independent experiments. Correlation was analyzed by Spearman correlation analysis (see material and methods for detailed information). Fluorescence values of GFP and InvA$_{HA}$ are indicated in arbitrary units (AU). **C)** Quantitative analysis of the data set from B. The upper and lower graphs display the percentages of cells displaying GFP or Cy5 (for InvA$_{HA}$) fluorescence, respectively. The thresholds for GFP and Cy5 (for InvA$_{HA}$) fluorescence were set by the maximum values in the GFP or Cy5 channel of the wt strain, respectively. Z555 and Z537 are the controls, harboring only the *gfp* or the *invA*$_{HA}$ reporter, respectively. Z536 harbors both reporters, *gfp* and *invA*$_{HA}$. Median is plotted. **D)** Flow cytometric analysis of the same cells as in B). The upper and lower graph display the percentages of T1^{+} cells, measured by the GFP and Alexa Fluor 647 (for InvA$_{HA}$) excitations. Statistical significance was assessed using the Mann-Whitney test. **E)** Growth analysis of the chromosomally tagged strains. Mean and standard deviation of three independent experiments are shown. "wt" = wild type SKI-12. ns = not significant; *** p<0.0002.

Expression of the *gfp* and *invA*$_{HA}$ reporters under the control of the same promoter

So far, we have demonstrated that the use of the P*sicA*-driven *invA*$_{HA}$ reporter can monitor T1 expression. However, the correlation with the P*prgH-gfp* reporter was below 100%. It had remained unclear if slight levels of divergence might arise from the different folding/maturation kinetics of the two reporters, the noisiness in promoter expression or to other so far unidentified effects. In a first attempt to address this, we wanted to test whether the combination of both reporters under the control of the same promoter will result in a similar pattern of correlation. For this purpose, we generated a transcriptional fusion of both constructs downstream of *sipA*, thus placing both constructs under the control of the *sicA* promoter (Figure 2.5A). To control for any artefacts caused by the order of reporters, we generated strains with either sequence order of the two reporters *gfp* and *invA*$_{HA}$. This yielded the two strains harboring either *sipA-invA*$_{HA}$*-gfp* (Z567) or *sipA-gfp-invA*$_{HA}$ (Z574). Microscopic analysis revealed that both reporters are expressed and that their expression was correlated (Z567: r=0.630, p<0.0001; Z574 r=0.654, p<0.0001). This correlation was similar to that observed in Z536 (r=0.518, p<0.0001) (Figure 2.5B). The two control strains Z537 and Z555 displayed exclusive InvA$_{HA}$ and GFP expression, respectively. However, a few cells displayed false positive signals. This was most likely caused by contamination during the handling procedures of the staining protocol. It should be noted that the percentage of T1^{+} cells was much higher in the case of Z555 (P*prgH-gfp*) than in Z567 and Z574, which expressed *gfp* under the control of the P*sicA* promoter. This indicates that the P*sicA* promoter is much weaker than the P*prgH* promoter is. However, additional factors (e.g. attenuated growth of the expressing fraction) might also be involved, as indicated by the intermediate *gfp* expression level of Z536

(Figure 2.5C). Similar observations were made using the $InvA_{HA}$ reporter. However, here all four constructs were expressed under the control of the P*sicA* promoter. Thus, it is not surprising that the differences in the expression levels were much less pronounced than in the case of the *gfp* reporter. The GFP and $InvA_{HA}$ protein presence was further confirmed by Western Blot (Figure 2.5D).

In conclusion, we observed similar correlation patterns in all strains harboring the two-promoter constructs. Our data confirmed that $InvA_{HA}$ can be used as reporter system to visualize gene expression and that this system can be used in combination with the *gfp* reporters.

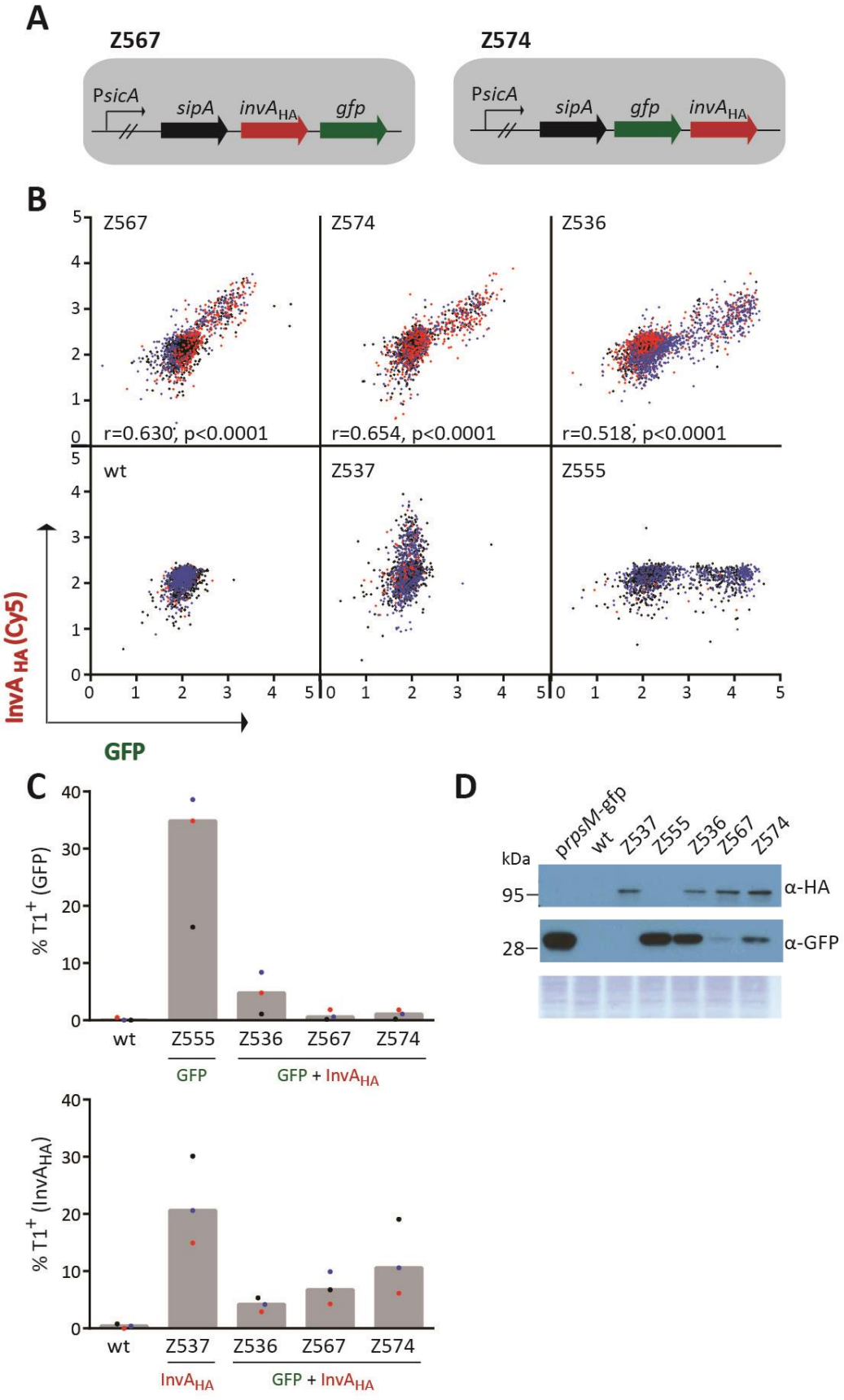
A
Z567
PsicA
sipA
invA HA
gfp
Z574
PsicA
sipA
gfp
invA HA
B
Z567
Z574
Z536
r=0.630; p<0.0001
r=0.654, p<0.0001
r=0.518; p<0.0001
wt
Z537
Z555
InvA HA (Cy5)
GFP
C
% T1+ (GFP)
wt
Z555
Z536
Z567
Z574
GFP
GFP + InvAHA
% T1+ (InvAHA)
wt
Z537
Z536
Z567
Z574
InvAHA
GFP + InvAHA
D
prpsM-gfp
wt
Z537
Z555
Z536
Z567
Z574
kDa
95
28
α-HA
α-GFP

Figure 2.5. Expression of the two reporters *gfp* and *invA*$_{HA}$ under the control of the same P*sicA* promoter.
A) Scheme of the transcriptional fusions of the *gfp* and *invA*$_{HA}$ reporters, which were inserted downstream of *sipA*. **B)** Microscopic analysis of GFP and InvA$_{HA}$ fluorescence levels (measured by the Cy5 exciting laser for microscopy) of the indicated strains. The three colors indicate the data from different experiments. The correlation was analyzed by Spearman correlation analysis. GFP and InvA$_{HA}$ fluorescence intensities are indicated in arbitrary units (AU). **C)** Quantitative analysis of the data set from B. The upper and lower graph display the percentages of cells expressing GFP or Cy5 (for InvA$_{HA}$) fluorescence, respectively. The thresholds for GFP and Cy5 (for InvA$_{HA}$) fluorescence were set using the maximum values in the GFP or Cy5 channel of the wt untagged strain, respectively. Z555 and Z537 were used as controls, harboring only the *gfp* or the *invA*$_{HA}$ reporter, respectively. Z536 harbors both reporters (*gfp* or the *invA*$_{HA}$) under the control of two different SPI-1 promoters. Z567 and Z574 harbor both reporters under *sicA* promoter control. **D)** Western blot analysis of GFP and HA protein levels in the indicated strains. p*rpsM-gfp* (pM965, (Stecher et al., 2004)) served as a positive control for GFP expression. GFP size= ~27 kDa, HA size ~94 kDa. The Coomassie stained membrane serves as loading control. "wt" = SKI-12.

2.4 Discussion

Here, we established a novel system for the analysis of *S*. Tm gene expression at the single cell level. This strategy employs the epitope-tagged autotransporter invasin (InvA$_{HA}$). Most previous reports studying the expression of individual promoters of interest within single cells have used fluorophores as reporter system (Elowitz et al., 2002; Hautefort et al., 2003; Saini et al., 2010a; Temme et al., 2008). Using strains expressing *gfp* and *invA*$_{HA}$ reporters from the same promoter (P*sicA*, Figure 2.5) or from two SPI-1 promoters (P*prgH* and P*sicA*, Figure 2.4), which were thought to be co-regulated, we could verify the suitability of this approach.

In theory, autotransporters like InvA should therefore provide distinct advantages when compared to *gfp*-based reporters. This is particularly relevant for cases when more than one promoter has to be analyzed per cell. First, it might offer a strategy to circumvent problems associated with the different folding/maturation half-lives observed with different fluorescent protein variants. Current approaches using different fluorophores for expression analysis within a single cell (Elowitz et al., 2002) impair accuracy due to different folding or maturation times. Using a set of InvA$_{HA}$ variants with equivalent maturation dynamics may allow such multi-gene expression analysis if one inserts multiple *invA* genes, harboring different epitope tags, e.g. *invA*$_{HA}$ for P*prgH* and *invA*$_{Strep}$ for P*sicA* expression analysis. Thus, it will be an important task for future work to establish the folding/maturation kinetics of the InvA$_{HA}$ reporter and verify that the kinetics are not affected by exchanging the HA epitope for other epitope members.

Our current InvA$_{HA}$ reporter system is limited to the expression analysis in O-antigen-deficient *S*. Tm strains, as the full-length LPS layer prevents antibody binding of the HA epitope (Figure 2.1B). This is a result of its close proximity to the outer membrane, as the HA epitope is located within an extracellular loop of the β-barrel. For many applications, the O-antigen-deficient background is not optimal, including our studies of T1 expression in wt *S*. Tm (Figure 2.3).

In previous reports analyzing the role of the O-antigen in *S*. Tm, an increased susceptibility to complement and antimicrobial peptides as well as a reduced colonization of mice was demonstrated in strains lacking the O-antigen (Ilg et al., 2009; Kong et al., 2011). Thus, the O-antigen-deficient background is not very well suited for *in vivo* studies. In order to circumvent this problem, one could choose another position for introducing the epitope into *invA*. Repositioning of the epitope tag to the outmost C-terminal part of the passenger domain, as described by Oberhettinger and colleagues recently for the autotransporter intimin (Oberhettinger et al., 2015), should be sufficient to locate the epitope sufficiently far out to allow antibody binding in the face of the O-antigen-proficient *S*. Tm strain SB300. This should alleviate the technical problems arising from the use of the O-antigen-deficient strain.

S. Tm is exquisitely sensitive to the expression of T1. The reduced growth rate of T1$^+$ *S*. Tm cells is attributable (at least in part) to the metabolic costs associated with the expression of the T1 apparatus and the large pools of the pre-formed effector proteins (Ackermann et al., 2008; Diard et al., 2013; Sturm et al., 2011). It is known that the co-expression of T1 with a *gfp* reporter further enhances theses costs. Thus, monitoring T1 expression represents a highly sensitive system to probe the "burden" imposed by any reporter construct. Indeed, when analyzing T1 expression using the P*sicA*-*invA*$_{HA}$ reporter (Z537, Z536, Z567, Z574), we observed some evidence for a burden (Figure 2.5C). The strains displaying both reporters, *gfp* and *invA*$_{HA}$ (Z536, Z567 and Z574), showed a reduction in InvA$_{HA}$ expression compared to the equivalent strain harboring only the *invA*$_{HA}$ reporter (Z537). However, this burden is equivalent to that imposed by the *gfp* reporter tested. Here, we also observed a reduction of the T1$^+$ subpopulation when two reporters were present (Z536, Z567 and Z574), in contrast to the strains with one reporter (Z555) (Figure 2.5C). Furthermore, we observed an additional reduction of the T1$^+$ subpopulation in those strains that indicated T1 expression by both reporters (Z536, Z567 and Z574) when visualized by GFP. However, as the *gfp* reporter in Z536 is driven by P*prgH*, in contrast to Z567 and Z574 that express *gfp* under the control of P*sicA*,

this reduction is probably caused by different promoter strengths of P*prgH* and P*sicA*. Altogether, this suggests that $InvA_{HA}$ reporters should be quite well suited to replace *gfp* reporters for applications like the parallel analysis of several reporters of bacterial cells featuring a particular expression pattern, e.g. by MACS sorting.

In *S*. Tm, phenotypic diversity in the expression of the T1 virulence factor is well known (Ackermann et al., 2008; Diard et al., 2013; Hautefort et al., 2003; Saini et al., 2010a; Sturm et al., 2011; Temme et al., 2008) and the core regulation factors controlling and fine tuning this system are established (for excellent reviews see (Ellermeier and Slauch, 2007; Moest and Meresse, 2013). However, the exact mechanism behind the bistable behavior of the T1 system remains unknown. Analyzing the dynamics of the multiple transcription factors controlling the T1 regulatory cascade (e.g. HilD, HilC, HilA) within single cells would allow a deeper analysis of the fundamental organization of the complex regulatory cascade. An InvA system combining multiple *invA* genes with different epitope tags located at the outmost C-terminal region may provide a pioneering system for accurate assessment of T1 regulatory circuits (Figure 2.6). This would give further insights into the mechanisms behind the phenotypic diversity of the *S*. Tm T1 expression.

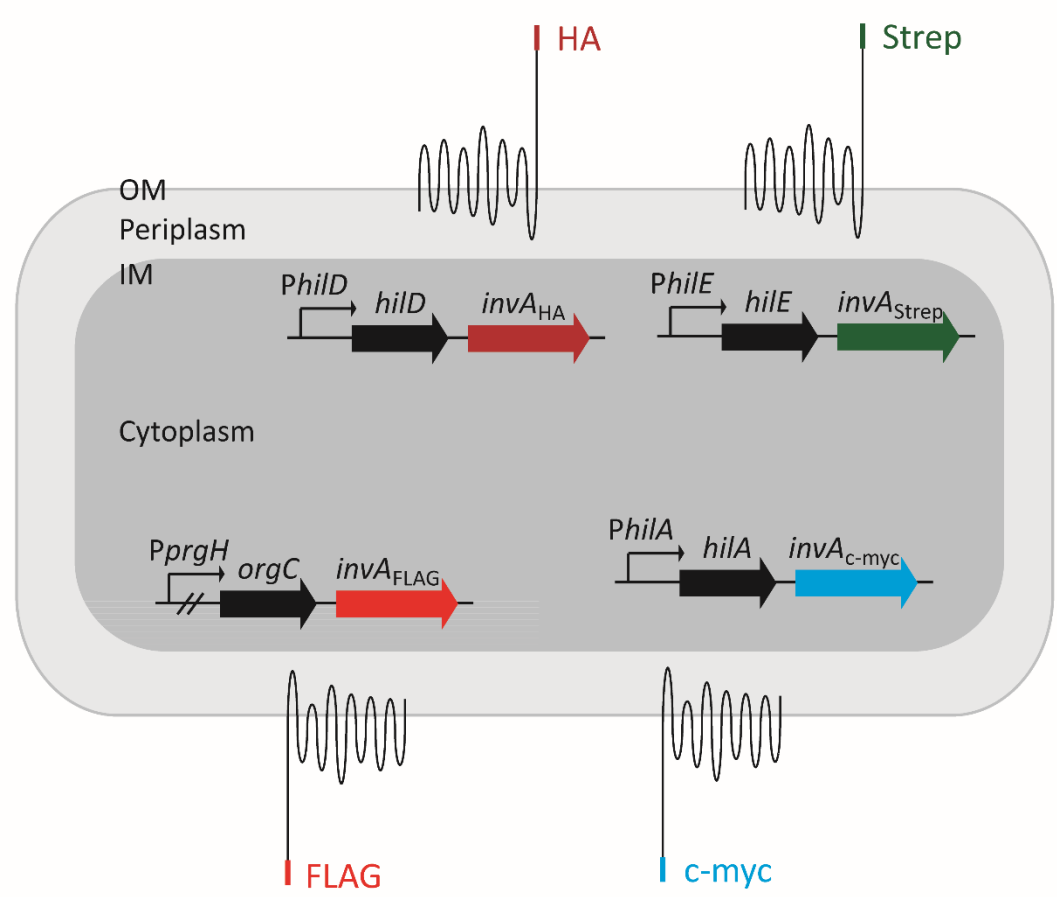

Figure 2.6. Potential extension to a multidimensional *invA*-based reporter system.
Scheme of an *invA*-based reporter system employing four differentially tagged invasin autotransporters carrying epitopes inserted into the C-terminal region of the extracellular passenger domain. Surface staining for the epitope tags HA, Strep, c-myc, FLAG epitopes would thereby allow monitoring the intracellular expression of *hilD, hilC, hilA* and *prgH* by individual *S*. Tm cells (epitope tags and the corresponding genes are indicated by the same color). OM= outer membrane, IM = inner membrane

2.5 Materials and Methods

Plasmid constructions

A list with all plasmids in provided in Supplementary Table S2.1. The suicide plasmid pZ503 harboring $invA_{HA204}$ downstream of a truncated *sipA* (**sipA*; nucleotide 1156-2058 of the open reading frame (orf)) was constructed as follows. The **sipA* fragment and $invA_{HA204}$ fragments were amplified by PCR from pM1300 and pInvA, respectively, using the primer combinations #52/#53 and #54/#55, respectively. Both fragments were fused by a subsequent amplification step using primers with overlapping restriction sites for *BamH*I (primer #52) and *Not*I (primer #55) and digestion by the restriction endonucleases *BamH*I and *Not*I. The **sipA-invA*$_{HA204}$

carrying fragment was ligated into pSB377, which was previously cleaved by the same restriction enzymes, resulting in pZ503.

The suicide plasmid pZ526, carrying the *sipA*-*invA*$_{HA204}$-*gfp* insert, was constructed by cleaving the *gfp* fragment from pM972 using *Not*I and *Sac*II and its ligation into the previously *Not*I- and *Sac*II- digested plasmid pZ503. The suicide plasmid pZ522, harboring the *sipA*-*gfp*-*invA*$_{HA204}$ insert, was constructed in three steps, following a modified protocol from An and colleagues (An et al., 2010). First, the three fragments **sipA*, *gfp* and *invA*$_{HA204}$ were amplified using primers with specific overhanging restriction sites to allow directed ligation of all fragments. The amplification of **sipA* was done using the primers #124/#125 (overlapping restriction sites *Spe*I and *Afl*II, respectively). The *gfp* fragment was created by amplification with the primers #126/#127 (overlapping restriction sites *Afl*II and *Sal*I, respectively). Finally, *invA*$_{HA204}$ was produced using the primers #128/#129 (overlapping restriction sites *Sal*I and *Sac*II, respectively). The **sipA* and *gfp* fragments were each transferred into the pGEM-T easy cloning vector, resulting in pZ523 and pZ524, respectively. In the second step, the **sipA* and *gfp* fragments were combined. The **sipA* fragment was cut out from pZ523 using the restriction enzymes *Spe*I, *Afl*II. The *gfp* fragment was cut out from pZ524 using *Afl*II and *Sal*I. Both fragments were combined by ligation and subsequent PCR amplification using the primers #124/#127 (*Spe*I and *Sal*I overhangs). The resulting **sipA*-*gfp* containing PCR fragment was introduced into the pGEM-T easy vector (Promega), creating pZ527. In the third step, the **sipA*-*invA*$_{HA204}$ fragment was retrieved from pZ527 by *Spe*I and *Sal*I and ligated with the previously amplified and *Sal*I- and *Sac*II- digested *invA*$_{HA204}$ fragment. After the following PCR amplification step using the primers #124/#129 (harboring *Spe*I and *Sac*II overhangs, respectively), the **sipA*-*gfp*-*invA*$_{HA204}$ fragment was digested with *Spe*I and *Sac*II and ligated into the pSB377 vector, cut with the same restriction endonucleases. The final ligation step resulted in pZ522. All plasmids were verified by sequencing.

Bacterial strains

All strains used in this study were derived from *Salmonella* Typhimurium SL1344 (Hoiseth and Stocker, 1981). The Supplementary Table S2.2 and Supplementary Table S2.3 list all bacterial strains and primer sequences.

The suicide plasmid pZ503 was introduced into M3142 and the unflagellated non-motile strain χ8602 (Curtiss and Kang, 2004) by conjugation, thereby creating Z531 and Z532, respectively. In the strains Z531, Z532 and M3142, the *wbaP* gene was deleted as previously described (Datsenko and Wanner, 2000). In short, the primers #62 and #63, harboring the λ recombinase recognition sites and sequences adjacent to the *wbaP* gene, were used to amplify the kanamycin resistance cassette from pKD4. The PCR product was electroporated into Z531, Z532 and M3142, each harboring pKD46 to create an in-frame deletion of *wbaP* directly in the desired strains. The pKD46 plasmid was directly transformed into the strains of interest to avoid the need for an additional P22 phage transduction step (note: P22 phage binds to the O-antigen, which is deleted in these strains). Thereby, the final strains Z536, Z537 and Z555, respectively, were constructed. The presence of the insert was verified by PCR using the primers #68/#70. The primer combinations #64/#65 and #64/#66, respectively, were used to confirm the *wbaP* deletion.

The suicide plasmids pZ526 and pZ522, carrying the *sipA-invA*$_{HA204}$*-gfp* insert and *sipA-gfp-invA*$_{HA204}$ inserts, respectively, were each individually integrated into the chromosome of SB300. This created the strains Z562 and Z569, respectively. Subsequently, P22 phage transduction was performed to introduce the inserts of pZ526 and pZ522 individually into the χ8602 background, resulting in Z565 and Z572, respectively. To obtain Z567 and Z574, the *wbaP* gene was replaced by a chloramphenicol resistance gene cassette by amplification of the resistance cassette from pKD3, as described before. The integration of the two inserts was verified by PCR using the primers #68/#70. For confirming the *wbaP* exchange by the chloramphenicol cassette, the primer combination #64 and #65 was used.

Culturing of bacterial strains

Overnight cultures were diluted 1:20 in fresh LB broth (0.1 M NaCl) and grown for 4h at 37°C, before aliquots for Western blot analysis were taken and subsequent staining was performed. For the growth-curve experiments, overnight cultures were diluted 1:100 and the optical density (OD_{600}) was measured at the indicated time points. In all induction experiments, we either used anhydrotetracycline (ATc, Chemie Brunschwig AG) or L-arabinose at the stated concentrations. Except otherwise stated, the induction was done immediately after dilution of the overnight culture.

Immunofluorescence measurements

Subcultures were grown for 4h as described before. 10µl of the subculture containing approximately $1x10^7$ cells, were transferred onto V-shaped 96-well plates (Nunc 96-well polypropylene MicroWell Plates, Thermo Scientific). Before staining, cells were washed 2x with 200µl washing buffer (PBS, 4% sucrose, 0.02% sodium azide) on the plate by centrifuging at 4°C at 4000 rpm for 10 min. Blocking was done with 200µl blocking buffer (washing buffer containing 3% bovine serum albumin (BSA)) for 1h at 4°C, before cells were stained in 25µl blocking buffer containing first the monoclonal mouse anti-HA (1:1000, clone HA-7, Sigma) and then the secondary goat anti-mouse-Cy5 antibody (1:200, Jackson ImmunoResearch) for 1 h, 4°C. Washing between and after the staining steps was done with PBS as described above. Finally, the cells were resuspended in 200µl PBS and surface staining of the HA tag was analyzed by flow cytometry and fluorescence microscopy.

Flow cytometric analysis was done using an LSR II analyzer (BD Biosciences) by measuring forward and sideward scatter of bacterial cells in addition to GFP, representing the respective transcriptional fusions, and the surface-stained HA tag (GFP and Alexa Fluor 647 laser, respectively). The data was analyzed with FlowJo software (version 10.0.8).

For microscopy, 150µl of the previously stained cells were transferred onto gelatin (0.2%) coated cover slips. Cover slips were prepared as previously described (Schlumberger et al., 2005). The cover slips harboring stained bacterial cells were mounted onto glass slides using Mowiol and kept in the dark at RT overnight before placing them at 4°C to store for further analysis. The fixed slides were analyzed the next day using an Axiovert 200m microscope with a spinning disc confocal laser unit (Visitron) and a solid state laser unit (Toptica). The samples were analyzed using the lasers for either GFP (488 nm) or Cy5 (647 nm) excitation. Data analysis was done using Volocity 6.3 and GraphPad Prism (version 6.07). The correlation analysis was performed using the Spearman correlation analysis in GraphPad Prism. Spearman rank correlation is a non-parametric test to measure the degree of association between two variables. In contrast to linear regression analysis, this test does not make assumptions about the distribution of the samples or the dependency of the analyzed parameters and is used for ordinal or nominal data.

For Figure 2.1B, a quick staining protocol was applied. In short, bacteria from 1.5 ml of the 4h subculture were pelleted and washed in blocking buffer (PBS containing 5% BSA). Blocking was done in 1 ml volumes for 1 h at 4°C, before the mouse anti-HA (1:5000, clone 12CA5, Roche) and goat anti-mouse-Cy5 (1:200, Jackson ImmunoResearch) antibodies were added. Antibody incubation was done at 4°C for 1 h. Cells were then transferred onto agarose pads (1% agarose in PBS) and analyzed using the Zeiss Axioplan 2 microscope (Zeiss) using the same software as described above.

Western blot analysis

Whole cell lysates of bacteria were prepared by resuspending bacterial pellets in Laemmli Sample Buffer to obtain $1x10^9$ bacteria/ml, before incubation at 95°C for 5 min. The proteins were resolved by SDS-PAGE and subsequently transferred onto nitrocellulose membranes. Subsequently, the membranes were Coomassie-stained to obtain protein loading controls. In short, membranes were washed 3x for 2 min in ddH_2O, before they were stained with the filter stain (Coomassie brilliant blue R 0.05% final concentration). Membranes were de-stained for 5 min with the de-stain solution to allow protein visualization and dried at RT. For the antibody staining, the membranes were blocked overnight at 4°C or 1h at room temperature (RT) in PBS/T (PBS, 0.1% Tween20) containing 5% milk powder. The blots were stained with monoclonal mouse anti-HA (1:1000, clone HA-7, Sigma), monoclonal mouse anti-GFP (1:2000, clone 7.1 and 13.1, Roche) and secondary peroxidase-conjugated goat anti-mouse antibody (1:4000, Sigma). The Page Ruler Plus Prestained Protein Ladder (10-250 kDa, Thermo Scientific) was used as molecular size marker.

Supplementary Table S2.1. Plasmids used in this study.

Plasmid	Characteristics	Resistance	Reference
pM1300	*sipA;* pSB377 derivative	tet	(Sturm et al., 2011)
pM972	*sicA-gfpmut2;* pBR322 derivative with *gfpmut2* (Cormack et al., 1996) expression under the promoter control of *sicA*	amp	(Sturm et al., 2011)
pM965	*rpsM-gfpmut2*; pBR322 derivative with constitutive *gfp* expression under the promoter control of *rpsM*	amp	(Stecher et al., 2004)
pTet-*gfp*	pGM-Tet-GFP; ATc-inducible expression of *gfp*; high copy	amp	(Neuenschwander, 2007)
pInvA$_{HA}$	pASK-IBA2-*invA*$_{HA204}$; HA-tagged *invA* in pASK-IBA2 vector; ATc-inducible promoter	amp	(Oberhettinger et al., 2012)
pZ503	**sipA-invA*$_{HA204}$; pSB377 derivative with InvA$_{HA}$ under the control of the *sicA* promoter which controls the *sicAsipBCDA* operon	tet	This study
pZ522	**sipA-gfpmut2-invA*$_{HA204}$; pSB377 derivative with GFPmut2 and InvA$_{HA}$ under the control of the *sicA* promoter which controls the *sicAsipBCDA* operon	tet	This study
pZ523	**sipA*; *sipA* in pGEM-T easy vector (Promega)	amp	This study
pZ524	*gfpmut2*; *gfpmut2* in pGEM-T easy vector (Promega)	amp	This study
pZ526	*sipA-invA*$_{HA204}$*-gfpmut2;* pZ503 (pSB377) derivative with InvA$_{HA}$ and GFPmut2 under the control of the *sicA* promoter which controls the *sicAsipBCDA* operon	tet	This study
pZ527	**sipA-gfpmut2*; *sipA-gfpmut2* in pGEM-T easy vector (Promega)	amp	This study
pZ543	pASK-IBA2 expression vector; ATc-inducible promoter	amp	This study

*truncated *sipA* carrying only nucleotides 1156-2058 of the orf

Supplementary Table S2.2. Strains used in this study.

Strain	Relevant genotype	Derivative of	Resistance	Reference
SB300	wt *S*. Tm	SL1344	sm	(Hoiseth and Stocker, 1981)
SKI-12	Δ*wbaP*	SL1344	sm	(Ilg et al., 2009)
M3142	*prgH-gfp+*	JH3010, SL1344 (Hautefort et al., 2003)	cm	Diard et al., unpublished; *gfp+:* (Scholz et al., 2000)
Z531*	*prgH-gfp+, sipA-invA*$_{HA204}$	M3142	cm, tet	This study
Z536*	*prgH-gfp+, sipA-invA*$_{HA204}$ *wbaP::aphT*	Z531	cm, tet, kan	This study
Z532*	*sipA-invA*$_{HA204}$	χ8602, SL1344 (Curtiss and Kang, 2004)	sm, tet	This study
Z537*	*sipA-invA*$_{HA204}$ *wbaP::aphT*	Z532	sm, tet, kan	This study
Z555*	*prgH-gfp+ wbaP::aphT*	M3142	sm, kan, cm	This study
Z562	*sipA-invA*$_{HA204}$*-gfpmut2*	SB300	sm, tet	This study; *gfpmut2:* (Cormack et al., 1996)
Z565*	*sipA-invA*$_{HA204}$*-gfpmut2*	X8602	sm, tet	This study
Z567*	*sipA-invA*$_{HA204}$*-gfpmut2 wbaP::cat*	Z565	sm, tet, cm	This study
Z569	*sipA-gfpmut2-invA*$_{HA204}$	SB300	Sm, tet	This study
Z572*	*sipA-gfpmut2-invA*$_{HA204}$	X8602	sm, tet	This study
Z574*	*sipA-gfpmut2-invA*$_{HA204}$ *wbaP::cat*	Z572	sm, tet, cm	This study

* Unflagellated non-motile χ8602 background (Δ*fliC*, Δ*fljB*); wt= wild type, sm= streptomycin, cm= chloramphenicol, tet= tetracycline, kan= kanamycin, amp= ampicillin

Supplementary Table S2.3. Primer sequences used in this study.

#	Primer	Primer sequence 5`-3`	Purpose
52	SipA-BamHI-fw	GATGACGGATCCATTGACCATGGCATCGCGGG	1)
53	SipA-InvA-rv	CACAGTTAGCGTATTAAAAAATGAATACATTGAATTCCTCC TCTAACGCTGCATGTGCAAGCCATC	1)
54	InvA-fw	ATGTATTCATTTTTTAATACGCTAACTG	1)
55	InvA-NotI-rv	GACGATGCGGCCGCCTATTGAGGCTCCGCACACAG	1)
10	_hilEM45-ctrl-Fw2	GACAACAAGCCAGGGATGTAAC	3)
11	_hilEM45-ctrl-Rv2	GGGAGTAAACAGGAGACAAGTG	3)
60	SipA-seq	TATCGGCAAGCCGGTACAGG	3)
61	SipA-seq2	GGCGTGGATCGGGTTATTAC	3)
48	InvA-seq4	CGCTGGAAGCGGAGACTATAATG	3)
42	InvA-seq2	GGCGGTCAATACCTATACCC	3)
43	InvA-seq3	CCGGCATTAACGTGAATGGTG	3)
68	SipA-ko-ctrl-fw	CGTTGATCTGACGCCATTAC	2)
70	InvA-SipA-rv	TAATGTTGCTGTGAGAACCCATA	2)
71	InvA-SipA-fw	TCTAATCCAGCTACGTTGAC	2)
69	SipA-ko-ctrl-rv	GAGTCAGCGTAAAGATCCTC	2)
62	wbaP-pkd-fw	CTTAATATGCCTATTTTATTTACATTATGCACGGTCAGAGG GTGAGGATTAAGTGTAGGCTGGAGCTGCTTC	1)
63	wbaP-pkd-rv	GATTTTACGCAGGCTAATTTATACAATTATTATTCAGTACT TCTCGGTAAGCCATATGAATATCCTCCTTAGTTCCTATTCC	1)
64	wbaP-ko-ctrl-fw	CCAACTCGTTACACCCATTC	2)
65	wbaP-ko-ctrl-rv	TCGATAGCTGCATCAGTACC	2)
66	aphT-ctrl-rv	CGGGTAGCCAACGCTATGTC	2)
67	aphT-ctrl-fw	CCGGTGCCCTGAATGAACTG	2)
124	_sipA-SpeI-fw	GATGACACTAGTATTGACCATGGCATCGCGG	1)
125	_sipA-AflII-rv	GACGATCTTAAGCTAACGCTGCATGTGCAAG	1)
126	GFP-AflII-fw	GATGACCTTAAGCTGCAGGAATTCAGGAGGT	1)
127	GFP-SalI-rv2	GACGATGTCGACTTATTTGTATAGTTCATCC	1)
128	InvA-SalI-fw	GATGACGTCGACAGGAGGAATTCAATGTATTCATTT	1)
129	InvA-SacII-rv	GACGATCCGCGGCTATTGAGGCTCCGCACACAG	1)
144	sipA-seq-rv	CGCTGCATGTGCAAGCCATCAAC	3)
145	InvA-seq-rv	ACGGTCAACGTAGCTGGATTAG	3)

Purpose: 1) strain/plasmid construction, 2) PCR verification, 3) sequencing

2.6 References

Ackermann, M. 2013. Microbial individuality in the natural environment. *The ISME journal* 7:465-467.

Ackermann, M. 2015. A functional perspective on phenotypic heterogeneity in microorganisms. *Nature reviews. Microbiology* 13:497-508.

Ackermann, M., B. Stecher, N.E. Freed, P. Songhet, W.D. Hardt, and M. Doebeli. 2008. Self-destructive cooperation mediated by phenotypic noise. *Nature* 454:987-990.

An, Y., W. Wu, and A. Lv. 2010. A PCR-after-ligation method for cloning of multiple DNA inserts. *Analytical biochemistry* 402:203-205.

Arnoldini, M., I.A. Vizcarra, R. Pena-Miller, N. Stocker, M. Diard, V. Vogel, R.E. Beardmore, W.D. Hardt, and M. Ackermann. 2014. Bistable expression of virulence genes in salmonella leads to the formation of an antibiotic-tolerant subpopulation. *PLoS biology* 12:e1001928.

Choi, P.J., L. Cai, K. Frieda, and X.S. Xie. 2008. A stochastic single-molecule event triggers phenotype switching of a bacterial cell. *Science* 322:442-446.

Cormack, B.P., R.H. Valdivia, and S. Falkow. 1996. FACS-optimized mutants of the green fluorescent protein (GFP). *Gene* 173:33-38.

Cummings, L.A., W.D. Wilkerson, T. Bergsbaken, and B.T. Cookson. 2006. In vivo, fliC expression by Salmonella enterica serovar Typhimurium is heterogeneous, regulated by ClpX, and anatomically restricted. *Molecular microbiology* 61:795-809.

Curtiss, R., and H. Kang. 2004. Modulation of immune responses to foreign antigens expressed by recombinant attenuated bacterial vectors. In 30.

Datsenko, K.A., and B.L. Wanner. 2000. One-step inactivation of chromosomal genes in Escherichia coli K-12 using PCR products. *Proceedings of the National Academy of Sciences of the United States of America* 97:6640-6645.

Diard, M., V. Garcia, L. Maier, M.N. Remus-Emsermann, R.R. Regoes, M. Ackermann, and W.D. Hardt. 2013. Stabilization of cooperative virulence by the expression of an avirulent phenotype. *Nature* 494:353-356.

Ellermeier, J.R., and J.M. Slauch. 2007. Adaptation to the host environment: regulation of the SPI1 type III secretion system in Salmonella enterica serovar Typhimurium. *Current opinion in microbiology* 10:24-29.

Elowitz, M.B., A.J. Levine, E.D. Siggia, and P.S. Swain. 2002. Stochastic gene expression in a single cell. *Science* 297:1183-1186.

Frankel, G., A.D. Phillips, I. Rosenshine, G. Dougan, J.B. Kaper, and S. Knutton. 1998. Enteropathogenic and enterohaemorrhagic Escherichia coli: more subversive elements. *Molecular microbiology* 30:911-921.

Golding, I., J. Paulsson, S.M. Zawilski, and E.C. Cox. 2005. Real-time kinetics of gene activity in individual bacteria. *Cell* 123:1025-1036.

Grassl, G.A., E. Bohn, Y. Muller, O.T. Buhler, and I.B. Autenrieth. 2003. Interaction of Yersinia enterocolitica with epithelial cells: invasin beyond invasion. *International journal of medical microbiology : IJMM* 293:41-54.

Hautefort, I., M.J. Proenca, and J.C.D. Hinton. 2003. Single-Copy Green Fluorescent Protein Gene Fusions Allow Accurate Measurement of Salmonella Gene Expression In Vitro and during Infection of Mammalian Cells. *Applied and environmental microbiology* 69:7480-7491.

Hoiseth, S.K., and B.A. Stocker. 1981. Aromatic-dependent Salmonella typhimurium are non-virulent and effective as live vaccines. *Nature* 291:238-239.

Ilg, K., K. Endt, B. Misselwitz, B. Stecher, M. Aebi, and W.D. Hardt. 2009. O-antigen-negative Salmonella enterica serovar Typhimurium is attenuated in intestinal colonization but elicits colitis in streptomycin-treated mice. *Infect Immun* 77:2568-2575.

Kaern, M., T.C. Elston, W.J. Blake, and J.J. Collins. 2005. Stochasticity in gene expression: from theories to phenotypes. *Nature reviews. Genetics* 6:451-464.

Kong, Q., J. Yang, Q. Liu, P. Alamuri, K.L. Roland, and R. Curtiss, 3rd. 2011. Effect of deletion of genes involved in lipopolysaccharide core and O-antigen synthesis on virulence and immunogenicity of Salmonella enterica serovar typhimurium. *Infect Immun* 79:4227-4239.

Leo, J.C., I. Grin, and D. Linke. 2012. Type V secretion: mechanism(s) of autotransport through the bacterial outer membrane. *Philosophical transactions of the Royal Society of London. Series B, Biological sciences* 367:1088-1101.

Leo, J.C., P. Oberhettinger, M. Schütz, and D. Linke. 2015. The inverse autotransporter family: intimin, invasin and related proteins. *International journal of medical microbiology : IJMM* 305:276-282.

Maamar, H., and D. Dubnau. 2005. Bistability in the Bacillus subtilis K-state (competence) system requires a positive feedback loop. *Molecular microbiology* 56:615-624.

Mills, D.M., V. Bajaj, and C.A. Lee. 1995. A 40 kb chromosomal fragment encoding Salmonella typhimurium invasion genes is absent from the corresponding region of the Escherichia coli K-12 chromosome. *Molecular microbiology* 15:749-759.

Moest, T.P., and S. Meresse. 2013. Salmonella T3SSs: successful mission of the secret(ion) agents. *Current opinion in microbiology* 16:38-44.

Neuenschwander, M. 2007. High-throughput assays for detecting enzymatic activities in living cells. In ETH Zurich, Zurich.

Oberhettinger, P., J.C. Leo, D. Linke, I.B. Autenrieth, and M.S. Schütz. 2015. The inverse autotransporter intimin exports its passenger domain via a hairpin intermediate. *The Journal of biological chemistry* 290:1837-1849.

Oberhettinger, P., M. Schütz, J.C. Leo, N. Heinz, J. Berger, I.B. Autenrieth, and D. Linke. 2012. Intimin and invasin export their C-terminus to the bacterial cell surface using an inverse mechanism compared to classical autotransport. *PloS one* 7:e47069.

Raj, A., and A. van Oudenaarden. 2008. Nature, nurture, or chance: stochastic gene expression and its consequences. *Cell* 135:216-226.

Rosenfeld, N., J.W. Young, U. Alon, P.S. Swain, and M.B. Elowitz. 2005. Gene regulation at the single-cell level. *Science* 307:1962-1965.

Saini, S., J.R. Ellermeier, J.M. Slauch, and C.V. Rao. 2010. The role of coupled positive feedback in the expression of the SPI1 type three secretion system in Salmonella. *PLoS pathogens* 6:e1001025.

Sanchez-Vargas, F.M., M.A. Abu-El-Haija, and O.G. Gomez-Duarte. 2011. Salmonella infections: an update on epidemiology, management, and prevention. *Travel medicine and infectious disease* 9:263-277.

Schlumberger, M.C., A.J. Muller, K. Ehrbar, B. Winnen, I. Duss, B. Stecher, and W.D. Hardt. 2005. Real-time imaging of type III secretion: Salmonella SipA injection into host cells. *Proceedings of the National Academy of Sciences of the United States of America* 102:12548-12553.

Scholz, O., A. Thiel, W. Hillen, and M. Niederweis. 2000. Quantitative analysis of gene expression with an improved green fluorescent protein. p6. *European journal of biochemistry / FEBS* 267:1565-1570.

Smits, W.K., O.P. Kuipers, and J.W. Veening. 2006. Phenotypic variation in bacteria: the role of feedback regulation. *Nature reviews. Microbiology* 4:259-271.

Stecher, B., S. Hapfelmeier, C. Muller, M. Kremer, T. Stallmach, and W.D. Hardt. 2004. Flagella and chemotaxis are required for efficient induction of Salmonella enterica serovar Typhimurium colitis in streptomycin-pretreated mice. *Infect Immun* 72:4138-4150.

Stewart, P.S., and M.J. Franklin. 2008. Physiological heterogeneity in biofilms. *Nature reviews. Microbiology* 6:199-210.

Sturm, A., M. Heinemann, M. Arnoldini, A. Benecke, M. Ackermann, M. Benz, J. Dormann, and W.D. Hardt. 2011. The cost of virulence: retarded growth of Salmonella Typhimurium cells expressing type III secretion system 1. *PLoS pathogens* 7:e1002143.

Suel, G.M., J. Garcia-Ojalvo, L.M. Liberman, and M.B. Elowitz. 2006. An excitable gene regulatory circuit induces transient cellular differentiation. *Nature* 440:545-550.

Temme, K., H. Salis, D. Tullman-Ercek, A. Levskaya, S.H. Hong, and C.A. Voigt. 2008. Induction and relaxation dynamics of the regulatory network controlling the type III secretion system encoded within Salmonella pathogenicity island 1. *Journal of molecular biology* 377:47-61.

Wendland, M., and D. Bumann. 2002. Optimization of GFP levels for analyzing Salmonella gene expression during an infection. *FEBS letters* 521:105-108.

Yu, J., J. Xiao, X. Ren, K. Lao, and X.S. Xie. 2006. Probing gene expression in live cells, one protein molecule at a time. *Science* 311:1600-1603.

Zhou, D., M.S. Mooseker, and J.E. Galan. 1999. Role of the S. typhimurium actin-binding protein SipA in bacterial internalization. *Science* 283:2092-2095.

3 Chapter 3 - The microfluidic device as tool for single cell gene expression analysis

Ismeta Curkić[1], Markus Arnoldini[2, 3], Ima Avalos Vizcarra[4], Daniel Kiviet[2], Markus Schlumberger[1], Peter Kaiser[5], Martin Ackermann[2], Wolf-Dietrich Hardt[1]

[1]Institute of Microbiology, Department of Biology, ETH Zurich, Zurich, Switzerland

[2]Institute of Biochemistry and Pollutant Dynamics, ETH Zurich and Department of Environmental Microbiology, Eawag, Zurich, Switzerland

[3]current address: Department of Physics, University of California San Diego, San Diego, California

[4]Laboratory of Applied Mechanobiology, Department of Health Sciences and Technology, ETH Zurich, Zurich, Switzerland

[5]Visitron Systems GmbH, Puchheim, Germany

Author contributions: I performed all experiments, strain constructions and establishment work described in this chapter. Markus Arnoldini and Ima Avalos Vizcarra supported during the microfluidics microscopy establishment and movie analysis. Ima Avalos Vizcarra designed the chromium mask and produced the silicon master. Daniel Kiviet supported during movie analysis. Peter Kaiser and Markus Schlumberger helped during microscopy establishment and macro-design.

3.1 Introduction

Traditionally, microbial research made use of bacterial populations to investigate microbial properties (Kreibich and Hardt, 2015; Veening et al., 2008). However, these studies did not consider phenotypic diversity among genetically identical cells within these cultures. Therefore, they most likely overlooked subpopulations, which harbored different phenotypes than the majority of cells. In the last 10 years, a novel technology combining microfabrication with bacteriology has emerged, providing unique tools to study basic questions in bacteriology (Hol and Dekker, 2014). The pioneering study of Wang and colleagues combined microfluidics with microbiology and provided new insights into bacterial growth and death in *E. coli* that were only possible to gain by the observation of bacteria over multiple generations (Wang et al., 2010). In their setup, they analyzed the growth and death behavior in *E. coli* over 200 generations in a controlled microenvironment, using a microfluidic setup exhibiting growth channels for the analysis of a single cell at the bottom of the channel ("mother cell" after which the device was named "mother machine").

The type three secretion system 1 (T1) in *Salmonella enterica* subspecies enterica serovar Typhimurium (*S*. Typhimurium or *S*. Tm) is essential for invasion into eukaryotic cells. All genes required for a functional T1 synthesis are encoded on the *Salmonella* pathogenicity island 1 (SPI-1). These include the genes encoding structural proteins of the T1 needle (e.g. PrgH), effectors mediating engulfment of the bacteria by host cells (e.g. SipA, SopE, SopE2) and transcription factors that coordinate and regulate T1 expression (e.g. HilD, HilA, HilC). The complex regulatory cascade includes the SPI-1 encoded regulatory genes *hilD, hilA* and *hilC* and the genes *rtsA* and the major negative regulator *hilE* that are encoded elsewhere in the chromosome (Ellermeier and Slauch, 2007).

In this technical chapter, we will describe the establishment of a microfluidics setup in our laboratory, similar to that described by Wang and colleagues (Wang et al., 2010). Our new wafer design allowed up to four parallel experimental setups. We used the bistably expressed T1 virulence factor to experimentally establish the microfluidics system. We were able to reproduce T1 induction by spent medium by analyzing a T1-driven *gfp* reporter and the reduced cell size and growth retardation of T1 expressing ($T1^+$) cells (Arnoldini et al., 2014; Sturm et al., 2011). The experimental system allowed monitoring of bacteria in a controlled

microenvironment for up to 20 hours. Additionally, we reproduced the reduced growth phenotype of $T1^+$ cells and monitored changes in cell length upon induction of the T1 virulence factor, which were reversible after T1 expression had ceased.

3.2 Results

Design of the chromium mask for wafer production

To produce the microfluidic devices (chips) and increase the number of chips during one manufacturing process, we designed a silicon master allowing the manufacturing of seven chip replicates at once. For this, two chrome masks were designed, one harboring the main trench structures and the other displaying the growth channels. Both masks were aligned during the two-step fabrication of the silicon master to obtain the structure as shown in Figure 3.1A). Single microfluidic devices were replica molded using polydimethylsiloxane (PDMS) with this silicon master, yielding individual chips with four parallel channel structures (Figure 3.1B). The channels displayed either one or two inlets in addition to an outlet to allow constant perfusion with growth medium. Each channel displayed two parallel trenches (in blue, Figure 3.1C), with growth channels perpendicular to the main trench (red area, Figure 3.1C) to harbor single bacterial cells. The length and width of the main trench was 4.2 mm and 100 µm, respectively. The growth channels were enumerated and displayed an increasing width from 0.8 to 1.2 µm. Their length was 20 µm and 25 µm, on either side of the main trench respectively (Figure 3.1D). The height of the silicon master was ~0.9 µm.

Thus, the newly designed silicon master allowed the fabrication of up to seven polydimethylsiloxane (PDMS) chips within one processing step. With one microfluidic device, it was possible to perform up to four parallel experiments with different strains and nutrient media. The existence of two inlets in some of the devices enables the controlled mixing of two different media during an experiment (gradients, step gradients etc.).

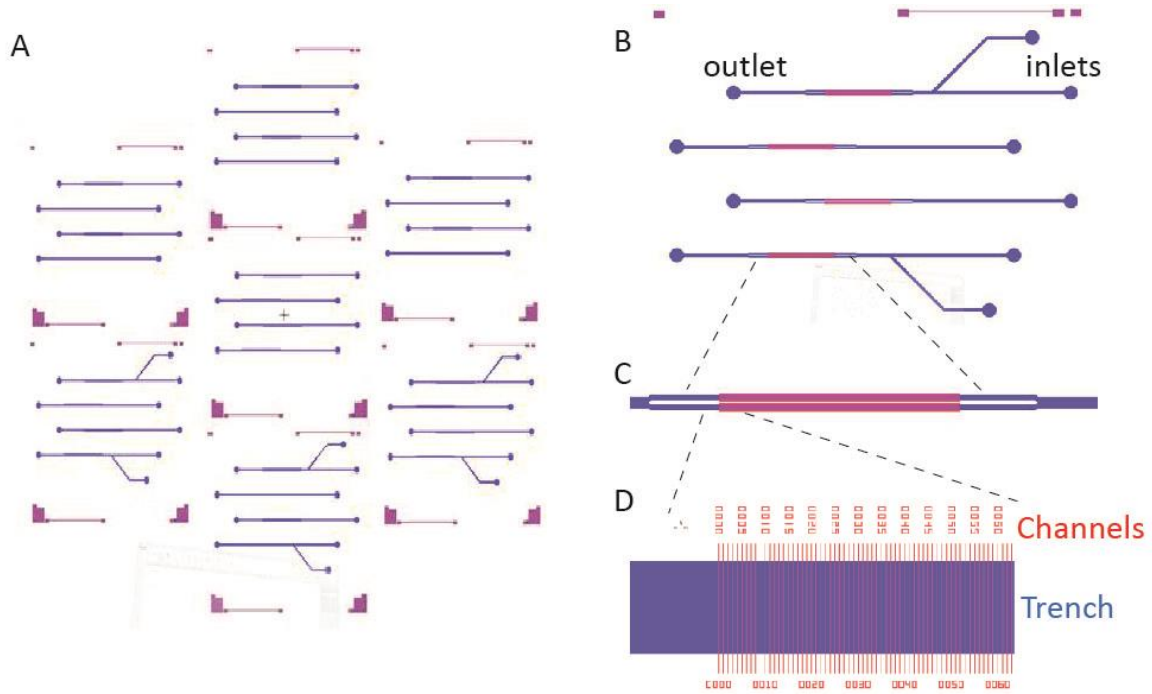

Figure 3.1. Design of chromium mask and individual microfluidic devices.
A) Chromium mask harboring seven designs for microfluidic chips. **B)** Structure of one microfluidic device. **C)** Zoom in into B) showing two main trenches (blue), with the area of the growth channels (red area). **D)** Zoom in into C). The growth channels (red) are numbered.

The CRISP Hardware Autofocus System

For long-term monitoring of bacterial cells, we installed the CRISP Hardware Autofocus System on our microscope. This autofocus system keeps the focal plane of the bacteria constant over the experimental period. It is based on an infrared (IR) LED light (850 nm) that is injected into the microscope and provides a reflected beam that is captured by a positon-sensitive detector (PSD) to determine the focal plane. Using the IR-LED, the hardware autofocus (HW-AF) uses the point of refraction between the glass of the cover slip and the applied medium in the microfluidic chip as reference. By default, this point is used as reference layer to define the focal plane. However, to set the focal plane to the optimal focal plane of the bacteria (=offset layer), calibration of the HW-AF is required. The calibration is done in the following three steps: i. gain calibration; ii. Dithering/ Error definition; iii. Offsetting. During gain calibration, the HW-AF measures the difference in the incoming signal on the detector when the IR-LED is on and off, respectively. To increase the difference between these two signals, the incoming signal when the IR-LED is on, is amplified to reach 75% of the maximum light level in the detector (gain amplification). The amplification is displayed by a signal-to-noise (SNR) value, which should optimally be ~4 dB. During the 2nd calibration step (Dither state), the HW-AF

controller uses the Piezo stepper from the microscope to move the focal position up and down in the Z-axis to define the maximum range in Z that can be used by the HW-AF during the experiment (calibration range). The focus change is displayed by lateral movement of the objects during live view using the Visiview software and is additionally visualized on the display of the HW-AF controller as error signal (Err number in Figure 3.2). To increase the error signal, the lateral adjustment screw on the detector has to be adjusted. The maximum error values that could be achieved during microfluidic experiments ranged between 60 and 90. With the third calibration step, the error value is set as zero, thereby setting the previously defined focal position in one of the Z directions as new offset.

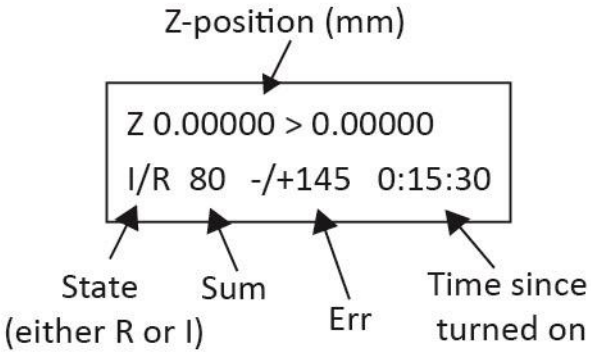

Figure 3.2. Display of the HW-AF controller.
The display of the HW-AF controller displays several indicators, including the Z position, which is relevant to show the Z drift during the experiment and the state (I= idle, IR-LED is turned off; R= Ready, IR-LED is on). The Err (error) value is relevant during calibration and can be both positive and negative. For further details, the reader is referred to the CRISP Autofocus Manual (ASI Applied Scientific Instrumentation, 2014).

For the experimental procedure, we created a Macro for the Visiview software, which allows measuring of several positions of the microfluidic chip during one experiment. This also allowed using different channels of the microfluidic chip to perform several experiments simultaneously. By default, the HW-AF is active during the entire course of the experiment, which includes incubation times without movement, but also the times for stage movement to measure all configured positions.

However, as soon as the HW-AF reaches areas consisting of PDMS, it cannot keep the previously installed focal position. This technical problem was solved by the following work-around: With the help of the "CRISP_Test" Macro, the HW-AF is turned off during stage move

(LK F=85, Figure 3.3), but is turned on again as soon as the installed position is reached (LK F=83, Figure 3.3).

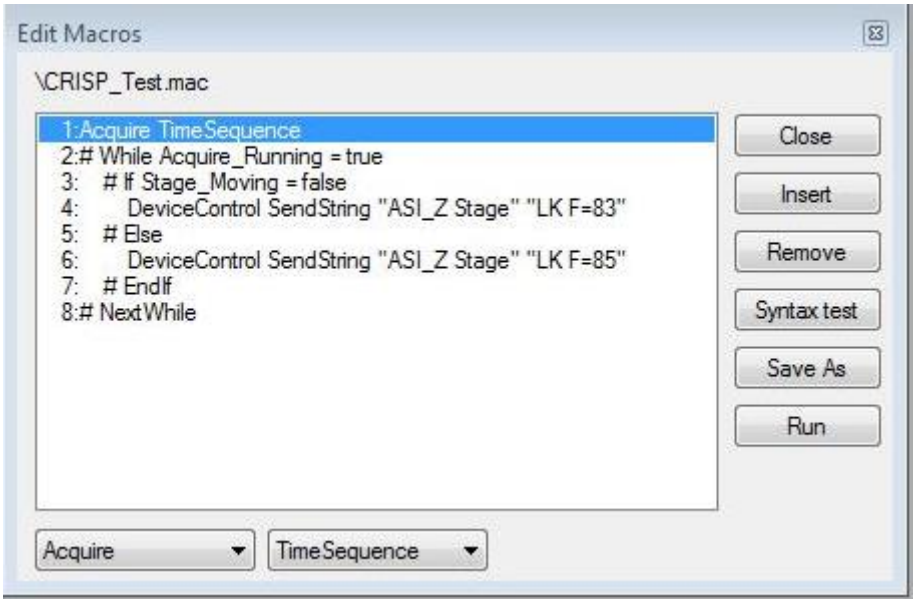

Figure 3.3. Snapshot of "CRISP_Test" macro commands.
Macro used for image acquisition during time laps movies with different positions using the Visiview software. The individual commands mean the following: 1. when time sequence experiments are performed; 2. when image acquisition takes place ("Acquire_Running"); 3. When the stage does not move (stage is at a specific position); 4. turn on the HW-AF ("LK F=83"); 5. otherwise (which means, in case the stage is moving to a position), do following; 6. turn off the HW-AF ("LK F=85"); 7. end of "if command from point 3; 8. Start over with command from point 2.

In conclusion, the HW-AF allows long-term experiments using microfluidic devices. Before use, a three-step calibration procedure has to be performed to define the focal plane of the bacteria as offset Z-position. During the experiment, the use of our newly created macro "CRISP_Test" is essential to allow the parallel measurement at different positions of the microfluidic device.

Analysis of cell growth and division rates in a constant microenvironment

To test our microfluidic setup, we decided to characterize the growth behavior of different *S*. Tm mutants in constant microenvironmental conditions by applying a constant flow of fresh LB medium. All strains analyzed in the microfluidic device were genetically deficient for swimming motility to prevent swimming out of the bacteria during the experiment. As our model system, we chose the T1 virulence factor of *S*. Tm. All analyzed strains harbored a chromosomal *gfp* reporter, which was under the control of the promoter for the gene encoding the T1 structural protein PrgH (P*prgH-gfp*) (Hautefort et al., 2003). We grew the

subcultures until they reached early logarithmic growth phase and concentrated the culture 10x to obtain a high amount of bacteria for injection into the microfluidic device. After injection, we allowed diffusion of the bacteria from the main trench into the growth channels for 1 to 2 hours. Subsequently, we applied constant LB supply and started the long-term analysis of cells at different positions of the microfluidic device. Figure 3.4A depicts the cell length and division rate of the wild-type (wt) strain, harboring P*prgH*-driven *gfp*. The bottom cell ("mother cell") in the indicated channel (yellow box) was analyzed. The cell length remained constant (median 30 pixels, px) during the entire course of the experiment, except for the peak in length at the time point ~630 min. However, this peak is probably a result of a missed segmentation event during image analysis, as occasionally the segmentation cannot be recognized clearly during analysis. The median time between two division events was 40 min. Because we applied fresh LB during the experiment, T1 expression was not induced in the cells. Except for a few cells in the beginning of the experiment, which harbored T1 expression from induction during overnight incubation, there was no GFP signal reported (data not shown). We also investigated the cell size and division rate of a mutant strain, which lacked *hilD*, the gene encoding the master regulator of T1 expression (Schechter et al., 1999; Schechter and Lee, 2001). Those cells were not capable of inducing T1 expression. The mother cell in the indicated channel in Figure 3.4B, displayed a median cell length of 30 px and a median division rate of 40 min, very similar to the wt in Figure 3.4A.

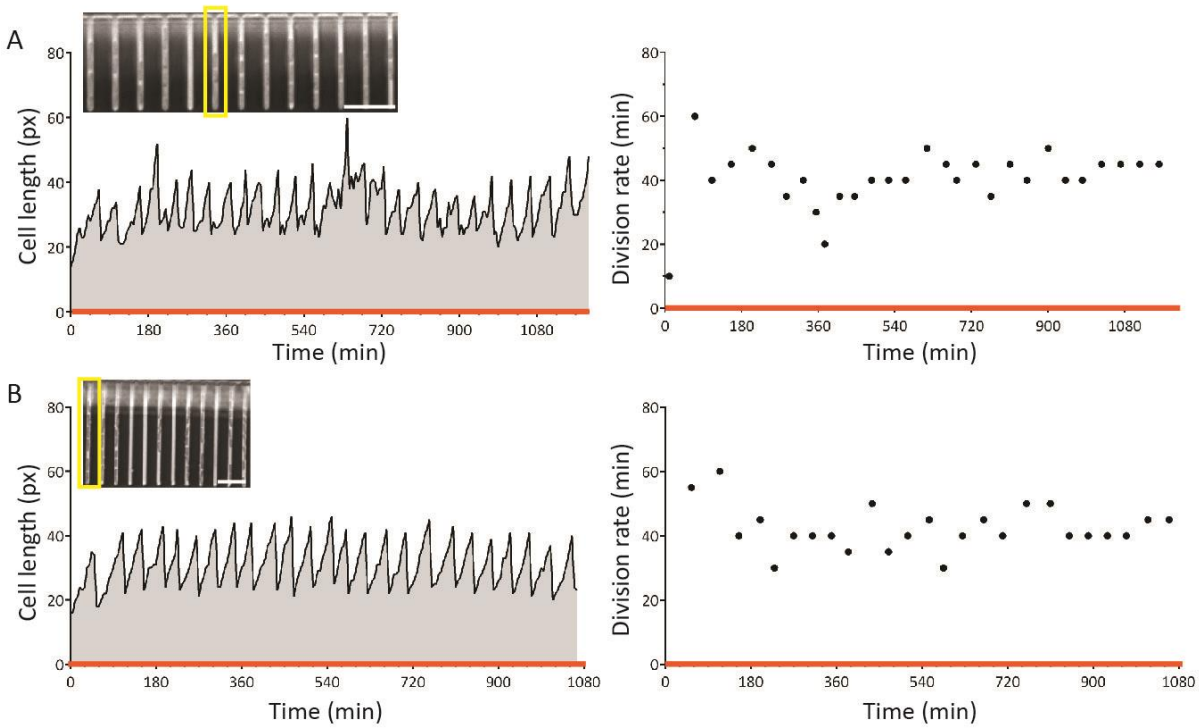

Figure 3.4. Characterization of wt and Δ*hilD* strains during long-term growth in fresh LB.
Bacteria (2h subculture, OD600 ~0.2) harboring a P*prgH*-driven *gfp* reporter in a wt (M3142) **(A)** and a Δ*hilD* mutant background (Z529) **(B)** were loaded into the microfluidic device and imaged every 5 min for 20h at 37°C. Cell length and division rate were assessed using phase contrast images. The cells were incubated in fresh LB throughout the experiment (orange bottom line). The insert displays the field of view of the analyzed position after 9h of incubation (time point 540 min). The bottom cell in the indicated channel (yellow box) of the insert was analyzed. Horizontal white bar indicates 10 µm. px = pixel.

Finally, we investigated a mutant lacking *hilE*, the major repressor of the T1 in *S*. Tm (Baxter et al., 2003) and not surprisingly found an increased number of cells expressing T1 (visualized by GFP). Figure 3.5A displays a cell expressing T1 throughout the experiment (median GFP level 90). The cell length was markedly reduced compared to $T1^-$ cells (median 13 px as opposed to 33 px in $T1^-$ cell in Figure 3.5B). Furthermore, the time between divisions was increased and very heterogeneous (median 80 min), in contrast to the analyzed $T1^-$ cell (median 40 min, Figure 3.5B). The cell length was constant throughout the experiment (median 30 px), except for two exceptions at time at ~600 and 800 min, which were probably resulting from segmentation problems during image analysis, as already described.

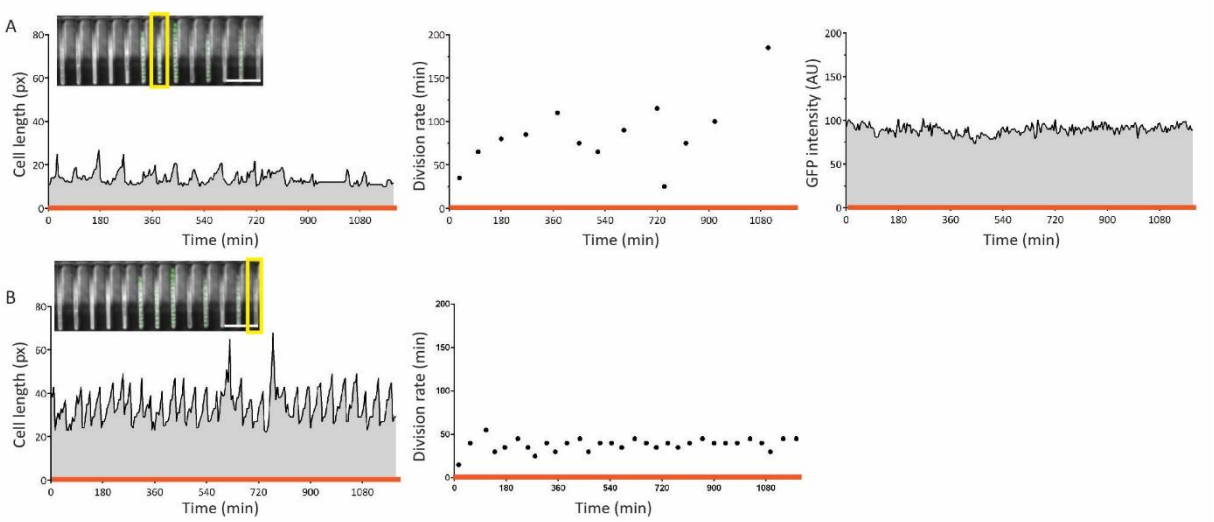

Figure 3.5. Analysis of Δ*hilE* mutant during long-term growth in fresh LB.
Bacteria harboring a P*prgH*-driven *gfp* reporter in a Δ*hilE* mutant background (Z530) were analyzed. LB was applied throughout the experiment (orange line). **A)** Cell length, division rate and GFP fluorescence are displayed for a $T1^+$ cell. GFP fluorescence was normalized to background fluorescence of an area between two growth channels. **B)** Cell length and division rate for a $T1^-$ cell are illustrated. The same experimental setup as described for Figure 3.4 was used. The insert displays the field of view of the analyzed position after 9h of incubation (time point 540 min). The bottom cell in the indicated channel (yellow box) of the insert was analyzed. Horizontal white bar indicates 10 µm. px= pixel.

In summary, we could successfully monitor bacterial growth and correlate it to T1 expression for periods of over 20h. We show one position of each analyzed strain as representative examples. However, during each experiment, we performed parallel measurements at 5 to 10 different positions. In this experimental setup, we performed one experiment at a time and did not use two parallel channel structures. We were able to reproduce the previously shown growth retardation and reduced cell size of $T1^+$ bacteria (Sturm et al., 2011). More repetitions are required to reproduce these data.

Induction of T1 expression using spent medium

In an additional approach, we aimed to reproduce the already known induction of T1 by spent medium (Arnoldini et al., 2014; Sturm et al., 2011). We therefore used the wt strain (P*prgH*-driven *gfp* reporter), cultured and injected the cells into the microfluidic device as described above. After an initial incubation time of 3h to allow adaptation of bacteria, we induced T1 expression by application of spent medium for ~2h. We measured T1 induction in a few cells after switching back to LB incubation upon treatment with spent medium. A representative example for T1 induction is displayed in Figure 3.6B. T1 expression is accompanied by a reduction of cell length (median 22 px) and larger time intervals between two divisions (Figure

3.6B). The non-induced cell displayed a slight reduction of cell length and an increased division rate upon treatment with spent medium. However, it returned to the initial growth rates after switching back to LB (Figure 3.6).

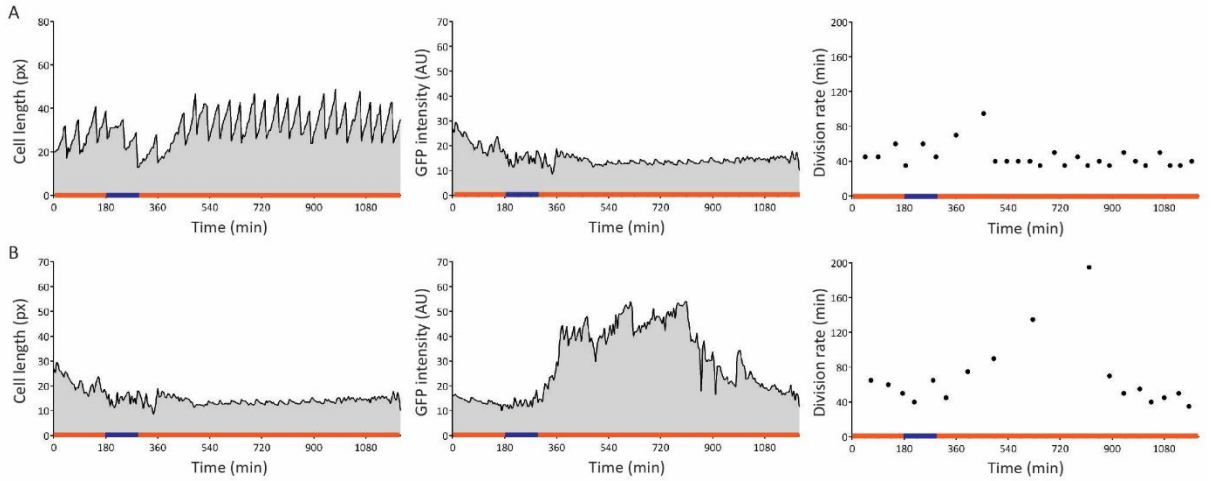

Figure 3.6. T1 is induced upon treatment with spent medium in the microfluidics setup.
Bacteria harboring the P*prgH*-driven *gfp* reporter (M3142; 2h subculture, OD600 ~0.2) were loaded into the microfluidic device and imaged every 5 min for 20h at 37°C. Growth and division rate were assessed using phase contrast images. T1 expression was visualized by measuring GFP fluorescence. The cells were incubated with LB for 3h (orange line), before spent medium was applied (blue line) for 2h and subsequent incubation with LB (orange line) for the residual experiment. Cell length, GFP intensity and division rates are displayed for a $T1^-$ **(A)** and $T1^+$ **(B)** cell. GFP fluorescence was normalized to background fluorescence of an area between two growth channels. px= pixel

We quantified the difference in growth rate between different $T1^+$ and $T1^-$ cells throughout the experiment after switching back to LB incubation (Figure 3.7). We found a slower growth rate for $T1^+$ cells compared to $T1^-$ cells ($\mu_{T1^-} = 1.04$ vs. $\mu_{T1^+} = 0.76$). These values are similar to the previously reported data by Sturm and colleagues, who used an agar pad setup for measuring bacterial growth (Sturm et al., 2011).

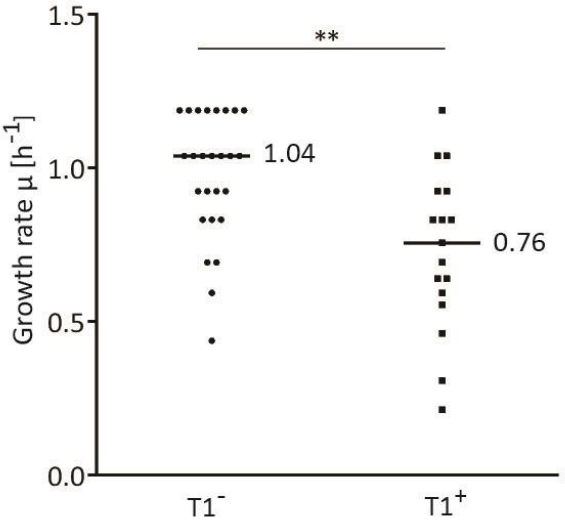

Figure 3.7. Reduced growth rate of T1$^+$ cells compared to T1$^-$ cells.
The growth rates of the experiment illustrated in Figure 3.6 were assessed. In addition to mother cells at the bottom of the growth channels, other bacteria in different growth channels were included for analysis. Only the second LB incubation period was used for analysis. Growth was assessed using phase contrast images. T1 expression was measured in the GFP fluorescence channel. The median growth rate is indicated. Statistical significance was assessed using the Mann-Whitney test. ** $p<0.0018$

Concluding, with our microfluidics device experimental setup, we could reproduce T1 induction and demonstrated the retarded growth phenotype of T1$^+$ cells, as previously described.

3.3 Discussion

Studies analyzing phenotypes of single cells provide important groundwork for analyzing phenotypic diversity within isogenic bacterial populations. We established here a microfluidics microscopy setup, similar to the already described one by Wang and colleagues (Wang et al., 2010). We were able to increase efficiency during microfluidic device fabrication by designing a new chromium mask, which allows the simultaneous preparation of up to seven PDMS devices. With the newly installed HW-AF setup, the focal plane can be stabilized over 20h time course experiments. During our testing period, we could verify previously published phenotypic traits of $T1^+$ subpopulation of *S*. Tm (e.g. slower growth, smaller cell size).

Despite the successful establishment of the microfluidics microscopy system, the following points should be considered when performing microfluidics time-course experiments: i) Before preparation of the microfluidics experimental setup, it is crucial to align the illumination pathway of the microscope to your sample by Köhler illumination. Thereby the contrast of the bacterial cells and thereby image quality are significantly increased. ii) Despite the stabilizing properties of the HW-AF, this system is highly sensitive to perturbations, which frequently results in low quality images and also complete loss of the focal plane. When setting up the different stage positions for microscopy, it is crucial to have the main trench in the center of the live picture of the Visiview software and as little PDMS as possible. The HW-AF is configured to send the IR-LED light beam to the center of the field of view. However, PDMS can perturb the light reflection and increase the amount of diffuse light arriving at the PSD detector. This leads to an unstable HW-AF function.

We could successfully use the microfluidics setup for our experiments and do a first characterization of cell length, division time and T1 expression in wt strains, as well as in Δ*hilD* and Δ*hilE* mutants harboring a T1-*gfp* reporter. When *hilE* was deleted, we observed an increased number of cells expressing T1 compared to wt. These cells displayed either transient expression of the T1 (data not shown) or stayed $T1^+$ throughout the experiment during growth in fresh LB incubation (Figure 3.5). This is in contrast to the wt bacteria (Figure 3.4A), which did not feature any T1 expression. The lack of $T1^+$ cells was not surprising, as we constantly exposed the cells to SPI-1 repressing conditions by continuous supply of fresh nutrients through LB and through the aerobic environment. T1 induction is known to be induced during

late logarithmic growth phase in liquid culture assays, where nutrients and oxygen are already depleted (Saini et al., 2010b; Sturm et al., 2011). Ellermeier and colleagues reported a weak *hilA* expression in the absence of *hilD* (Ellermeier et al., 2005). However, we did not observe T1 expression in the analyzed movie in the Δ*hilD* background (Figure 3.4B). This is might be attributable to the combination of the lack of *hilD* and incubation in SPI-1 repressing conditions (continuous supply of fresh LB). This prevented reaching the T1 activation threshold in individual cells, which was previously described by Saini and colleagues to be necessary for activation (Saini et al., 2010a).

When deleting *hilE*, we observed an increased number of cells displaying T1 expression. This was in accordance to previous reports (Diard et al., 2013) and further supports the finding about the activation threshold by Saini and colleagues (Saini et al., 2010a), as the $T1^-$ cells in our system did probably not reach the threshold for T1 activation. However, the existence of other SPI-1 repressors acting on different transcriptional regulators of the T1 regulatory cascade is well known. Global SPI-1 repressors, such as the small nucleoid-binding protein H-NS and the global carbon metabolism regulator CsrA (carbon storage regulator A) act on the transcription of *hilA* and *hilD*, respectively (Martinez et al., 2011; Schechter et al., 2003b).

With our microfluidics setup, we were able to induce T1 expression using spent medium, which should contain all metabolic cues from the late logarithmic growth phase, as described previously by Sturm and colleagues (Sturm et al., 2011). Arnoldini and colleagues also made use of this T1 induction technique and observed an increased resistance to antibiotic killing during T1 expression by the imposed growth burden in this subpopulation (Arnoldini et al., 2014). However, the exact T1 triggering components remain unknown. We analyzed the growth rate the $T1^+$ and $T1^-$ cells in this setup (Figure 3.7) and found similar growth rates as described previously by Sturm and colleagues (Sturm et al., 2011). Interestingly in both groups, we observed both, fast and slow growing bacteria. This might be explained by slow maturation kinetics of GFP folding, resulting in non-fluorescent cells that already express T1, but are categorized as $T1^-$. The second "delay" is most likely caused by dilution of the GFP fluorophore, which renders cells fluorescent after T1 expression was ceased.

In general, the established microfluidics system provides a useful tool to study T1 expression in *S*. Tm. Besides fluorophores, the epitope-tagged autotransporter system, described in

Chapter 2 of this thesis, is a valuable option to study the dynamics of the T1 core regulatory factors. This system may enhance our capacity to study expression of different T1 regulatory genes. It would be of particular interest if such an autotransporter reporter would circumvent the technical problems arising from the slow folding/maturation kinetics of GFP.

3.4 Materials and Methods

Bacterial strains

The strains used in this study are derivatives of *Salmonella* Typhimurium SL1344 (Hoiseth and Stocker, 1981). All strains are listed in the Supplementary Table S3.1.

The strains Z524 and Z525 were constructed by P22 phage-mediated transduction of *hilD::aphT* from Z37 and *hilE::cat* from M3106, respectively, into the non-flagellated χ8602 (Δ*fliC*, Δ*fljB*). The resistance cassettes were subsequently removed by Flp-catalyzed excision (Cherepanov and Wackernagel, 1995). In short, the strains Z524 and Z525 were transformed with the Flp-recombinase-encoding temperature sensitive helper plasmid pCP20 (replication at 30°C). Upon induction of Flp synthesis at 37°C, the Flp-recombinase recognizes the FRT-flanked resistance genes and flips out the resistance cassette. During flipping, the resulting strains lose the helper plasmid and are selected by the loss of the previous antibiotic resistance. Accordingly, the strains Z527 and Z528 were constructed by flipping out the *aphT* gene from Z524 and the *cat* gene from Z525, respectively. By subsequent P22 transduction of the P*prgH-gfp+* gene fragment from the JH3010 strain into Z527 and Z528, we created the strains Z529 and Z530, respectively. All strains harbor the non-flagellated background and were verified by PCR.

Production of microfluidic devices

The production of microfluidic devices was performed similar as described by Wang and colleagues (Wang et al., 2010). In short, the wafer was produced by two-step photolithography using SU8 2002 and SU8 3025 photoresists (Microchem), respectively. First, the main trench and subsequently the growth channels were produced by spincoating the resists and subsequent UV exposure at 365 nm. The growth channel length was 20 µm and 25

µm, on either side of the main trench, respectively, with an increasing width from 0.8 to 1.2 µm. The length and width of the main trench was 4.2 mm and 100 µm, respectively. The microfluidic device was replica molded from the silicon master using the PDMS elastomer Sylgard 184 Silicone (Bisterfeld Spezialchemie Helvetia GmbH). The PDMS base and curing agent were mixed in a 10:1 ratio (w/w) and subsequently degassed by vacuum, before curing at 80°C for 1h. Before the final step of bonding, the inlet and outlet holes were produced using reusable biopsy punchers (0.75 mm; World Precision Instruments). Finally, the PDMS device was covalently bonded to a glass cover slip after surface activation by air plasma treatment in the plasma cleaner PDC-32G (Harrick Plasma) for 30 seconds.

Culturing of bacterial strains and microfluidics microscopy

Bacterial cultures were grown over night, before they were diluted 1:100 in 5 ml of fresh LB broth (0.1M NaCl) and grown at 37°C until they reached the early logarithmic growth phase (OD600 ~0.20; ~2h). Cells were then concentrated 10x and loaded into the microfluidic device. Bacteria either were incubated with LB or spent medium, as indicated. 0.1% of Tween20 were supplemented to the LB broth to prevent adhesion of bacteria to the PDMS surface. Spent medium was prepared by diluting the overnight cultures 1:100 and culturing them until they enter the late logarithmic growth phase (OD600 ~0.9). The culture was pelleted and the supernatant (=spent medium) was filter-sterilized to remove residual bacterial cells.

Before injection of the bacterial cells, the microfluidic device was coated with LB broth containing 1.5% of 10 mg/ml Bovine Serum Albumin (BSA; Invitrogen AG) and 0.5% of 10 mg/ml Salmon Sperm DNA (Invitrogen AG) to prevent adhesion of bacterial cells to the PDMS surface. The medium was applied through the PTFE microbore tubing (0.012``ID x 0.0.0``OD; Fisher Scientific), which was connected to a syringe pump via the Tygon-tubing (S54HL 0.76 mm; Fisher Scientific). During microfluidics microscopy, LB broth or spent medium was continuously supplied via the tubing system by a pump at a constant rate of 2 ml/h. The experiments were performed in an incubation chamber (Pecon/Visitron) at 37°C. For each experiment, one position covering eleven to thirteen channels was observed and images were acquired every 5 min for the indicated time period using the Visiview software (version 2.1.4; Visitron Systems GmbH) by a Zeiss Axiovert 200m inverted microscope with a 100x/1.3 oil immersion objective (PLAN-Neofluar Zeiss). During each experiment, phase contrast and GFP

fluorescence images were acquired. The focal position was stabilized by the CRISP Hardware Autofocus System (ASI).

Semi-automatic analysis of movies

The movies were analyzed using the MMJ plugin (available at https://github.com/ccg-esb/mmJ) for ImageJ (Schneider et al., 2012). The plugin extracts data on fluorescence intensities and cell length of the cell at the bottom of each channel. Based on the cell length, the division of individual cells was measured. Before MMJ analysis, the movies were pre-processed. For this the following plugins were installed in imageJ: "javacv.jar", "jna.jar", "Template_Matching.jar", "reAlign_slices.class", "reAlign_slices.java", and "MMJ_.jar".

During the pre-processing stage in ImageJ, the movies (phase contrast and fluorescence channels) were converted to 8-bit format and rotated straight up. Subsequently, the phase contrast movies were corrected for small movements during the movie. During the corrections, an excel file is generated, which contained information on the corrections that had to be applied to the pictures of the fluorescence channel. Before MMJ analysis of the phase contrast movies was done, they were cropped to see the growth channels only. For a description of how the MMJ plugin is used, please refer to the webpage https://github.com/ccg-esb/mmJ. The MMJ analysis was done on phase contrast movies first to segment cells and afterwards these segmentation data was transferred to the fluorescence channels. The extracted data on segmentation (time between two divisions; indicated as division rate) and fluorescence was plotted by GraphPad Prism (version 6.07).

The fluorescence data in Figure 3.6 was normalized using the background fluorescence values of the region between the channels, showing no fluorescence.

The growth rate μ in Figure 3.7 was assessed as described previously by calculating ln2/(time(h)) (Sturm et al., 2011).

Supplementary Table S3.1. Strains used in this study.

Strain	Relevant genotype	Derivative of	Resistance	Reference
SB300	*S*. Tm	SL1344	sm	(Hoiseth and Stocker, 1981)
JH3010	P*prgH-gfp+*	SL1344	cm	(Hautefort et al., 2003) *gfp+:* (Scholz et al., 2000)
M3142*	wt; P*prgH-gfp+*	JH3010, SL1344 (Hautefort et al., 2003)	cm	Diard *et al*., unpublished;
Z37	*hilD::aphT*	SB300		Studer *et al*., unpublished
Z524*	*hilD::aphT*	χ8602, SL1344 (Curtiss and Kang, 2004)	sm, kan	This study
Z527*	*ΔhilD*	Z524	sm	This study
Z529*	*ΔhilD,* P*prgH-gfp+*	Z527	sm, cm	This study
M3106	*hilE::cat*	SB300	cm	Diard *et al*., unpublished
Z525*	*hilE::cat*	χ8602, SL1344 (Curtiss and Kang, 2004)	sm, cm	This study
Z528*	*ΔhilE*	Z525		This study
Z530*	*ΔhilE,* P*prgH-gfp+*	Z528	sm, cm	This study

*indicates an unflagellated non-motile χ8602 background (Δ*fliC*, Δ*fljB*); sm= streptomycin, cm= chloramphenicol, tet= tetracycline, kan= kanamycin, amp= ampicillin

3.5 References

Arnoldini, M., I.A. Vizcarra, R. Pena-Miller, N. Stocker, M. Diard, V. Vogel, R.E. Beardmore, W.D. Hardt, and M. Ackermann. 2014. Bistable expression of virulence genes in salmonella leads to the formation of an antibiotic-tolerant subpopulation. *PLoS biology* 12:e1001928.

ASI Applied Scientific Instrumentation. 2014. CRISP Autofocus System Manual. In Applied Scientific Instrumentation.

Baxter, M.A., T.F. Fahlen, R.L. Wilson, and B.D. Jones. 2003. HilE Interacts with HilD and Negatively Regulates hilA Transcription and Expression of the Salmonella enterica Serovar Typhimurium Invasive Phenotype. *Infection and Immunity* 71:1295-1305.

Cherepanov, P.P., and W. Wackernagel. 1995. Gene disruption in Escherichia coli: TcR and KmR cassettes with the option of Flp-catalyzed excision of the antibiotic-resistance determinant. *Gene* 158:9-14.

Curtiss, R., and H. Kang. 2004. Modulation of immune responses to foreign antigens expressed by recombinant attenuated bacterial vectors. In 30.

Diard, M., V. Garcia, L. Maier, M.N. Remus-Emsermann, R.R. Regoes, M. Ackermann, and W.D. Hardt. 2013. Stabilization of cooperative virulence by the expression of an avirulent phenotype. *Nature* 494:353-356.

Ellermeier, C.D., J.R. Ellermeier, and J.M. Slauch. 2005. HilD, HilC and RtsA constitute a feed forward loop that controls expression of the SPI1 type three secretion system regulator hilA in Salmonella enterica serovar Typhimurium. *Molecular microbiology* 57:691-705.

Ellermeier, J.R., and J.M. Slauch. 2007. Adaptation to the host environment: regulation of the SPI1 type III secretion system in Salmonella enterica serovar Typhimurium. *Current opinion in microbiology* 10:24-29.

Hautefort, I., M.J. Proenca, and J.C.D. Hinton. 2003. Single-Copy Green Fluorescent Protein Gene Fusions Allow Accurate Measurement of Salmonella Gene Expression In Vitro and during Infection of Mammalian Cells. *Applied and environmental microbiology* 69:7480-7491.

Hoiseth, S.K., and B.A. Stocker. 1981. Aromatic-dependent Salmonella typhimurium are non-virulent and effective as live vaccines. *Nature* 291:238-239.

Hol, F.J., and C. Dekker. 2014. Zooming in to see the bigger picture: microfluidic and nanofabrication tools to study bacteria. *Science* 346:1251821.

Kreibich, S., and W.D. Hardt. 2015. Experimental approaches to phenotypic diversity in infection. *Current opinion in microbiology* 27:25-36.

Martinez, L.C., H. Yakhnin, M.I. Camacho, D. Georgellis, P. Babitzke, J.L. Puente, and V.H. Bustamante. 2011. Integration of a complex regulatory cascade involving the SirA/BarA and Csr global regulatory systems that controls expression of the Salmonella SPI-1 and SPI-2 virulence regulons through HilD. *Molecular microbiology* 80:1637-1656.

Saini, S., J.R. Ellermeier, J.M. Slauch, and C.V. Rao. 2010a. The role of coupled positive feedback in the expression of the SPI1 type three secretion system in Salmonella. *PLoS pathogens* 6:e1001025.

Saini, S., J.M. Slauch, P.D. Aldridge, and C.V. Rao. 2010b. Role of cross talk in regulating the dynamic expression of the flagellar Salmonella pathogenicity island 1 and type 1 fimbrial genes. *Journal of bacteriology* 192:5767-5777.

Schechter, L.M., S.M. Damrauer, and C.A. Lee. 1999. Two AraC/XylS family members can independently counteract the effect of repressing sequences upstream of the hilA promoter. *Molecular microbiology* 32:629-642.

Schechter, L.M., S. Jain, S. Akbar, and C.A. Lee. 2003. The Small Nucleoid-Binding Proteins H-NS, HU, and Fis Affect hilA Expression in Salmonella enterica Serovar Typhimurium. *Infection and Immunity* 71:5432-5435.

Schechter, L.M., and C.A. Lee. 2001. AraC/XylS family members, HilC and HilD, directly bind and derepress the Salmonella typhimurium hilA promoter. *Molecular microbiology* 40:1289-1299.

Schneider, C.A., W.S. Rasband, and K.W. Eliceiri. 2012. NIH Image to ImageJ: 25 years of image analysis. *Nature methods* 9:671-675.

Scholz, O., A. Thiel, W. Hillen, and M. Niederweis. 2000. Quantitative analysis of gene expression with an improved green fluorescent protein. p6. *European journal of biochemistry / FEBS* 267:1565-1570.

Sturm, A., M. Heinemann, M. Arnoldini, A. Benecke, M. Ackermann, M. Benz, J. Dormann, and W.D. Hardt. 2011. The cost of virulence: retarded growth of Salmonella Typhimurium cells expressing type III secretion system 1. *PLoS pathogens* 7:e1002143.

Veening, J.W., W.K. Smits, and O.P. Kuipers. 2008. Bistability, epigenetics, and bet-hedging in bacteria. *Annual review of microbiology* 62:193-210.

Wang, P., L. Robert, J. Pelletier, W.L. Dang, F. Taddei, A. Wright, and S. Jun. 2010. Robust growth of Escherichia coli. *Current biology : CB* 20:1099-1103.

4 Chapter 4 - The quest for cause and consequence on the expression of the *Salmonella* Typhimurium type three secretion system 1 and the RpoE-mediated stress response

Ismeta Curkić[1], Barbara Müller[1], Nicolas Studer[1, 2], Alexander Sturm[1,3], Wolf-Dietrich Hardt[1]

[1]Institute of Microbiology, Department of Biology, ETH Zurich, Zurich, Switzerland

[2]Institute of Infectious Diseases, University of Bern, Bern, Switzerland

[3]Broad Institute of MIT and Harvard, Cambridge, MA 02142, USA

Author contributions: I performed all experiments (except Figure 1C-H) in this chapter and constructed several strains. Nicolas Studer performed the experiments for Figure 1C-H and several strain constructions. Barbara Müller performed the plasmid constructions of the arabinose-inducible plasmids in Figure 6. Alexander Sturm performed the proteome analysis, constructed some of the used strains and established the initial version of this project.

4.1 Abstract

The envelope of a bacterium provides the first shield of protection against stress factors in the environment. Therefore, bacteria have evolved membrane stress response systems to encounter these stresses. The RpoE-mediated stress response in *Salmonella* Typhimurium (*S*. Tm) represents one of these response systems and is activated upon accumulation of misfolded or unfolded proteins in the periplasm. *S.* Tm virulence is governed by the expression of the type three secretion system 1 (T1) needle, which is encoded on the *Salmonella* Pathogenicity Island 1 (SPI-1) that mediates invasion into eukaryotic host cells. The T1 needle is bistably expressed, resulting in two distinct subpopulations within an isogenic population in a given environment. We tested the co-regulation of T1 and RseP, one of the activators of RpoE. Using a m*Cherry* reporter for T1 expression, we observed a bimodal distribution of *rseP*, similar to T1. However, without the T1-driven *mCherry* reporter, we could not observe bimodality of RseP. We subsequently investigated the role of inducible *mCherry* in *rseP* expression, but did not find any increase in RseP levels upon overproduction of mCherry within the cytoplasm. Furthermore, *rseP* deletion did not affect the growth rate of *S*. Tm. Deletion of the T1 regulatory genes *hilD* and *hilA* and the entire SPI-1 locus resulted in a reduced *rseP* expression. In contrast, deletion of *invF*, a *hilA*-regulated downstream transcription factor, did not affect *rseP* expression. Furthermore, the deletion of T1 assembly genes (which may lead to the accumulation of T1 apparatus assembly modules and thereby enhance membrane stress) did not increase *rseP* levels. Overall, we could not clearly elucidate if and how T1 or cytoplasmic mCherry expression are connected to the RpoE stress response in *S*. Tm.

4.2 Introduction

Salmonella enterica subspecies enterica serovar Typhimurium (*S*. Typhimurium or *S*. Tm) is a pathogen that encounters various stresses during its lifetime. These stress factors include temperature fluctuations, shifts in pH or osmolarity, the presence of antimicrobial peptides or antibiotics and nutrient scarcity in environments both inside and outside the host (Runkel et al., 2013). Thus, the ability to encounter these stresses successfully is essential to ensure survival. *S*. Tm has evolved various protection mechanisms that are activated when

encountering specific environmental signals. As an interface between a bacterial cell and its environment, the bacterial envelope plays an important role in these response mechanisms that usually trigger the expression of specific genes and thereby provide an adaptation to the imposed danger signal (Ruiz et al., 2006). *S*. Tm encodes numerous membrane stress response systems, including the CpxAR two-component system (Cosma et al., 1995; Duguay and Silhavy, 2004), the phage shock protein (PSP) system (Brissette et al., 1990) the Bae pathway (Leblanc et al., 2011) and the RpoE $\delta^{E/24}$ pathway (Duguay and Silhavy, 2004; Erickson and Gross, 1989). Although each of the systems reacts to specific environmental cues, cross talk between some systems has been suggested (McBroom and Kuehn, 2007; Runkel et al., 2013). The RpoE-mediated stress response is initiated upon accumulation of misfolded or unfolded proteins in the periplasm (Mecsas et al., 1993; Runkel et al., 2013). Since its discovery in 1989, where it was described in the context of the heat shock response in *E. coli* (Erickson and Gross, 1989), other inducers have been described. Cues that trigger the RpoE pathway include heat, ethanol, antimicrobial peptides, pH changes, osmotic and oxidative stress and shifts to some carbon sources (Bang et al., 2005; Erickson and Gross, 1989; Kenyon et al., 2005; McMeechan et al., 2007).

S. Tm virulence is dependent on the type three secretion system 1 (T1) virulence factor, which is encoded on the *Salmonella* Pathogenicity island 1 (SPI-1). So far, it has been recognized that this virulence factor is bistably expressed within a genetically homogeneous population that shares the same microenvironment (Ackermann et al., 2008; Hautefort et al., 2003; Saini et al., 2010a; Sturm et al., 2011; Temme et al., 2008). Another study analyzing the effects of T1 expression on the bacterial cells found that T1 expression reduces *S*. Tm fitness in *in vitro* settings by imposing a growth burden onto the cell (Sturm et al., 2011). The T1 displays a syringe like structure, which spans through both, the inner and outer membrane (Cornelis, 2010; Moest and Meresse, 2013). The needle is assembled by a number of structural proteins (e.g. InvG, InvH) and is associated with a translocon (the ATPase InvC) that facilitates translocation of effector proteins through the needle (Akeda and Galan, 2005; Moest and Meresse, 2013). T1 expression is governed by a complex set of proteins, including proteins encoded on SPI-1 (e.g. HilD, HilA, SipA, SicA) but also affected by global regulators (H-NS, PhoQ/P) (Groisman et al., 1989; Miller et al., 1989; Schechter et al., 2003a).

As the expression of the T1 needle results in reduced growth rates (Sturm et al., 2011), we were initially hypothesizing that this "cost" of expression might also include increased envelope stress. T1 assembly itself might lead to increased envelope stress and the RpoE stress response might help to alleviate this imposed burden. In this chapter, we present a study, which was initially based on the hypothesis that RseP, a zinc-metalloprotease involved in the RpoE-mediated stress response, is co-regulated with T1. We found hints of co-regulation of *rseP* and *t1* by analyzing *t1* expression by a T1-driven *mCherry* reporter, as *rseP* expression displayed a similar bimodal distribution as previously observed for *t1*. However, follow-up work revealed that the bimodal distribution occurred only when we use the cytoplasmic fluorophore mCherry as transcriptional reporter. This led us to hypothesize that the cytoplasmic mCherry fluorophore might induce the RpoE-mediated stress response by increasing *rseP* expression. However, when testing the effect of an inducible *mCherry* reporter on *rseP* expression, we did not detect increased RseP levels. Thus, we could not clearly elucidate the role of T1 expression or overexpression of the cytoplasmic fluorophore mCherry in the RpoE-mediated stress response.

4.3 Results

rseP and *t1* are co-regulated in the presence of the T1 reporter plasmid p*sicA-mCherry*

This project was initiated after a proteomic analysis of the T1 expressing ($T1^+$) subpopulation using a plasmid-based *gfp* reporter as T1 indicator for flow cytometric sorting (Sturm *et al*., unpublished). In the proteomic analysis, RpoE levels were increased in the $T1^+$ cells, which led to the hypothesis that the RpoE-mediated stress response was involved in alleviating membrane stress caused by the expression of the T1 needle in *S.* Tm. However, subsequent validation of the involvement of RpoE during T1 expression did not substantiate a direct link (Dormann *et al*., Studer *et al*.; unpublished). Based on this finding, Nicolas Studer (MSc) and Alexander Sturm (PhD) decided to investigate a potential involvement of the zinc-metalloprotease RseP in *t1* expression. RseP is part of the activation cascade of RpoE and releases RpoE from its sequestered state by proteolytic cleavage of the RpoE sequestering anti-sigma factor RseA (Figure 4.1B). They hypothesized that *rseP* is bistably expressed and

thereby renders the activation of the sigma factor RpoE regulon bistable, as described for T1. To study gene expression of *t1*, *rpoE* and *rseP* in single cells, Studer used the chromosomal tsr_{venus} reporter (Yu et al., 2006), fused to the respective promoter. The chromosomal T1 reporter harbored the tsr_{venus} gene downstream of the *sicAsipBCDA* operon (Figure 4.1) (Sturm et al., 2011). Furthermore, they used a second T1 reporter to analyze simultaneous expression of the respective genes with T1 using a plasmid-based *mCherry* reporter under the control of the promoter of the *sicAsipBCDA* operon (p*sicA-mCherry*) (Sturm et al., 2011). They performed a time course to investigate the simultaneous expression of *sipA, rseP* and *rpoE* (chromosomal tsr_{venus} reporter fusions) with *t1* (plasmid-based *mCherry* reporter). Bacteria were grown for 6h, sampled at the indicated time points and analyzed on agar pads by microscopy. They found a bimodal distribution pattern of the *sicA*-tsr_{venus}-harboring strain in the course of 6h, as previously described for T1 (Hautefort et al., 2003; Saini et al., 2010a; Sturm et al., 2011). Furthermore, both reporters for T1 (chromosomal *sipA*-tsr_{venus} and plasmid-based p*sicA-mCherry*) expression displayed a similar expression pattern (Figure 4.1C) and a correlative expression ($r=0.7136$, $p<0.0001$) (Figure 4.1D). They further found that the *rseP*-tsr_{venus}-harboring strain containing the p*sicA-mCherry* plasmid displayed a bimodal distribution of Venus fluorescence (Figure 4.1E) as the *sipA*-tsr_{venus} strain (Figure 4.1C). The expression of both reporters, *rseP*-tsr_{venus} and *sipA*-tsr_{venus} displayed a positive correlation ($r=0.8252$, $p<0.0001$) (Figure 4.1F). In contrast, the expression of *rpoE*-tsr_{venus} increased slightly over time but did not correlate with *t1* ($r=0.2254$, p 0.0169) (Figure 4.1H). The wild-type (wt) control SB300, lacking any fluorophores were used as negative controls for the assessment of background fluorescence.

In conclusion, the time course experiment performed by Studer using chromosomal tsr_{venus} reporters in combination with a plasmid-based T1 reporter (T1 visualization by mCherry) identified a bimodal distribution of *rseP* expression, which is similar to that of T1. In contrast, *rpoE* expression did not correlate with *t1* expression. From this, they concluded that *rseP* but not *rpoE* was co-regulated with *t1*.

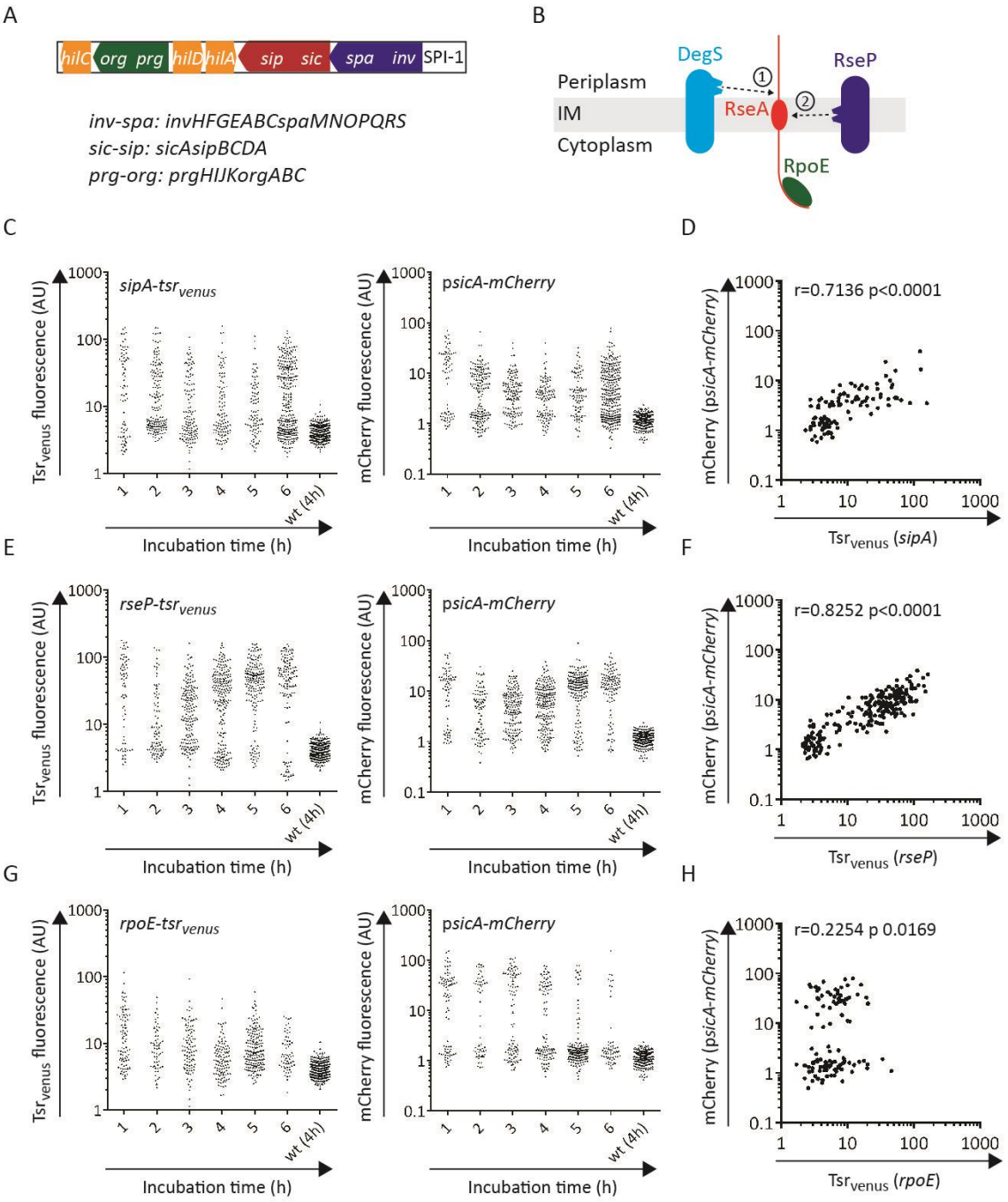

Figure 4.1. Scheme of SPI-1 and *rpoE* activation and time course experiment of *sipA, rseP* and *rpoE* expression. A) Scheme of the three biggest operons encoded on SPI-1, including the *inv-spa*, *sic-sip* and *prg-org* operons. The transcription factors *hilC*, *hilD* and *hilA* are depicted in orange. Adapted from (Ellermeier and Slauch, 2008; Lostroh and Lee, 2001). **B)** Scheme of RpoE sequestration to the inner membrane (IM) by RseA in a non-stressed environment. Upon stress induction, DegS senses misfolded or unfolded proteins in the periplasm and initiates the first cleavage of RseA, which is followed by a second cleavage step by RseP. The released RpoE subsequently induces gene expression of target genes to induce a stress response. Adapted from (Osterberg et al., 2011) **C, E, G)** Microscopic analysis of the combined expression of T1 (p*sicA-mCherry*; pM2833) with *sipA-tsr*$_{venus}$ (**C**; M2000-pM2833, *rseP-tsr*$_{venus}$ (**E;** Z6-pM2833) and *rpoE-tsr*$_{venus}$ (**G**; M2519-pM2833) during a time course of 6h. Tsr$_{venus}$ and mCherry fluorescence indicate the expression of the respective chromosomal promoter (P*sicA* for SipA expression and P*rseP* and P*rpoE*) and the plasmid-based T1 reporter, respectively. The wt control (SB300) is only shown for the 4h time point. **D, F, H)** Analysis of correlative expression of the data from the 4h time points depicted in **C, E** and **G**. *t1* (p*sicA-mCherry*) expression was correlated with *sipA-tsr*$_{venus}$ **(D)**, *rseP-tsr*$_{venus}$ **(F)** and *rpoE-tsr*$_{venus}$ **(H)**. **D, F, H)** Correlation was statistically tested using Spearman correlation analysis. **C-H)** Experiments were performed by N. Studer (unpublished).

In our study, we aimed to reproduce these data and analyzed the respective gene expression during late logarithmic growth. We cultured bacteria for 4h and analyzed the expression of either *rseP-tsr*$_{venus}$, *rpoE-tsr*$_{venus}$ or *sipA-tsr*$_{venus}$ and the plasmid-based T1 reporter p*sicA-mCherry*. We could verify the bimodal *rseP* distribution and observed a similar expression pattern of *rseP tsr*$_{venus}$ when using the p*sicA-mCherry* T1 reporter (Figure 4.2C). Further, the expression of *rseP* and *t1* displayed a positive correlation (r=0.8667, p<0.0001) (Figure 4.2D). In contrast, *rpoE* did not show correlation with *t1* expression (r=0.06260, p=0.0006; Figure 4.2F). The *rpoE* distribution was unimodal within the population, despite the presence of a bimodal *t1* expression pattern (Figure 4.2E). Finally, the control strain harboring two T1 reporters, *sipA-tsr*$_{venus}$ and p*sicA-mCherry*, respectively, also displayed a bimodal distribution with both reporters (Figure 4.2A) as well as a positive correlation (r=0.7081, p<0.0001) (Figure 4.2B).

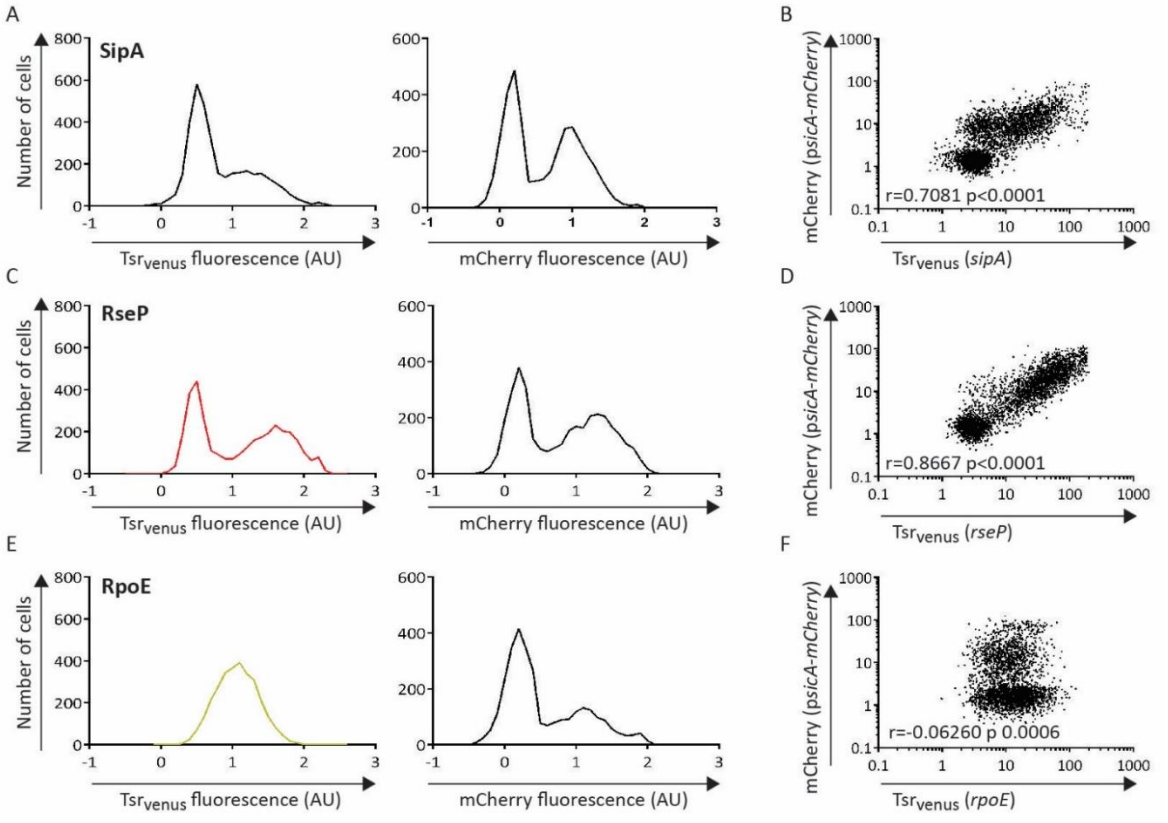

Figure 4.2. Co-expression analysis of *t1* with *sipA, rseP* and *rpoE*.
Microscopic analysis of combined expression of T1 with the respective promoters at 4h (late logarithmic growth) as seen in Figure 4.1C-H. **A, C, E)** Histogram of the distribution of SipA **(A),** RseP **(C)** and RpoE **(E)** visualized by Tsr$_{venus}$ fluorescence and the corresponding T1 distribution visualized by mCherry (p*sicA-mCherry*; pM2833). For the combined analysis, bacteria harbored the p*sicA-mCherry* plasmid (pM2833) as follows: *sipA-tsr*$_{venus}$ **(A;** M2000-pM2833), *rseP-tsr*$_{venus}$ **(C;** Z6-pM2833) and *rpoE-tsr*$_{venus}$ **(E**; M2519-pM2833). **B, D, F)** Correlation analysis of the data from A, C, E. The correlation of *t1* (p*sicA-mCherry*) expression was analyzed versus the expression of *sipA-tsr*$_{venus}$ **(B)**, *rseP-tsr*$_{venus}$ **(D)** on *rpoE-tsr*$_{venus}$ **(F)**. Correlation was statistically tested using Spearman correlation analysis. Data from three independent experiments is shown.

We could reproduce the bimodal expression of *rseP* in the presence of the T1 reporter plasmid p*sicA-mCherry*, which was previously observed by Studer and Sturm (Studer *et al*.; unpublished). Interestingly, the *rseP-tsr*$_{venus}$ distribution within the bacterial population displayed a very similar pattern as the mCherry fluorescence signal (Figure 4.2C), indicating that the expression of *rseP* and of *t1* are functionally linked. The nature of this link remained to be established.

Single cell analysis of an *rseP* mutant reveals no effect on the growth rate of *S*. Tm

We next decided to investigate the effect of RseP on the growth rate of *S*. Tm on single cell level. As we hypothesized that *t1* and *rseP* were co-regulated during expression, a bulk growth analysis would not provide the precise information of the desired T1$^+$ subpopulation, which is retarded in growth (Sturm et al., 2011) and therefore is easily overgrown by the T1$^-$ population. We therefore applied a microfluidics setup to monitor the growth phenotype of individual cells in the presence and absence of *rseP*. We monitored T1 expression using a chromosomally encoded *gfp* reporter upon activation of the P*prgH* promoter (P*prgH-gfp*). PrgH is a structural component of the T1 needle (Figure 4.5B) and should therefore be a suitable indicator for T1 expression. Growth rates of the P*prgH-gfp*-harboring strain and an isogenic *rseP* mutant (P*prgH-gfp ΔrseP*) were assessed during a long-term incubation of ~18h (Figure 4.3). In both backgrounds, the T1 non expressing (T1$^-$) bacteria grew faster than the T1 expressing (T1$^+$) cells (μ_{T1^-} = 0.76 and 0.73 for P*prgH-gfp* and P*prgH-gfp ΔrseP*, respectively, vs. μ_{T1^+} = 0.36 and 0.34 for P*prgH-gfp* and P*prgH-gfp ΔrseP*, respectively) (Figure 4.3B). However, deletion of *rseP* did not seem to influence the growth rate of the T1$^+$ cells.

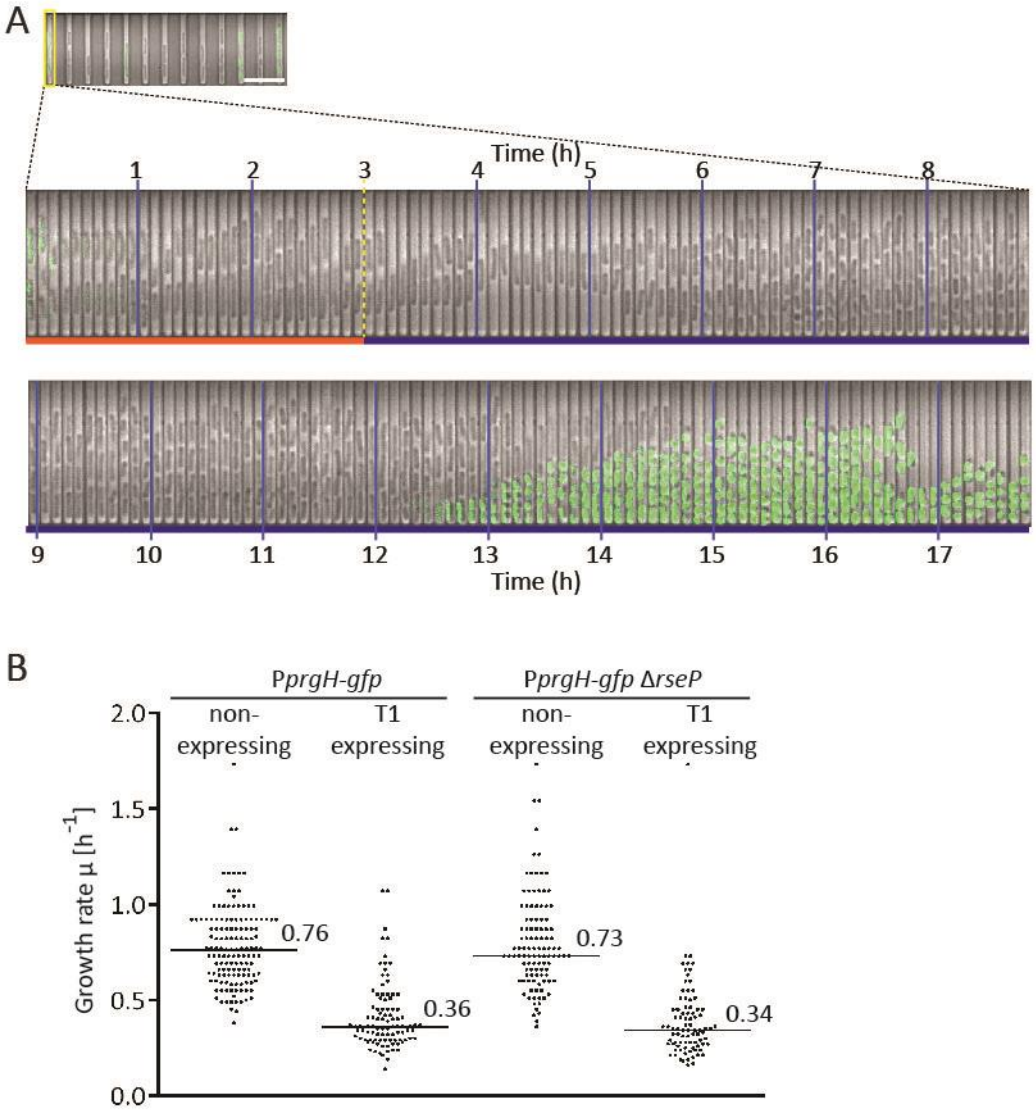

Figure 4.3. Analysis of growth rate effects upon *rseP* deletion on single cells during long-term observation.
A) Representative image representing long-term growth of the P*prgH-gfp* Δ*rseP* mutant (Z535) from the indicated channel. Bacteria were cultured for 2h before (exponential growth phase; OD ~0.2) loading into the microfluidic device. Cells were incubated for 18h and imaged every 3 min. The yellow dashed line indicates the time point of medium switch from fresh LB (orange bottom line) and spent medium (blue bottom line). The onset of green fluorescence represents the onset of *t1* gene expression. Horizontal white bar in the insert represents 10 µm. **B)** Quantification of growth rates for $T1^+$ and $T1^-$ cells of P*prgH-gfp* (M3142) and P*prgH-gfp* Δ*rseP* (Z535) strains. T1 expression was analyzed with the P*prgH-gfp* reporter. A single point represents the growth rate of a single cell. The growth rates were assessed only during incubation with spent medium. Data from three independent experiments is shown. The median is indicated by the horizontal black lines. The numbers indicate the median growth rates.

In summary, r*seP* does not affect growth rate of the $T1^+$ subpopulation of *S*. Tm. This might be because of the presence of other compensatory envelope stress systems.

rseP expression is unimodal in the absence of the p*sicA-mCherry* T1 reporter plasmid

We next tested the expression of *rseP-tsr*$_{venus}$ in the absence of the plasmid-based T1 reporter (p*sicA-mCherry*). Surprisingly, we could not observe the bimodal expression pattern (Figure 4.4A) as described with the strains harboring the p*sicA-mCherry* plasmid (Figure 4.2C and Figure 4.4B). The *rseP* distribution was unimodal, similar to the *rpoE* distribution. We included the *sipA-tsr*$_{venus}$ reporter strain as a positive control to verify T1 expression at the analyzed time point. The wild-type (wt) control, lacking any fluorophores, was used to determine the T1^{-} population. Furthermore, we included another negative control to assess background fluorescence in a *tsr*$_{venus}$-harboring strain during an inactive promoter state. For this, we deleted *hilD*, the major inducer of T1 controlling the expression of the *sicAsipBCDA* operon through *hilA* (Figure 4.1A), in the *sipA-tsr*$_{venus}$-harboring strain. As expected, the background fluorescence of both the wt strain without any fluorophores and the *sipA-tsr*$_{venus}$-harboring strain, lacking *hilD*, overlap (blue curve and grey area Figure 4A).

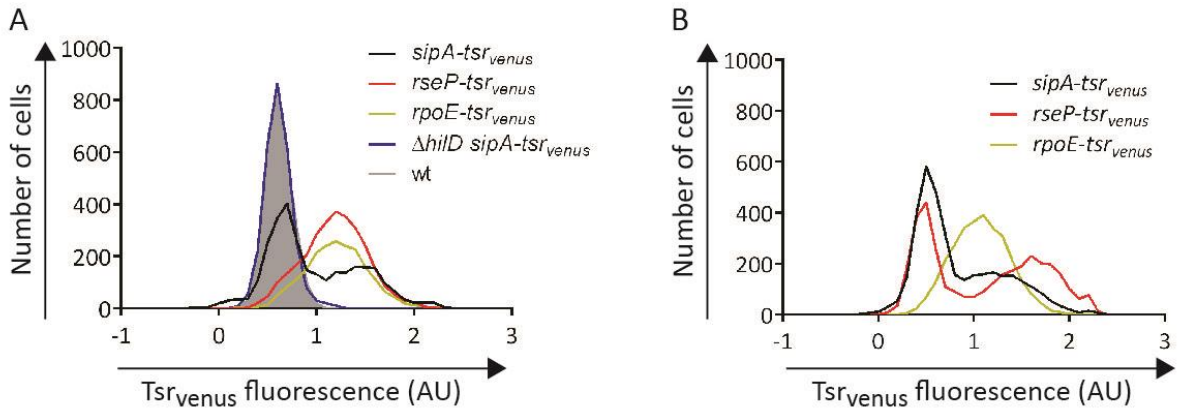

Figure 4.4. Expression analysis of the *rseP-tsr*$_{venus}$ reporter.
Histograms displaying the reporter gene expression of the strains harboring *sipA-tsr*$_{venus}$ (M2000), *rseP-tsr*$_{venus}$ (Z6) and *rpoE-tsr*$_{venus}$ (M2519) with **(B)** and without **(A)** the plasmid-based T1 reporter p*sicA-mCherry* (pM2833). **A)** The wt (SB300) and Δ*hilD sipA-tsr*$_{venus}$ (M2020) strains served as negative controls. **B)** Overlay of the Tsr$_{venus}$ fluorescence signals from the *sipA-tsr*$_{venus}$ (M2000), *rseP-tsr*$_{venus}$ (Z6) and *rpoE-tsr*$_{venus}$ (M2519) strains from Figure 4.2. The displayed data is pooled from three independent experiments. The indicated strains were analyzed during late logarithmic growth phase (4h culture) by microscopy.

In conclusion, we found that *rseP* expression was bimodal in the presence, but unimodal in the absence of the p*sicA-mCherry* plasmid. The reasons for this remained unclear.

Effects of deletion of T1 regulators and T1 assembly genes on *rseP* expression

To analyze whether *t1* expression and T1 needle assembly might generate membrane stress per se and thereby induce *rseP*, we decided to investigate *rseP-tsr*$_{venus}$ expression upon deletion of single genes of the T1 regulatory cascade or the T1 assembly machinery (Figure 4.5A, B). To assess the effects of deletions of the T1 regulatory genes, we deleted the following genes in an *rseP-tsr*$_{venus}$ reporter strain: *hilA* (Δ*hilA rseP-tsr*$_{venus}$), *hilD* (Δ*hilD rseP-tsr*$_{venus}$) and *invF* (Δ*invF rseP-tsr*$_{venus}$). InvF is a transcription factor that is directly controlled by *hilA* (Lostroh and Lee, 2001). Further, we constructed a strain carrying a deletion of the entire SPI-1 island (Δ*spi-1 rseP-tsr*$_{venus}$). The mutant strains lacking *hilA* and *hilD* are incapable of expressing T1, as both genes are essential for the induction of this virulence factor. For all strains, *rseP-tsr*$_{venus}$ expression was analyzed at late stationary phase (4h culture) by microscopy. The *rseP-tsr*$_{venus}$ reporter strain displaying the unimodal distribution was the positive control (Figure 4.5C). The wt control, lacking fluorophore reporters, and the Δ*hilD sipA-tsr*$_{venus}$ strain served as negative controls. The deletion of *spi-1*, *hilA* or *hilD* decreased *rseP-tsr*$_{venus}$ levels, in contrast to *invF* deletion, indicating either a direct regulation of *rseP* by *hilA* or the presence of an additional regulatory cue that acts between *hilA* and *invF*.

We also created additional *rseP-tsr*$_{venus}$ reporter strains displaying deletions of some structural and functional T1 components to induce direct stress to the envelope. We deleted *invH* (Δ*invH rseP-tsr*$_{venus}$), the ATPase *invC* (Δ*invC rseP-tsr*$_{venus}$) and the *inv-spa* and *prg-org* operon (Δ*inv-spa-prg-org rseP-tsr*$_{venus}$). InvH is a structural component of the outer ring of the T1 needle (Figure 4.5B). By its deletion, we hypothesized to infer inner membrane stress, which would be resolved by the RpoE-mediated membrane stress system. The ATPase InvC is required for the translocation of T1 effector proteins through the needle complex into the host cytoplasm. It releases chaperones from their cognate T1 substrates before translocation and might also provide energy for the export (Akeda and Galan, 2005; Eichelberg et al., 1994). Through its close association to the inner membrane (IM), we hypothesized that the deletion could infer increased membrane stress due to stalled translocation of proteins. Through the deletion of the entire *inv-spa* and *prg-org* operon, the entire ring assembly of the T1 needle is impaired and we thereby hypothesized an increased stress imposed on the bacterial envelope. However, neither of these gene deletions lead to an elevation of RseP levels (Figure 4.5D),

indicating that RseP is not affected by the presence, absence or assembly of T1 structural components.

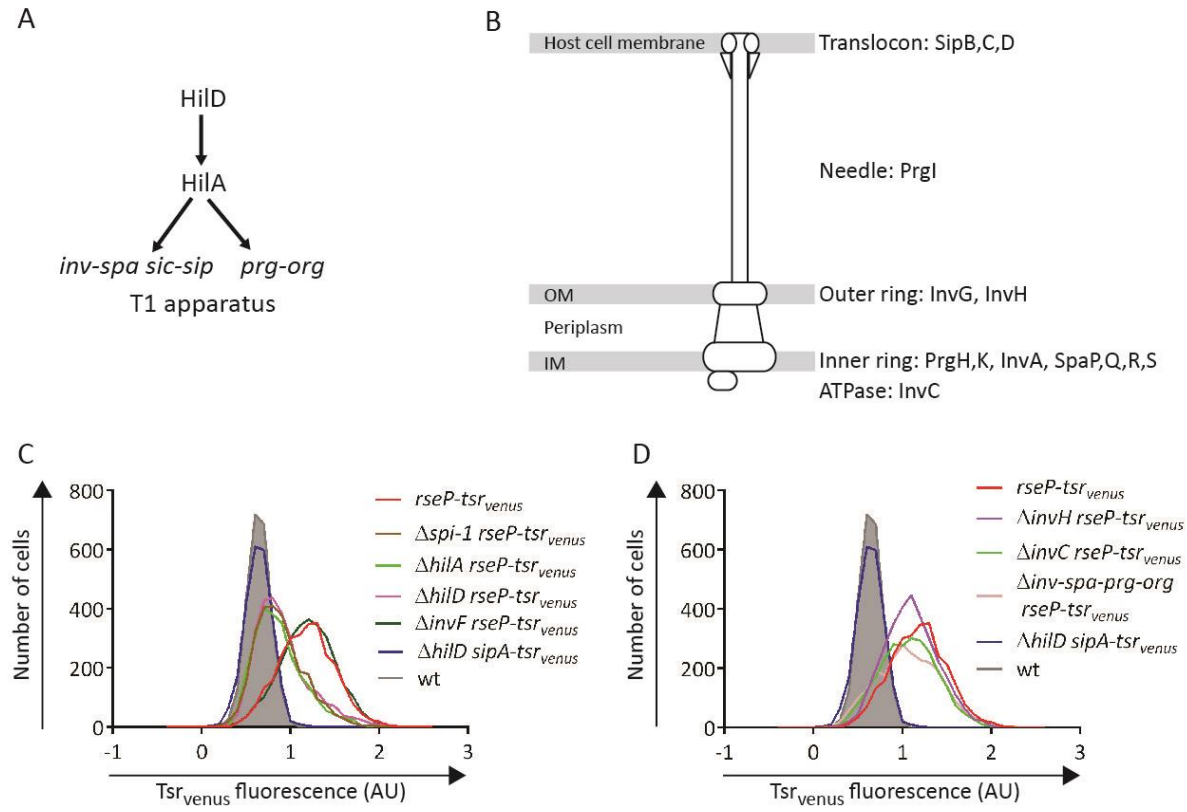

Figure 4.5. Schemes of the T1 needle and the T1 regulation cascade and how deleting T1 regulatory proteins and assembly genes affects *rseP-tsrvenus* expression.
A) Scheme of the T1 regulation cascade. The transcriptional regulators *hilD* and *hilA* induce the expression of downstream operons, including *inv-spa, sic-sip* and *prg-org*. HilD is bistably expressed, resulting in a bistable expression of the downstream regulatory proteins (Saini et al., 2010a). **B)** The T1 needle is composed of numerous structural and functional components, including the inner and outer ring, the needle and the translocon. Figure adapted from (Hoelzer, 2010; Moest and Meresse, 2013). **C)** Effect of deletion of T1 regulatory proteins on *rseP-tsr*$_{venus}$. Microscopic analysis of *rseP-tsr*$_{venus}$ when the transcription factors *hilA* (Δ*hilA rseP-tsr*$_{venus}$*;* Z26*)*, *hilD* (Δ*hilD rseP-tsr*$_{venus}$*;* Z28) and *invF* (Δ*invF rseP-tsr*$_{venus}$*;* Z557) are deleted. The entire SPI-1 island was deleted (Δ*spi-1 rseP-tsr*$_{venus}$*;* Z25) and *rseP-tsr*$_{venus}$ was analyzed. **D)** Analysis of *rseP-tsr*$_{venus}$ upon deletion of T1 assembly and functional components. The *rseP-tsr*$_{venus}$-harboring strains were deleted for *invH* (Δ*invH rseP-tsr*$_{venus}$*;* Z558), *invC* (Δ*invC rseP-tsr*$_{venus}$*;* Z559), and the *inv-spa* and *prg-org* operons (Δ*inv-spa-prg-org rseP-tsr*$_{venus}$*;* Z560). **C, D)** The wt (SB300) and Δ*hilD sipA-tsr*$_{venus}$ (M2020) strains served as negative controls. The *rseP-tsr*$_{venus}$-harboring strain served as positive control. All strains were incubated until they reached late exponential growth (4h cultures), before imaging.

Concluding, we observed a reduction in *rseP* transcription levels when deleting the major T1 regulators *hilD* and *hilA* and the entire SPI-1 island. However, the downstream transcription factor *invF* did not affect *rseP* expression, suggesting an *rseP* regulation by either *hilA* or unknown factors that regulate between HilA and InvF. Furthermore, *rseP* expression is independent of envelope stress that might be caused by the deletion of the structural and functional T1 needle components tested.

Overproduction of mCherry by an arabinose-inducible system does not increase RseP levels

From our previous findings that the expression of *rseP-tsr*$_{venus}$ (but not *rpoE-tsr*$_{venus}$) displayed a bimodal distribution in the presence of the cytoplasmic mCherry fluorophore, we hypothesized that cytoplasmic overproduction of the *mCherry* reporter might play a role. This may link the RpoE-mediated envelope stress response system with cytoplasmic stress. Therefore, we decided to investigate the role of mCherry in RseP expression. We constructed an arabinose-inducible *mCherry* construct to investigate the *rseP-tsr*$_{venus}$ expression when *mCherry* is overexpressed. We grew the strains until late logarithmic growth phase for 4h and analyzed *rseP-tsr*$_{venus}$ expression as described for the previous experiments (see description above and in the materials and methods part). We did not observe any increase in *rseP-tsr*$_{venus}$ expression upon arabinose-dependent *mCherry* overexpression (*rseP-tsr*$_{venus}$ pBAD-*mCherry*; Figure 4.6A). The distribution of *rseP-tsr*$_{venus}$ upon arabinose induction of *mCherry* (*rseP-tsr*$_{venus}$ pBAD-*mCherry* (+); Figure 4.6B) remained similar to the non-induced control (*rseP-tsr*$_{venus}$ pBAD-*mCherry* (-)) and the empty vector control strain, harboring the same plasmid without the *mCherry* gene (*rseP-tsr*$_{venus}$ pBAD-*mCherry* e.v.). However, the arabinose-inducible *mCherry* induction was verified (*rseP-tsr*$_{venus}$ pBAD-*mCherry* (+) vs. (-); Figure 4.6B). The mCherry fluorescence levels of the arabinose-inducible *mCherry* reporter (*rseP-tsr*$_{venus}$ pBAD-*mCherry* (+)) reached similar intensities compared to that of the p*sicA*-driven *mCherry* (*rseP-tsr*$_{venus}$ p*sicA-mCherry*).

Interestingly, in this experiment we observed an overall increase of *rseP-tsr*$_{venus}$ expression in the *S*. Tm strain harboring *rseP-tsr*$_{venus}$ reporter in the presence of the p*sicA-mCherry* plasmid (*rseP-tsr*$_{venus}$ p*sicA-mCherry*; Figure 4.6B), instead of a bimodal distribution as previously observed (Figure 4.2C). However, this is probably because the *mCherry* reporter displayed an increased expression level, in contrast to the bistable distribution observed before.

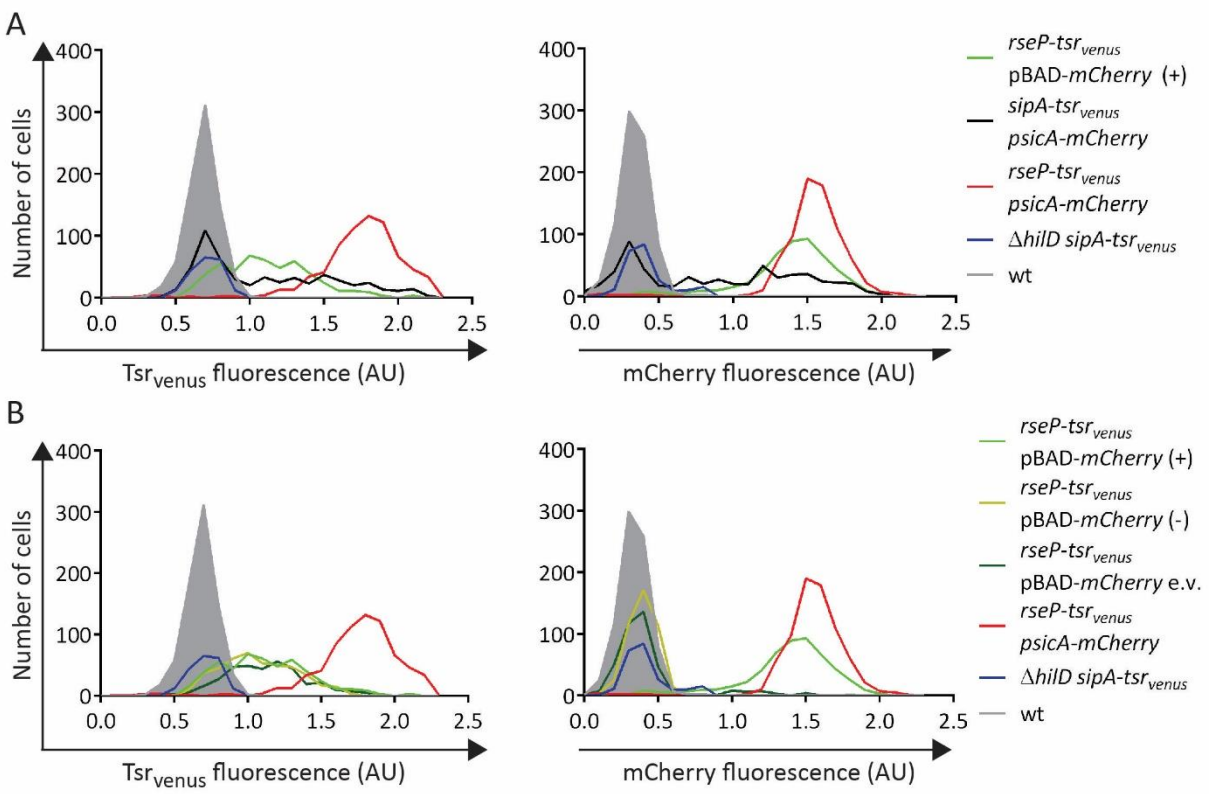

Figure 4.6. Effect of arabinose-inducible *mCherry* on *rseP-tsr*$_{venus}$ expression.
A) The induction of *mCherry* by arabinose was tested. 0.01% arabinose was added during growth of the displayed strains. *rseP-tsr*$_{venus}$ pBAD-mCherry (Z6-pZ515), *sipA-tsr*$_{venus}$ p*sicA-mCherry* (M2000-pM2833), *rseP-tsr*$_{venus}$ p*sicA-mCherry* (Z6-pM2833) were analyzed. **B)** The induction and the "empty" control vector for panel A are shown. The strain *rseP-tsr*$_{venus}$ (Z6) with the arabinose-inducible pBAD-*mCherry* (pZ515) and its empty vector control (e.v.; pZ518) are displayed. The presence or absence of 0.01% arabinose during growth is indicated by "+" or "-", respectively. The wt (SB300) and Δ*hilD sipA-tsr*$_{venus}$ (M2020) strains served as negative controls. All strains were cultured for 4h analyzed by microscopy.

Concluding, we did not observe an increased expression of *rseP* when cytoplasmic mCherry was over-expressed by an arabinose-inducible system. The effect that *rseP-tsr*$_{venus}$ expression "followed" the same pattern as the mCherry fluorophore, expressed under the promoter control of P*sicA*, was confirmed by this experiment. The t*1* expression visualized by mCherry, did not display a bimodal distribution, but rather an increased expression within the whole population. The reasons for this have remained unclear. Nevertheless, this shift was also observed by the Tsr$_{venus}$ distribution. From this data, we can conclude that the T1-driven *mCherry* reporter has an effect on *rseP*, in contrast to the arabinose-inducible pBAD-*mCherry* reporter. However, it remained unclear how and why p*sicA-mCherry* affected *rseP* expression. The presence or absence of mCherry protein (or folding intermediates) do not seem to be sufficient to explain this phenomenon.

4.4 Discussion

In the beginning of this study, we aimed to investigate the role of the zinc-metalloprotease RseP during T1 expression. RseP is involved in the RpoE-mediated stress response system, which lead us to hypothesize that T1 expression causes stress on the envelope that might be alleviated by the RpoE-membrane stress response system. Previous work by Studer and Sturm (Studer *et al*.; unpublished) revealed a co-expression of *rseP* and *t1*. However, we could only observe a bimodal RseP distribution in the presence of a T1-driven *mCherry* reporter. Consequently, this lead us to hypothesize that the cytoplasmic fluorophore mCherry and not T1 might affect *rseP* expression. As previous work by Arnoldini and colleagues has demonstrated a negative effect on growth by overexpression of the *S.* Tm foreign protein LacZ (Arnoldini et al., 2014), the idea that overproduction of the cytoplasmic fluorophore mCherry might have an effect on cell viability and membrane integrity seemed reasonable. When testing this hypothesis with an arabinose-inducible *mCherry* reporter, we did not observe elevated RseP levels upon *mCherry* induction. This refuted the existence of a link between cytoplasmic protein overproduction and the envelope stress response governed by RpoE.

The deletion of *rseP* did not have any effect on the growth rate of the T1 expressing cells. The absence of any effect might be due to the existence of other envelope stress responses, which complement each other. One of these stress systems is the CpxAR two-component system, which is required for pilus assembly and has been shown to be highly activated in an *rpoE* mutant in *S*. Tm (Humphreys et al., 2004). Both systems are triggered by system-specific environmental cues; however, they also share common inducing factors, such as the presence of misfolded proteins in the periplasm and their regulons partially overlap (Duguay and Silhavy, 2004).

We observed a reduction in *rseP* levels upon deletion of the entire SPI-1 island and the major inducers of T1, *hilD* and *hilA*, but not the downstream transcription factor *invF* (Figure 4.5C). This finding indicates an unknown regulation of *rseP* by *hilA*, which is further strengthened by the presence of a *hilA* recognition motif in the *rseP* promoter region (Studer *et al*.; unpublished). However, to investigate the interaction of *hilA* with the *rseP* promoter region, further studies are required. Interestingly, the deletion of T1 assembly genes, which are integrated in the inner and outer membranes of the bacterial envelope, did not affect the

expression of *rseP* (Figure 4.5D). However, as we used the RpoE system as readout for envelope stress, we cannot exclude the involvement of other envelope stress responses to maintain envelope homeostasis. Envelope stress responses have been implicated with virulence in several pathogens. In *S*. Tm, the deletion of *rpoE* impairs virulence and *rpoE* mutants do not survive in macrophages (Humphreys et al., 1999). The RpoE-mediated membrane stress response is essential for survival of *E. coli* (De Las Penas et al., 1997). In *Yersinia* spp., studies have shown a direct link between the lack of envelope stress response systems CpxAR and RpoE to reduced adhesion or translocation of effector proteins during infection (Carlsson et al., 2007a; Carlsson et al., 2007b).

Our study could not clarify the role of T1 or the cytoplasmic fluorophore mCherry in the modulation of RseP and thereby in the RpoE-mediated stress response. The current experimental setup displays some limitations that have to be overcome for further continuation of this project. First, the microscopy protocol needs to be optimized, as all the microscopy data was generated using variable exposure times. Therefore, it is currently difficult to address the question whether the lack of *rseP* induction by the arabinose-inducible *mCherry* (*rseP-tsr*$_{venus}$ pBAD-*mCherry*; Figure 4.6A) compared to the p*sicA*-driven *mCherry* (*rseP-tsr*$_{venus}$ p*sicA-mCherry*) is due to different promoter strengths. Additionally, using the *sipA-tsr*$_{venus}$ strain for T1 visualization, the current 4h time point chosen for analysis has resulted in variable *t1* expression levels (data not shown). This large experimental variation compromises detailed analysis. In case of a correlative expression between *rseP* and *t1*, an earlier time point might reduce *t1* expression but may also alleviate the need for RpoE/RseP. Therefore, for future analyses a later time point displaying more stable *t1* expression might be beneficial.

4.5 Materials and Methods

Bacterial strains and plasmids

All strains used in this study were derivatives of *S*. Tm SL1344 (Hoiseth and Stocker, 1981). A complete list of strains and plasmids is provided in Supplementary Table S4.1 and S4.2, respectively.

For standard microscopy procedures, bacteria were cultured by diluting the overnight cultures 1:20 in LB broth (0.1M) for 4h at 37°C. Folding of the fluorophores was allowed by subsequent addition of spectinomycin to a final concentration of 500 µg/ml and an additional incubation step for 2h. In the induction experiments, expression of the desired proteins was induced by 0.01% arabinose.

Z535 was constructed by P22 transduction of the Z39 lysate (*rseP::aphT*) into M3142 (non-flagellated P*prgH-gfp* background). Z557, Z558 and Z559 were constructed by P22 transduction of the lysates of M2016 *(invF::cat)*, SB150 *(invH::aphT)* and SB566 *(invF::cat)*, respectively, into Z6 *(rseP-tsr$_{venus}$).* Z560 was constructed by P22 transduction of the Z6 lysate *(rseP-tsr$_{venus}$)* into M2072 (*inG-spaS::cat, prgH-org::aphT*). The arabinose-inducible plasmids pZ515 and pZ518 were constructed as follows. The *mCherry* fragment was PCR-amplified from pM2833 with *Nhe*I and *Hind*III overlapping restriction sites. The subsequent restriction digest of pBAD24 (Guzman et al., 1995) and of the *mCherry* construct by *Nhe*I and *Hind*III and ligation resulted in the plasmid pZ511 (pBAD-*mCherry*; ampR). To exchange the ampicillin resistance cassette by a chloramphenicol resistance cassette in pZ511, the *bla* gene was removed by restriction digest with *Hind*III and *Pvu*I and subsequent ligation with the *Hind*III and *Pvu*I digested chloramphenicol PCR fragment, previously amplified from pM2833. This resulted in pZ515 (pBAD-*mCherry*; catR).

The plasmid pZ518 is the empty vector control pZ515 (pBAD-*mCherry*; catR) and was constructed by removing *mCherry* using the restriction endonuclease *EcoR*I and subsequent re-ligation. All plasmids were verified by PCR using the primers indicated in Supplementary Table S4.3.

Fluorescence microscopy

The indicated strains were analyzed by fluorescence microscopy at the respective time points. After the additional incubation in the presence of spectinomycin, 1µl of the bacterial cells was added onto an agarose pad (1% agarose diluted in PBS). For image acquisition, we used the Zeiss Axioscope 2 with a Plan-APOCHROMAT 63x/1.4 oil objective. In addition to phase contrast, the fluorescence intensity of Tsr$_{venus}$ and mCherry was imaged using the appropriate channels. All images were acquired with variable exposure times. Image analysis of single bacteria was performed using Volocity (version 6.3). The maximum fluorescence intensity was

measured and normalized to its own background by subtracting the mean fluorescence intensity of the same area (max-mean fluorescence intensity of a single bacterium). All data were plotted using GraphPad Prism (version 6.07). The correlation analysis was performed using the Spearman correlation analysis in GraphPad Prism. Spearman rank correlation is a non-parametric test to measure the degree of association between two variables. In contrast to linear regression analysis, this test does not make assumptions about the distribution of the samples or the dependency of the analyzed parameters and is used for ordinal or nominal data.

Microfluidic fluorescence microscopy

Design and fabrication of microfluidic devices was performed similar to the procedure by Wang and colleagues (Wang et al., 2010). In short, the silicon master was manufactured using two-step photolithography with SU8 2002 and SU8 3025 (Microchem), first applying the main trench and in a second step the growth channels. The growth channel length was 25 µm, the width ranged from 0.8 µm - 1.2 µm. The length of the main trench was 4.2 mm with the width of 100 µm. The microfluidic device was replica molded from the silicon master by soft lithography using the PDMS elastomer Sylgard 184 Silicone (Bisterfeld Spezialchemie Helvetia GmbH). The PDMS base and curing agent were mixed in a 10:1 ratio (w/w) and subsequently degassed by vacuum, before curing at 80°C for 1h. Finally, the PDMS device was covalently bonded to a glass cover slip after surface activation by air plasma treatment in the plasma cleaner PDC-32G (Harrick Plasma) for 30 sec.

For microfluidics microscopy, the bacterial cells from overnight cultures were diluted 1:100 in 5 ml LB broth and grown at 37°C. They were cultured until reaching early logarithmic growth phase (OD600 ~0.20; ~2h). Cells were then prepared for loading by concentrating them 10x by centrifugation. Before injection of the bacterial cells, the microfluidic device was passivated with LB, containing 1.5% of 10 mg/ml bovine serum albumin (Invitrogen) and 0.5% of 10 mg/ml salmon sperm DNA (Invitrogen) to prevent adhesion of bacterial cells to the PDMS surface. Fresh or LB medium from spent cultures was continuously supplied as indicated by a pump at a constant rate of 2 ml/h. Spent medium was prepared by collecting the supernatant of bacterial cultures grown to late exponential phase (OD600 ~0.9). The supernatant was sterile filtered to remove residual bacterial cells. For each experiment, several positions of the

microfluidic device were imaged, each covering twelve channels. Images were acquired every 3 min using a Zeiss Axiovert 200m inverted microscope with a 100 x oil immersion objective (Plan-Neofluar 100x/1.3 oil, Zeiss) and the Visiview software (Visitron Systems GmbH). The experiments were performed in an incubation chamber (Pecon/Visitron) at 37°C and the focus position was maintained by the CRISP Hardware Autofocus System (ASI). Analysis of the time-lapse movies was performed using the ImageJ software.

Supplementary Table S4.1. Strains used in this study.

Strain	Relevant genotype	Derivative of	Resistance	Reference
SB300	*S*. Tm	SL1344	sm	(Hoiseth and Stocker, 1981)
M3142	wt; *prgH-gfp+; ΔfliC825, ΔfljB217*	JH3010, SL1344 (Hautefort et al., 2003)	cm	Diard *et al*., unpublished;
M2000	*sipA-tsr*$_{venus}$	SL1344	sm, tet	Sturm *et al*., unpublished
M2020	*sipA-tsr*$_{venus}$, *hilD::aphT*	SL1344	tet, kan	Sturm *et al*., unpublished
M2519	*rpoE-tsr*$_{venus}$	SL1344	sm, amp	Sturm *et al*., unpublished
Z6	*rseP-tsr*$_{venus}$	SL1344	sm, amp	Studer *et al*., unpublished
Z25	*spi-1::aphT*, *rseP-tsr*$_{venus}$	SL1344	amp, kan	Studer *et al*., unpublished
Z26	*rseP-tsr*$_{venus}$, *ΔhilA*	SL1344	sm, amp	Studer *et al*., unpublished
Z28	*rseP-tsr*$_{venus}$, *ΔhilD*	SL1344	sm, amp	Studer *et al*., unpublished
Z39	*rseP::aphT*	SL1344	sm, amp	Studer *et al*., unpublished
Z535	*rseP'*(1-142)::*aphT*, *PprgH::gfp*, *ΔfliC825, ΔfljB217*	SL1344; χ8602 (Curtiss and Kang, 2004)	kan, cm	This study
M2016	*invF::cat*	ATCC14028	cm	Sturm *et al*., unpublished
Z557	*rseP-tsr*$_{venus}$, *invF::cat*	Z6	amp, cm	This study
SB150	*invH::aphT*	SL1344	kan	(Altmeyer et al., 1993)
Z558	*rseP-tsr*$_{venus}$, *invH::aphT*	Z6	amp, kan	This study
SB566	*invC::aphT*	SL1344	sm, kan	(Eichelberg et al., 1994)
Z559	*rseP-tsr*$_{venus}$, *invC::aphT*	Z6	amp, kan	This study
M2072	*invG-spaS::cat*, *prgH-org::aphT*	SL1344	kan, cm	Sturm *et al*., unpublished
Z560	*rseP-tsr*$_{venus}$, *invG-spaS::cat*, *prgH-org::aphT*	M2072	amp, kan, cm	This study

sm= streptomycin, cm= chloramphenicol, tet= tetracycline, kan= kanamycin, amp= ampicillin

Supplementary Table S4.2. Plasmids used in this study.

Plasmid	Characteristics	Resistance	Reference
pM2838	p*sicA-mCherry*; *mCherry* under the control of the P*sicA* promoter	amp, cm	(Sturm et al., 2011)
pZ511	ampR; pBAD-*mCherry*; arabinose-inducible mCherry; pBAD24 derivative (pSBR322 ori)	amp	This study
pZ515	catR; pBAD-*mCherry*; arabinose-inducible mCherry; pBAD24 derivative	cm	This study
pZ518	Empty vector of pZ515; pBAD24 derivative	cm	This study

Supplementary Table S4.3. Primer sequences used in this study.

Primer	Primer sequence 5`-3`
GST NcoI fw	GATGACCCATGGATGTCCCCTATACTAGGTTA
GST XbaI rw	CATGGAGTCTAGAATTCCAC
mCh NheI fw	GATGACAAGCTTTAGAGAATAGGAACTTCGGA
mCh HindIII rv	GACCCGTAGAGATCGTACCG
cat PCR HindIII fw	GACAACAAGCCAGGGATGTAAC
cat PCR PvuI rv	GATGACCGATCGGAAAGTATAGGAACTTCGGC

4.6 References

Ackermann, M., B. Stecher, N.E. Freed, P. Songhet, W.D. Hardt, and M. Doebeli. 2008. Self-destructive cooperation mediated by phenotypic noise. *Nature* 454:987-990.

Akeda, Y., and J.E. Galan. 2005. Chaperone release and unfolding of substrates in type III secretion. *Nature* 437:911-915.

Altmeyer, R.M., J.K. McNern, J.C. Bossio, I. Rosenshine, B.B. Finlay, and J.E. Galan. 1993. Cloning and molecular characterization of a gene involved in Salmonella adherence and invasion of cultured epithelial cells. *Molecular microbiology* 7:89-98.

Arnoldini, M., I.A. Vizcarra, R. Pena-Miller, N. Stocker, M. Diard, V. Vogel, R.E. Beardmore, W.D. Hardt, and M. Ackermann. 2014. Bistable expression of virulence genes in salmonella leads to the formation of an antibiotic-tolerant subpopulation. *PLoS biology* 12:e1001928.

Bang, I.S., J.G. Frye, M. McClelland, J. Velayudhan, and F.C. Fang. 2005. Alternative sigma factor interactions in Salmonella: sigma and sigma promote antioxidant defences by enhancing sigma levels. *Molecular microbiology* 56:811-823.

Brissette, J.L., M. Russel, L. Weiner, and P. Model. 1990. Phage shock protein, a stress protein of Escherichia coli. *Proceedings of the National Academy of Sciences of the United States of America* 87:862-866.

Carlsson, K.E., J. Liu, P.J. Edqvist, and M.S. Francis. 2007a. Extracytoplasmic-stress-responsive pathways modulate type III secretion in Yersinia pseudotuberculosis. *Infect Immun* 75:3913-3924.

Carlsson, K.E., J. Liu, P.J. Edqvist, and M.S. Francis. 2007b. Influence of the Cpx extracytoplasmic-stress-responsive pathway on Yersinia sp.-eukaryotic cell contact. *Infect Immun* 75:4386-4399.

Cornelis, G.R. 2010. The type III secretion injectisome, a complex nanomachine for intracellular 'toxin' delivery. *Biological chemistry* 391:745-751.

Cosma, C.L., P.N. Danese, J.H. Carlson, T.J. Silhavy, and W.B. Snyder. 1995. Mutational activation of the Cpx signal transduction pathway of Escherichia coli suppresses the toxicity conferred by certain envelope-associated stresses. *Molecular microbiology* 18:491-505.

Curtiss, R., and H. Kang. 2004. Modulation of immune responses to foreign antigens expressed by recombinant attenuated bacterial vectors. In 30.

De Las Penas, A., L. Connolly, and C.A. Gross. 1997. SigmaE is an essential sigma factor in Escherichia coli. *Journal of bacteriology* 179:6862-6864.

Duguay, A.R., and T.J. Silhavy. 2004. Quality control in the bacterial periplasm. *Biochimica et biophysica acta* 1694:121-134.

Eichelberg, K., C.C. Ginocchio, and J.E. Galan. 1994. Molecular and functional characterization of the Salmonella typhimurium invasion genes invB and invC: homology of InvC to the F0F1 ATPase family of proteins. *Journal of bacteriology* 176:4501-4510.

Ellermeier, J.R., and J.M. Slauch. 2008. Fur regulates expression of the Salmonella pathogenicity island 1 type III secretion system through HilD. *Journal of bacteriology* 190:476-486.

Erickson, J.W., and C.A. Gross. 1989. Identification of the sigma E subunit of Escherichia coli RNA polymerase: a second alternate sigma factor involved in high-temperature gene expression. *Genes & development* 3:1462-1471.

Groisman, E.A., E. Chiao, C.J. Lipps, and F. Heffron. 1989. Salmonella typhimurium phoP virulence gene is a transcriptional regulator. *Proceedings of the National Academy of Sciences of the United States of America* 86:7077-7081.

Guzman, L.M., D. Belin, M.J. Carson, and J. Beckwith. 1995. Tight regulation, modulation, and high-level expression by vectors containing the arabinose PBAD promoter. *Journal of bacteriology* 177:4121-4130.

Hautefort, I., M.J. Proenca, and J.C.D. Hinton. 2003. Single-Copy Green Fluorescent Protein Gene Fusions Allow Accurate Measurement of Salmonella Gene Expression In Vitro and during Infection of Mammalian Cells. *Applied and environmental microbiology* 69:7480-7491.

Hoelzer, S. 2010. Functional analysis of the type III secretion systems in Salmonella enterica. In Naturwissenschaftliche Fakultät. Friedrich-Alexander-Universität Erlangen-Nürnberg (FAU), Nürnberg.

Hoiseth, S.K., and B.A. Stocker. 1981. Aromatic-dependent Salmonella typhimurium are non-virulent and effective as live vaccines. *Nature* 291:238-239.

Humphreys, S., G. Rowley, A. Stevenson, M.F. Anjum, M.J. Woodward, S. Gilbert, J. Kormanec, and M. Roberts. 2004. Role of the two-component regulator CpxAR in the virulence of Salmonella enterica serotype Typhimurium. *Infect Immun* 72:4654-4661.

Humphreys, S., A. Stevenson, A. Bacon, A.B. Weinhardt, and M. Roberts. 1999. The alternative sigma factor, sigmaE, is critically important for the virulence of Salmonella typhimurium. *Infect Immun* 67:1560-1568.

Kenyon, W.J., S.M. Thomas, E. Johnson, M.J. Pallen, and M.P. Spector. 2005. Shifts from glucose to certain secondary carbon-sources result in activation of the extracytoplasmic function sigma factor sigmaE in Salmonella enterica serovar Typhimurium. *Microbiology* 151:2373-2383.

Leblanc, S.K., C.W. Oates, and T.L. Raivio. 2011. Characterization of the induction and cellular role of the BaeSR two-component envelope stress response of Escherichia coli. *Journal of bacteriology* 193:3367-3375.

Lostroh, C.P., and C.A. Lee. 2001. The HilA box and sequences outside it determine the magnitude of HilA-dependent activation of P(prgH) from Salmonella pathogenicity island 1. *Journal of bacteriology* 183:4876-4885.

McBroom, A.J., and M.J. Kuehn. 2007. Release of outer membrane vesicles by Gram-negative bacteria is a novel envelope stress response. *Molecular microbiology* 63:545-558.

McMeechan, A., M. Roberts, T.A. Cogan, F. Jorgensen, A. Stevenson, C. Lewis, G. Rowley, and T.J. Humphrey. 2007. Role of the alternative sigma factors sigmaE and sigmaS in survival of Salmonella enterica serovar Typhimurium during starvation, refrigeration and osmotic shock. *Microbiology* 153:263-269.

Mecsas, J., P.E. Rouviere, J.W. Erickson, T.J. Donohue, and C.A. Gross. 1993. The activity of sigma E, an Escherichia coli heat-inducible sigma-factor, is modulated by expression of outer membrane proteins. *Genes & development* 7:2618-2628.

Miller, S.I., A.M. Kukral, and J.J. Mekalanos. 1989. A two-component regulatory system (phoP phoQ) controls Salmonella typhimurium virulence. *Proceedings of the National Academy of Sciences of the United States of America* 86:5054-5058.

Moest, T.P., and S. Meresse. 2013. Salmonella T3SSs: successful mission of the secret(ion) agents. *Current opinion in microbiology* 16:38-44.

Neuenschwander, M. 2007. High-throughput assays for detecting enzymatic activities in living cells. In ETH Zurich, Zurich.

Oberhettinger, P., M. Schütz, J.C. Leo, N. Heinz, J. Berger, I.B. Autenrieth, and D. Linke. 2012. Intimin and invasin export their C-terminus to the bacterial cell surface using an inverse mechanism compared to classical autotransport. *PloS one* 7:e47069.

Osterberg, S., T. del Peso-Santos, and V. Shingler. 2011. Regulation of alternative sigma factor use. *Annual review of microbiology* 65:37-55.

Ruiz, N., D. Kahne, and T.J. Silhavy. 2006. Advances in understanding bacterial outer-membrane biogenesis. *Nature reviews. Microbiology* 4:57-66.

Runkel, S., H.C. Wells, and G. Rowley. 2013. Living with Stress: A Lesson from the Enteric Pathogen Salmonella enterica. *Advances in applied microbiology* 83:87-144.

Saini, S., J.R. Ellermeier, J.M. Slauch, and C.V. Rao. 2010. The role of coupled positive feedback in the expression of the SPI1 type three secretion system in Salmonella. *PLoS pathogens* 6:e1001025.

Schechter, L.M., S. Jain, S. Akbar, and C.A. Lee. 2003. The small nucleoid-binding proteins H-NS, HU, and Fis affect hilA expression in Salmonella enterica serovar Typhimurium. *Infect Immun* 71:5432-5435.

Sturm, A., M. Heinemann, M. Arnoldini, A. Benecke, M. Ackermann, M. Benz, J. Dormann, and W.D. Hardt. 2011. The cost of virulence: retarded growth of Salmonella Typhimurium cells expressing type III secretion system 1. *PLoS pathogens* 7:e1002143.

Temme, K., H. Salis, D. Tullman-Ercek, A. Levskaya, S.H. Hong, and C.A. Voigt. 2008. Induction and relaxation dynamics of the regulatory network controlling the type III secretion system encoded within Salmonella pathogenicity island 1. *Journal of molecular biology* 377:47-61.

Wang, P., L. Robert, J. Pelletier, W.L. Dang, F. Taddei, A. Wright, and S. Jun. 2010. Robust growth of Escherichia coli. *Current biology : CB* 20:1099-1103.

Yu, J., J. Xiao, X. Ren, K. Lao, and X.S. Xie. 2006. Probing gene expression in live cells, one protein molecule at a time. *Science* 311:1600-1603.

5 Chapter 5 - General discussion

The importance of understanding phenotypic diversity within isogenic bacterial populations has been recognized during the last years. To understand the reasons behind the co-existence of different phenotypes within a genetically identical population, it is crucial to study the different subpopulations. In particular, analyzing the differential gene expression patterns between the subpopulations is of interest to understand different behavior of isogenic bacterial cells. In *S*. Tm, the existence of two phenotypes for type three secretion system 1 (T1) expression ($T1^+$= T1 expressing; $T1^-$= T1 non-expressing) has been subject of numerous studies (e.g. (Ackermann et al., 2008; Diard et al., 2013; Ellermeier and Slauch, 2003; Hautefort et al., 2003; Saini et al., 2010a; Temme et al., 2008)). These studies focus on the analysis of single genes regulating the T1. However, to reveal dynamic and mechanistic insights behind the bistable behavior of T1, the simultaneous analysis of several transcription factors regulating T1 expression is of major interest.

I present here two tools, the epitope-tagged autotransporter invasin for gene expression analysis in *S*. Tm and the microfluidics microscopy setup that allows gene expression analysis of subpopulations at single cell level. We show a proof-of-concept that the hemagglutinin-tagged invasin (*invA*$_{HA}$) provides a suitable alternative to the *gfp* fluorescent reporter for monitoring gene expression in *S*. Tm (Chapter 2). We further show the establishment of the microfluidics microscopy setup, a single cell analysis tool for gene expression analysis. We demonstrated *t1* gene expression using a *gfp* reporter that was under the control of the SPI-1 regulon (Chapter 3). Single cells that express genes transcriptionally fused to *invA*$_{HA}$ could also be analyzed in the microfluidics setup. For this, the medium providing continuous nutritional supply has to be supplemented with epitope-specific antibodies. Thereby, gene expression could be analyzed in real-time by specific staining of the surface localized epitope tags. Combined, these two tools provide a powerful means for the analysis of the T1 regulatory genes within single cells in constant environmental conditions.

5.1 The complexity and origin of T1 bistability in *S*. Tm

For a successful invasion into eukaryotic cells, *S*. Tm is dependent on a functional T1. The T1 mediates translocation of T1 effectors that trigger the engulfment of the bacterial cell by initiating actin re-arrangement within the host cell. For the expression of all T1 components, *S*. Tm faces a high metabolic burden, which results in a significant retardation of growth (Sturm et al., 2011). If during the infection of a mammalian host, the entire bacterial population expressed the T1 virulence factor, the reduced growth would pose a high threat to the survival of the entire genotype. Therefore, *S*. Tm has evolved different phenotypes in T1 expression, with only a subpopulation displaying the slow growing $T1^+$ phenotype, while the majority of cells remain fast growing and $T1^-$. This division of labor has been described to increase *S*. Tm fitness, as both populations are required for the successful infection process (Ackermann et al., 2008; Stecher et al., 2007).

Because of the high "cost", imposed by the metabolic burden caused by expressing T1, *S*. Tm needs to rigorously control the expression of this virulence factor. The regulation of T1 is a highly complex process, which relies on the presence of the transcription factors *hilD*, *hilC*, *hilA* and *rtsA* and the major negative regulator *hilE.* The former three transcription factors each display auto-regulatory loops and influence the expression of each other by positive stimulation (Figure 5.1A) (Ellermeier and Slauch, 2007; Moest and Meresse, 2013). In addition to the predisposition of the bacterial cell (e.g. by elevated molecule numbers of the T1 core regulatory proteins to reach the T1 activation threshold more easily), the timing for T1 expression is influenced by environmental stimuli, which are sensed by global regulators, such as BarA/SirA and PhoQ/PhoP. The BarA/SirA two-component system activates T1 expression by inhibiting the *csrA*-mediated repression of *hilD* when the nutrient availability changes (Martinez et al., 2011). In contrast, T1 is repressed in acidic environments and low Mg^{2+} levels by the PhoQ/PhoP two-component system through repression of SPI-1 encoded *prg* genes (PhoP-repressed genes) and *hilA* (Bajaj et al., 1996; Behlau and Miller, 1993; Pegues et al., 1995). Such environmental cues are probably found during the late logarithmic growth phase *in vitro*, in addition to low oxygen availability. The medium from these cells seems to contain all metabolites and cues required to induce other cells, which have not previously been expressing T1. Interestingly, although conditions with low-oxygen pressure favor T1 induction

(Sturm et al., 2011), low oxygen concentrations seem not to be crucial for the expression of T1, because T1 induction using this spent medium can also be achieved in the presence of oxygen (Chapter 3) (Arnoldini et al., 2014; Sturm et al., 2011). This indicates that the induction of T1 in *S*. Tm is driven by multiple factors, including environmental cues as well as the predisposition of the cell itself.

Although the main transcriptional regulators of the T1 cascade are quite well established, the origin of T1 bistability in *S*. Tm still remains unclear. A previous study by Temme and colleagues suggested the formation of bistability at the *invF* transcription level (downstream of *hilA*) by the formation of a "split" positive feedback loop formed by InvF and its chaperone SicA. However, in their study *hilD* did not display bistability (Temme et al., 2008). The study by Saini and colleagues demonstrated that bistability is generated by *hilD*, because bistable expression of T1 was converted into a rheostatic response after the promoter of *hilD* was replaced by the weaker *hilC* promoter (Saini et al., 2010a). Another study by Baxter and colleagues indicated the presence of a more upstream source of bistability by showing that T1 expression is controlled by HilE, via HilD repression (Baxter et al., 2003). The proven presence of a T1 regulator, which is encoded outside SPI-1 and acts on HilD, further complicates the search for the origin of bistability of T1.

5.2 Autotransporters as a multidimensional reporter system for T1 gene expression

As stated before, the predisposition to T1 expression of a bacterial cell seems to be an important factor determining a particular T1 phenotype. In an isogenic population, which shares the same environment, only a fraction of cells express T1 (Bumann, 2002; Diard et al., 2013; Hautefort et al., 2003; Sturm et al., 2011). Why is this? Depending on the levels of HilD and the other T1 core regulators within a cell, the unknown T1-inducing environmental cue can only induce T1 expression in those cells that reach the activation threshold to initiate the positive feedback loop and thereby trigger the expression of genes of the T1 machinery. To understand the involvement of the different transcription factors in T1 activation better, it is therefore essential to analyze their interplay prior to induction in a single cell. The dynamical

assessment of the expression of the T1 regulatory genes before T1 induction would therefore provide major insights into the mechanism of T1 expression. Previous studies analyzing T1 transcriptional regulators used amongst others β-galactosidase, luciferase or fluorescent proteins for the analysis of gene expression (e.g. (Bumann, 2002; Ellermeier et al., 2005; Ellermeier and Slauch, 2003; Saini et al., 2010a; Sturm et al., 2011)). While the first two options measure readouts on population level, only the latter provides single cell readouts. Most studies were performed using plasmid-based transcriptional fusions with the promoter of interest. In a highly sensitive and fine-tuned system like the T1 regulation cascade, the addition of an additional promoter might already change the promoter-transcription factor ratio and thereby skew the entire system. As most transcription factors are expressed at very low levels, the use of fluorophores might not provide enough sensitivity for detection. An alternative is presented by the use of the fusion of the membrane protein Tsr with Venus, as presented by Yu and colleagues. Tsr anchors the fluorescent protein Venus to the membrane and thereby increases the signal by concentrating it at one position (Yu et al., 2006). However, studies analyzing T1 regulatory genes using multiple reporters within single cells are lacking. Furthermore, for dynamical studies the use of different fluorescent proteins hinders accurate assessment of expression because of varying maturation kinetics.

We therefore aimed to set up an alternative system to fluorescent proteins to study multiple regulatory genes controlling T1 within single cells. The approach using the epitope-tagged autotransporter invasin (InvA), described in Chapter 2, will allow dynamical analysis of gene expression, in particular if we could verify that different InvA variants do feature equivalent maturation kinetics. Furthermore, by using chromosomal transcriptional fusions of the *invA* reporter downstream of the gene of interest, we should not interfere with the ratios of the promoters and the respective regulators.

We used a two-reporter setup with GFP and the HA-tagged invasin ($InvA_{HA}$) to demonstrate proof-of-principle for the suitability of $InvA_{HA}$ to display T1 gene expression. However, the current O-antigen-deficient strain background (Δ*wbaP*) is not optimal for studying T1 expression and additionally is not suited for *in vivo* applications. This is particularly true, as we detected a decrease of T1 expression upon deletion of the O-antigen (Chapter 2). Previous reports studying the effects of O-antigen deletion in *S*. Tm, observed an increased invasion into non-polarized HeLa and polarized MDCK cells, in addition to increased susceptibility to

complement and antimicrobial peptide killing (Holzer et al., 2009; Ilg et al., 2009; Kong et al., 2011). An increased invasiveness in strains with a modified O-antigen polysaccharide chain was also reported for other pathogens. In *Shigella* flexneri, LPS modification by glycosylation was directly linked to an increased invasiveness of the type three secretion system *in vivo*. West and colleagues showed that glycosylation rendered the LPS layer more compact, thereby reducing its length and consequently enhancing the access of the type three secretion system needle to the host cells (West et al., 2005). Similarly, *Pseudomonas aeruginosa* O-antigen mutants displayed increased secretion of type three secretion system effectors, thereby enhancing the severity of pathogenicity *in vivo* (Augustin et al., 2007).

Engineering the epitope tag into the SL1344 SB300 wild-type (wt) background would provide major advantages, as this strain has efficiently been used for *in vivo* infections and *in vitro* T1 analyses (e.g. (Ackermann et al., 2008; Barthel et al., 2003; Diard et al., 2014; Maier et al., 2014b; Sturm et al., 2011)). Future work should focus on placing the epitope tag to the outermost C-terminus of InvA, at a similar position as described for the Strep-tag of the autotransporter intimin (Oberhettinger et al., 2015). This might position the epitope tag suitably so that it can be stained on the bacterial surface in the presence of an intact O-side chain. The LPS of *S*. Tm and other serovars exhibits a complex surface structure with varying O-antigen lengths (short, long, very long O-antigen types) on the bacterial surface. The length depends on the number of O-antigen units attached to the core polysaccharide. In *S*. Tm, the O-antigen displays 16 to over 100 O-antigen repeats. However, the distribution of the differentially long O-antigen variants on the bacterial surface and the LPS length in *S*. Tm is not known (Holzer et al., 2009). Considering the different O-antigen variants, it is not clear whether the epitope-tagged InvA, with a reported length of 180 angstrom (~18 nm) (Hamburger et al., 1999) will be stained in the presence of long and very long O-antigen variants. To ensure epitope staining, one could test an adhesin with a length similar to the *S*. Tm giant adhesin SiiE, which was reported to reach out the LPS layer with a length of 175 ± 5nm (Barlag and Hensel, 2015; Griessl et al., 2013).

Once the *invA*$_{HA}$ reporter is integrated in SB300, future work could expand the *invA* reporter system to allow the analysis of multiple genes. This could be done by exchanging the HA epitope of the *invA* gene with other epitope tags, including Strep, c-myc or FLAG. Every gene of interest could then be transcriptionally fused with the different *invA* fusion genes,

harboring one of the mentioned epitopes. In an optimal scenario, as shown in Figure 5.1B, it would be possible to study the expression of multiple genes, by antibody staining of the corresponding epitopes. The expression of e.g. *hilD*, *hilE*, *hilA* and *prgH* could then be analyzed simultaneously by specific staining for the HA, Strep, c-myc or FLAG epitopes on the bacterial surface.

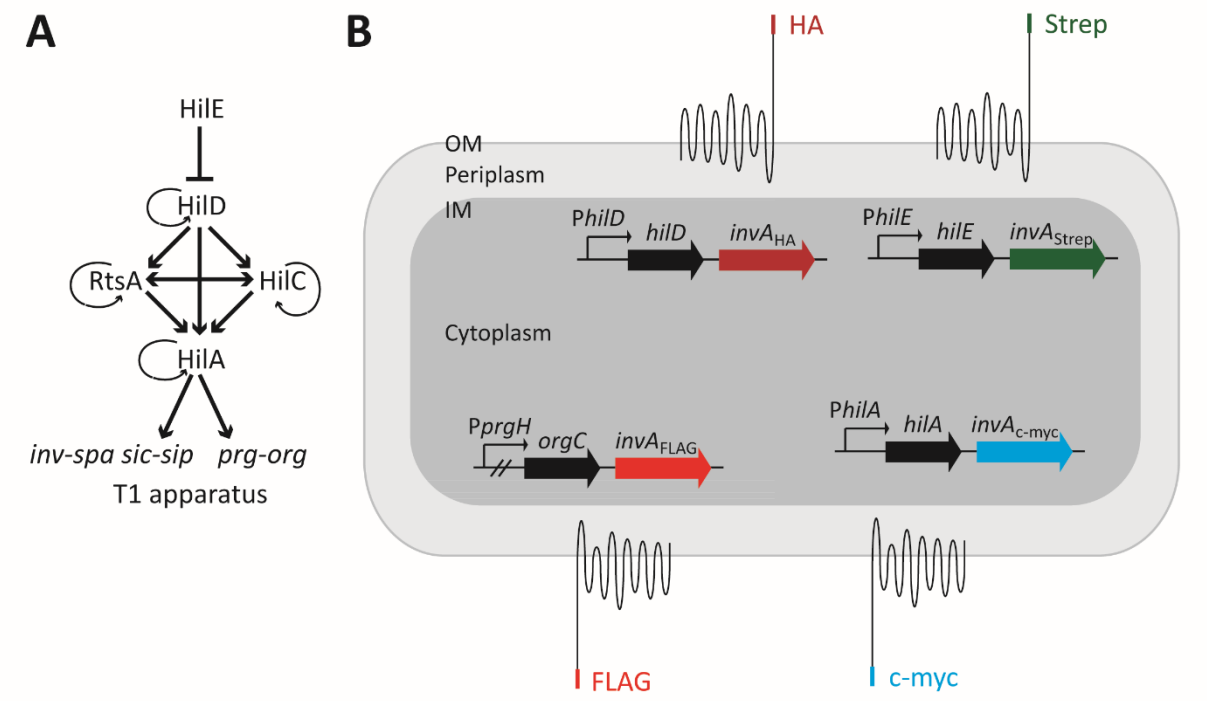

Figure 5.1. T1 regulation cascade and future perspective of a multidimensional *invA* reporter system.
A) T1 regulation cascade. The transcriptional regulators *hilD, hilC, hilA* and the three major operons *inv-spa, sic-sip* and *prg-org* operons are encoded on SPI-1. The major T1 repressor *hilE* and *rtsA* are encoded outside SPI-1. Figure adapted from (Ellermeier and Slauch, 2007). **B)** Scheme of a reporter system employing four differentially tagged invasin autotransporters carrying epitopes inserted into the C-terminal region of the extracellular passenger domain. Surface staining for the epitope tags HA, Strep, c-myc, FLAG epitopes would thereby allow monitoring the intracellular expression of *hilD, hilC, hilA* and *prgH* by individual *S*. Tm cells (epitopes and the corresponding genes are indicated by the same color). OM= outer membrane, IM = inner membrane

Overall, the advantages of the multidimensional *invA*-based reporter system over the fluorescent protein approach would be that i) multiple genes can be analyzed in real time during live microscopy ii) the maturation kinetics may be similar for all differentially tagged *invA* genes iii) the sensitivity might be higher as the fluorescence signal provided by the antibody-stained signal can be increased by introducing more than one fluorophore per antibody (or Fab fragment) in additional staining steps.

5.3 Microfluidics microscopy to analyze *t1* gene expression using epitope-tagged InvA

Traditionally, in microbial research conclusions were drawn from readouts that were obtained from bulk assay experiments. Culture-wide reporters, such as β-galactosidase or bioluminescence-based reporters fused to the promoter of interest, provided information on the general promoter activity. However, these assays usually assumed that all analyzed cells were similar and did not distinguish between differentially expressing cells. Thereby heterogeneity within the population was neglected and resulted in bulk readouts that generally provided information from a mixed population.

Advances in single cell studies using e.g. fluorescent molecules in combination with flow cytometry or microscopy have advanced the study of cellular individuality (Smits et al., 2006a; Smits et al., 2006b). However, flow cytometric analysis of bulk cultures still disregards the timing of events, which have led to the observed phenotype. More recent studies have used microfluidics to study individual bacterial cells within small channels that allow observation of single cells over extended time periods (Arnoldini et al., 2014; Hol and Dekker, 2014; Wang et al., 2010).

I show here that the microfluidic setup, similar to that described by Wang and colleagues (Wang et al., 2010), was successfully tested using a fluorescent reporter that indicated T1 expression. Using this setup, the *invA*$_{HA}$ reporter system, described in Chapter 3, can be analyzed in principle. During microfluidics microscopy, T1 expression in *S*. Tm cells can easily be induced using spent medium. The beauty of this system is that it allows live staining of surface exposed epitopes by applying epitope-specific antibodies with the medium that is continuously supplied throughout the experiment. Thus, using *S*. Tm strains, genetically encoding differentially tagged *invA* variants for the visualization of e.g. *hilD*, *hilC* and *hilA* (as depicted in Figure 5.1B), it would be possible to investigate their hierarchy and dynamic interaction before T1 expression occurs. By transcriptionally fusing the different epitope-tagged *invA* variants downstream of other genes of interest within single cells, gene expression could be analyzed, without introducing any bias by differential maturation kinetics, providing that the *invA* variants display similar folding times. However, the influence of the

different epitopes on the maturation or folding properties of InvA has to be tested first. Thereby, it would be possible to investigate the dynamical expression of the different T1 transcription factors. This would shed more light on the mechanism behind T1 bistability within individual cells.

5.4 The RpoE-mediated stress response and its role in during T1 expression in *S.* Tm

The bacterial membrane is a crucial first line of defense for bacteria to combat various stresses (e.g. antimicrobial peptides, oxidative stress) imposed by the host. We analyzed the role of the RpoE-mediated membrane stress response, in particular the role of the zinc-metalloprotease RseP and its involvement during T1 expression in *S*. Tm. With our current analysis setup, we could not demonstrate the involvement of RseP in T1 expression during late logarithmic growth. However, in the presence of a T1 reporter plasmid we observed an increased RseP response, which was uncoupled from RpoE. In *S*. Tm, so far RseP has only been described in the context of RpoE activation (Rowley et al., 2011). However, in *Vibrio cholerae*, RseP clearly serves additional functions. In addition to the activating role of RpoE, Chatterjee and colleagues found that RseP actively cleaves the central *V. cholerae* virulence regulator TcpP during conditions of extracytoplasmic stress. They induced envelope stress by the deletion of *fadD*, a gene encoding a long-chain fatty acyl-CoA ligase, which is responsible for the integration of TcpP into the inner membrane (Chatterjee and Chowdhury, 2013).

Thus, in *V. cholerae*, RseP displays an additional role in addition to its contribution to RpoE activation. We can speculate that in our presented *S*. Tm model RseP also serves an additional unknown function. The existence of such a function is suggested by the presence of a T1-driven (but not by an inducible) *mCherry* reporter plasmid, suggesting a dependency on both the fluorescent reporter and T1 expression. The T1 reporter plasmid might cause a certain envelope stress for the bacterial cell that does not activate RpoE directly, but rather activates RseP independently. However, to test whether the effect of increasing *rseP* expression by the T1-driven *mCherry* reporter is solely attributable to mCherry or also to other fluorescent proteins, other reporters, such as *gfp*, will have to be tested for their effect on *rseP*.

In *V. cholerae*, the RpoE-mediated stress response is induced in the *fadD* mutant as a result of the inability of the TcpP to integrate into the inner membrane (Chatterjee and Chowdhury, 2013). Interestingly, in our *S*. Tm system the deletion of genes encoding factors required for T1 assembly within the inner and outer membrane did not trigger any increase in RseP levels. This suggests that the truncated T1 needle either did not cause any membrane stress or that other envelope stress responses might have compensated the compromised T1 assembly. To investigate the effects of disturbed T1 needle assembly on membrane stress, future work could focus on investigating the involvement of other envelope stress response systems.

The dependency of *rseP* on *t1* gene expression is illustrated by the reduction of RseP levels in the absence of *hilA* and SPI-1 in general. This is further strengthened by the presence of a putative *hilA*-binding motif in the *rseP* promoter region (Studer and Sturm, unpublished). However, overexpression of *hilA* did not increase *rseP* (or *rpoE*) expression (Studer, unpublished), suggesting that an additional unknown factor might be involved in the *hilA*-mediated control of *rseP*.

It is tempting to speculate that RseP and thereby the RpoE-mediated stress response is involved during T1 needle assembly. Links between type three secretion and membrane stress responses have been demonstrated already in several pathogens. *S*. Tm mutants of *rpoE* or *rseP* display a highly attenuated phenotype *in vivo* and are not capable of surviving in the acidic intracellular environment within macrophages (Humphreys et al., 1999; Rowley et al., 2011). The presence of the RpoE-mediated membrane stress response in *E. coli* is essential for survival upon heat or ethanol stress conditions or misfolding of proteins in the periplasm (De Las Penas et al., 1997). Furthermore, in *Yersinia* spp. several envelope stress responses have been connected to virulence. Interestingly, the phage shock protein (Psp) response is induced by type three secretion system (TTSS) in *Yersinia* spp. There, this seems to mitigate the membrane stress imposed by the expression of the TTSS (Flores-Kim and Darwin, 2012).

Overall, the fluorescent reporter *mCherry* might not be the optimal tool for studying membrane stress responses. In our system, the mCherry fluorescent protein used as T1 reporter clearly affected the RseP response. However, the influence of other fluorescent proteins on RseP has to be tested.

5.5 Final remarks

A key step towards elucidating the origins of T1 bistability is the dynamic gene expression analysis of all T1 transcriptional regulators simultaneously within single cells. This study set out to establish an alternative gene expression reporter system to the standard *gfp* fluorescent reporter. Using the *invA*$_{HA}$ transcriptional reporter, we demonstrated that this reporter system displays *t1* expression equivalently to the *gfp* reporter. Because we used an O-antigen-deficient strain for our analysis, we found a reduction in the T1^{+} population. Future studies will have to relocate the HA epitope tag accordingly to enable the transfer of the *invA*$_{HA}$ reporter into the O-antigen-proficient background of the S. Tm SB300 strain. Further, we were able to establish a microfluidics microscopy technique. We demonstrated the functionality of this method for single cell analysis by analyzing T1 expression using a *gfp* reporter. The previously published T1 induction using spent medium was confirmed. Additionally we observed the increase in T1^{+} cells when deleting the major T1 repressor HilE, as shown in a previous study. This microfluidics microscopy technique could be used in combination with the *invA*$_{HA}$ reporters for single cell gene expression analysis by antibody staining of the surface exposed epitopes. Finally, we were not able to clarify the link between *t1* and *rseP* expression. This underlines the complexity of the T1 regulation network.

5.6 References

Acar, M., J.T. Mettetal, and A. van Oudenaarden. 2008. Stochastic switching as a survival strategy in fluctuating environments. *Nature genetics* 40:471-475.

Ackermann, M. 2013. Microbial individuality in the natural environment. *The ISME journal* 7:465-467.

Ackermann, M. 2015. A functional perspective on phenotypic heterogeneity in microorganisms. *Nature reviews. Microbiology* 13:497-508.

Ackermann, M., B. Stecher, N.E. Freed, P. Songhet, W.D. Hardt, and M. Doebeli. 2008. Self-destructive cooperation mediated by phenotypic noise. *Nature* 454:987-990.

Akeda, Y., and J.E. Galan. 2005. Chaperone release and unfolding of substrates in type III secretion. *Nature* 437:911-915.

Alpuche Aranda, C.M., J.A. Swanson, W.P. Loomis, and S.I. Miller. 1992. Salmonella typhimurium activates virulence gene transcription within acidified macrophage phagosomes. *Proceedings of the National Academy of Sciences of the United States of America* 89:10079-10083.

Altier, C. 2005. Genetic and environmental control of salmonella invasion. *Journal of microbiology* 43 85-92.

Altmeyer, R.M., J.K. McNern, J.C. Bossio, I. Rosenshine, B.B. Finlay, and J.E. Galan. 1993. Cloning and molecular characterization of a gene involved in Salmonella adherence and invasion of cultured epithelial cells. *Molecular microbiology* 7:89-98.

An, Y., W. Wu, and A. Lv. 2010. A PCR-after-ligation method for cloning of multiple DNA inserts. *Analytical biochemistry* 402:203-205.

Arnoldini, M., I.A. Vizcarra, R. Pena-Miller, N. Stocker, M. Diard, V. Vogel, R.E. Beardmore, W.D. Hardt, and M. Ackermann. 2014. Bistable expression of virulence genes in salmonella leads to the formation of an antibiotic-tolerant subpopulation. *PLoS biology* 12:e1001928.

ASI Applied Scientific Instrumentation. 2014. CRISP Autofocus System Manual. In Applied Scientific Instrumentation.

Audia, J.P., C.C. Webb, and J.W. Foster. 2001. Breaking through the acid barrier: an orchestrated response to proton stress by enteric bacteria. *International journal of medical microbiology : IJMM* 291:97-106.

Augustin, D.K., Y. Song, M.S. Baek, Y. Sawa, G. Singh, B. Taylor, A. Rubio-Mills, J.L. Flanagan, J.P. Wiener-Kronish, and S.V. Lynch. 2007. Presence or absence of lipopolysaccharide O antigens affects type III secretion by Pseudomonas aeruginosa. *Journal of bacteriology* 189:2203-2209.

Baek, C.H., S. Wang, K.L. Roland, and R. Curtiss, 3rd. 2009. Leucine-responsive regulatory protein (Lrp) acts as a virulence repressor in Salmonella enterica serovar Typhimurium. *Journal of bacteriology* 191:1278-1292.

Bajaj, V., R.L. Lucas, C. Hwang, and C.A. Lee. 1996. Co-ordinate regulation of Salmonella typhimurium invasion genes by environmental and regulatory factors is mediated by control of hilA expression. *Molecular microbiology* 22:703-714.

Bang, I.S., J.G. Frye, M. McClelland, J. Velayudhan, and F.C. Fang. 2005. Alternative sigma factor interactions in Salmonella: sigma and sigma promote antioxidant defences by enhancing sigma levels. *Molecular microbiology* 56:811-823.

Barlag, B., and M. Hensel. 2015. The giant adhesin SiiE of Salmonella enterica. *Molecules* 20:1134-1150.

Barnhart, M.M., and M.R. Chapman. 2006. Curli biogenesis and function. *Annual review of microbiology* 60:131-147.

Barthel, M., S. Hapfelmeier, L. Quintanilla-Martinez, M. Kremer, M. Rohde, M. Hogardt, K. Pfeffer, H. Russmann, and W.D. Hardt. 2003. Pretreatment of mice with streptomycin provides a Salmonella enterica serovar Typhimurium colitis model that allows analysis of both pathogen and host. *Infect Immun* 71:2839-2858.

Baxter, M.A., T.F. Fahlen, R.L. Wilson, and B.D. Jones. 2003. HilE Interacts with HilD and Negatively Regulates hilA Transcription and Expression of the Salmonella enterica Serovar Typhimurium Invasive Phenotype. *Infection and Immunity* 71:1295-1305.

Baxter, M.A., and B.D. Jones. 2005. The fimYZ genes regulate Salmonella enterica Serovar Typhimurium invasion in addition to type 1 fimbrial expression and bacterial motility. *Infect Immun* 73:1377-1385.

Becskei, A., and L. Serrano. 2000. Engineering stability in gene networks by autoregulation. *Nature* 405:590-593.

Behlau, I., and S.I. Miller. 1993. A PhoP-repressed gene promotes Salmonella typhimurium invasion of epithelial cells. *Journal of bacteriology* 175:4475-4484.

Belden, W.J., and S.I. Miller. 1994. Further characterization of the PhoP regulon: identification of new PhoP-activated virulence loci. *Infect Immun* 62:5095-5101.

Bigger, B.W. 1944. Treatment of staphylococcal infecitons with penicillin. *The Lancet* 244:497-500.

Bodelon, G., E. Marin, and L.A. Fernandez. 2009. Role of periplasmic chaperones and BamA (YaeT/Omp85) in folding and secretion of intimin from enteropathogenic Escherichia coli strains. *Journal of bacteriology* 191:5169-5179.

Bone, R.C. 1991. Gram-negative sepsis. Background, clinical features, and intervention. *Chest* 100:802-808.

Bonemann, G., A. Pietrosiuk, and A. Mogk. 2010. Tubules and donuts: a type VI secretion story. *Molecular microbiology* 76:815-821.

Bowe, F., C.J. Lipps, R.M. Tsolis, E. Groisman, F. Heffron, and J.G. Kusters. 1998. At least four percent of the Salmonella typhimurium genome is required for fatal infection of mice. *Infect Immun* 66:3372-3377.

Brass, J.M., C.F. Higgins, M. Foley, P.A. Rugman, J. Birmingham, and P.B. Garland. 1986. Lateral diffusion of proteins in the periplasm of Escherichia coli. *Journal of bacteriology* 165:787-795.

Brenner, F.W., R.G. Villar, F.J. Angulo, R. Tauxe, and B. Swaminathan. 2000. Salmonella nomenclature. *Journal of clinical microbiology* 38:2465-2467.

Brissette, J.L., M. Russel, L. Weiner, and P. Model. 1990. Phage shock protein, a stress protein of Escherichia coli. *Proceedings of the National Academy of Sciences of the United States of America* 87:862-866.

Brumell, J.H., O. Steele-Mortimer, and B.B. Finlay. 1999. Bacterial invasion: Force feeding by Salmonella. *Current Biology* 9:R277-R280.

Bumann, D. 2002. Examination of Salmonella gene expression in an infected mammalian host using the green fluorescent protein and two-colour flow cytometry. *Molecular microbiology* 43:1269-1283.

Bustamante, V.H., L.C. Martinez, F.J. Santana, L.A. Knodler, O. Steele-Mortimer, and J.L. Puente. 2008. HilD-mediated transcriptional cross-talk between SPI-1 and SPI-2. *Proceedings of the National Academy of Sciences of the United States of America* 105:14591-14596.

Cai, L., N. Friedman, and X.S. Xie. 2006. Stochastic protein expression in individual cells at the single molecule level. *Nature* 440:358-362.

Canals, R., M. McClelland, C.A. Santiviago, and H. Andrews-Polymenis. 2011. Genomics of Salmonella Species. 171-235.

Carlsson, K.E., J. Liu, P.J. Edqvist, and M.S. Francis. 2007a. Extracytoplasmic-stress-responsive pathways modulate type III secretion in Yersinia pseudotuberculosis. *Infect Immun* 75:3913-3924.

Carlsson, K.E., J. Liu, P.J. Edqvist, and M.S. Francis. 2007b. Influence of the Cpx extracytoplasmic-stress-responsive pathway on Yersinia sp.-eukaryotic cell contact. *Infect Immun* 75:4386-4399.

Centers for diesease control and prevention. 2011. National enteric surveillance: *Salmonella* surveillance overview. In.

Chatterjee, E., and R. Chowdhury. 2013. Reduced virulence of the Vibrio cholerae fadD mutant is due to induction of the extracytoplasmic stress response. *Infect Immun* 81:3935-3941.

Cherepanov, P.P., and W. Wackernagel. 1995. Gene disruption in Escherichia coli: TcR and KmR cassettes with the option of Flp-catalyzed excision of the antibiotic-resistance determinant. *Gene* 158:9-14.

Choi, P.J., L. Cai, K. Frieda, and X.S. Xie. 2008. A stochastic single-molecule event triggers phenotype switching of a bacterial cell. *Science* 322:442-446.

Chubiz, J.E., Y.A. Golubeva, D. Lin, L.D. Miller, and J.M. Slauch. 2010. FliZ regulates expression of the Salmonella pathogenicity island 1 invasion locus by controlling HilD protein activity in Salmonella enterica serovar typhimurium. *Journal of bacteriology* 192:6261-6270.

Cirillo, D.M., R.H. Valdivia, D.M. Monack, and S. Falkow. 1998. Macrophage-dependent induction of the Salmonella pathogenicity island 2 type III secretion system and its role in intracellular survival. *Molecular microbiology* 30:175-188.

Coburn, B., I. Sekirov, and B.B. Finlay. 2007. Type III secretion systems and disease. *Clinical microbiology reviews* 20:535-549.

Cormack, B.P., R.H. Valdivia, and S. Falkow. 1996. FACS-optimized mutants of the green fluorescent protein (GFP). *Gene* 173:33-38.

Cornelis, G.R. 2010. The type III secretion injectisome, a complex nanomachine for intracellular 'toxin' delivery. *Biological chemistry* 391:745-751.

Cosma, C.L., P.N. Danese, J.H. Carlson, T.J. Silhavy, and W.B. Snyder. 1995. Mutational activation of the Cpx signal transduction pathway of Escherichia coli suppresses the toxicity conferred by certain envelope-associated stresses. *Molecular microbiology* 18:491-505.

Cummings, L.A., W.D. Wilkerson, T. Bergsbaken, and B.T. Cookson. 2006. In vivo, fliC expression by Salmonella enterica serovar Typhimurium is heterogeneous, regulated by ClpX, and anatomically restricted. *Molecular microbiology* 61:795-809.

Curtiss, R., and H. Kang. 2004. Modulation of immune responses to foreign antigens expressed by recombinant attenuated bacterial vectors. In 30.

Darwin, K.H., and V.L. Miller. 2000. The putative invasion protein chaperone SicA acts together with InvF to activate the expression of Salmonella typhimurium virulence genes. *Molecular microbiology* 35:949-960.

Darwin, K.H., and V.L. Miller. 2001. Type III secretion chaperone-dependent regulation: activation of virulence genes by SicA and InvF in Salmonella typhimurium. *The EMBO journal* 20:1850-1862.

Datsenko, K.A., and B.L. Wanner. 2000. One-step inactivation of chromosomal genes in Escherichia coli K-12 using PCR products. *Proceedings of the National Academy of Sciences of the United States of America* 97:6640-6645.

De Las Penas, A., L. Connolly, and C.A. Gross. 1997. SigmaE is an essential sigma factor in Escherichia coli. *Journal of bacteriology* 179:6862-6864.

Delbruck, M. 1945a. The Burst Size Distribution in the Growth of Bacterial Viruses (Bacteriophages). *Journal of bacteriology* 50:131-135.

Delbruck, M. 1945b. The burst size distribution in the growth of bacterial viruses (bacteriophages). *Journal of bacteriology* 50:131-135.

Delepelaire, P. 2004. Type I secretion in gram-negative bacteria. *Biochimica et biophysica acta* 1694:149-161.

Desvaux, M., M. Hebraud, R. Talon, and I.R. Henderson. 2009. Secretion and subcellular localizations of bacterial proteins: a semantic awareness issue. *Trends in microbiology* 17:139-145.

Diard, M., V. Garcia, L. Maier, M.N. Remus-Emsermann, R.R. Regoes, M. Ackermann, and W.D. Hardt. 2013. Stabilization of cooperative virulence by the expression of an avirulent phenotype. *Nature* 494:353-356.

Diard, M., M.E. Sellin, T. Dolowschiak, M. Arnoldini, M. Ackermann, and W.D. Hardt. 2014. Antibiotic treatment selects for cooperative virulence of Salmonella typhimurium. *Current biology : CB* 24:2000-2005.

Dillon, S.C., and C.J. Dorman. 2010. Bacterial nucleoid-associated proteins, nucleoid structure and gene expression. *Nature reviews. Microbiology* 8:185-195.

Dubnau, D., and R. Losick. 2006. Bistability in bacteria. *Molecular microbiology* 61:564-572.

Duguay, A.R., and T.J. Silhavy. 2004. Quality control in the bacterial periplasm. *Biochimica et biophysica acta* 1694:121-134.

Eichelberg, K., C.C. Ginocchio, and J.E. Galan. 1994. Molecular and functional characterization of the Salmonella typhimurium invasion genes invB and invC: homology of InvC to the F0F1 ATPase family of proteins. *Journal of bacteriology* 176:4501-4510.

Ellermeier, C.D., J.R. Ellermeier, and J.M. Slauch. 2005. HilD, HilC and RtsA constitute a feed forward loop that controls expression of the SPI1 type three secretion system regulator hilA in Salmonella enterica serovar Typhimurium. *Molecular microbiology* 57:691-705.

Ellermeier, C.D., and J.M. Slauch. 2003. RtsA and RtsB Coordinately Regulate Expression of the Invasion and Flagellar Genes in Salmonella enterica Serovar Typhimurium. *Journal of bacteriology* 185:5096-5108.

Ellermeier, J.R., and J.M. Slauch. 2007. Adaptation to the host environment: regulation of the SPI1 type III secretion system in Salmonella enterica serovar Typhimurium. *Current opinion in microbiology* 10:24-29.

Ellermeier, J.R., and J.M. Slauch. 2008. Fur regulates expression of the Salmonella pathogenicity island 1 type III secretion system through HilD. *Journal of bacteriology* 190:476-486.

Elowitz, M.B., A.J. Levine, E.D. Siggia, and P.S. Swain. 2002. Stochastic gene expression in a single cell. *Science* 297:1183-1186.

Erickson, J.W., and C.A. Gross. 1989. Identification of the sigma E subunit of Escherichia coli RNA polymerase: a second alternate sigma factor involved in high-temperature gene expression. *Genes & development* 3:1462-1471.

Fabrega, A., and J. Vila. 2013. Salmonella enterica serovar Typhimurium skills to succeed in the host: virulence and regulation. *Clinical microbiology reviews* 26:308-341.

Flores-Kim, J., and A.J. Darwin. 2012. Links between type III secretion and extracytoplasmic stress responses in Yersinia. *Frontiers in cellular and infection microbiology* 2:125.

Flynn, J.M., I. Levchenko, R.T. Sauer, and T.A. Baker. 2004. Modulating substrate choice: the SspB adaptor delivers a regulator of the extracytoplasmic-stress response to the AAA+ protease ClpXP for degradation. *Genes & development* 18:2292-2301.

Food and Agriculture Organization of the United Nations. 2002. W.H.O (Risk assessment of *Salmonella* in eggs and broiler chickens). In.

Franchi, L., A. Amer, M. Body-Malapel, T.D. Kanneganti, N. Ozoren, R. Jagirdar, N. Inohara, P. Vandenabeele, J. Bertin, A. Coyle, E.P. Grant, and G. Nunez. 2006. Cytosolic flagellin requires Ipaf for activation of caspase-1 and interleukin 1beta in salmonella-infected macrophages. *Nature immunology* 7:576-582.

Frankel, G., A.D. Phillips, I. Rosenshine, G. Dougan, J.B. Kaper, and S. Knutton. 1998. Enteropathogenic and enterohaemorrhagic Escherichia coli: more subversive elements. *Molecular microbiology* 30:911-921.

Fraser, H.B., A.E. Hirsh, G. Giaever, J. Kumm, and M.B. Eisen. 2004. Noise minimization in eukaryotic gene expression. *PLoS biology* 2:e137.

Friebel, A., and W.D. Hardt. 2000. Purification and biochemical activity of Salmonella exchange factor SopE. *Methods in enzymology* 325:82-91.

Gal-Mor, O., D.L. Gibson, D. Baluta, B.A. Vallance, and B.B. Finlay. 2008. A novel secretion pathway of Salmonella enterica acts as an antivirulence modulator during salmonellosis. *PLoS pathogens* 4:e1000036.

Galan, J.E. 1996. Molecular genetic bases of Salmonella entry into host cells. *Molecular microbiology* 20:263-271.

Galan, J.E., and R. Curtiss, 3rd. 1989. Cloning and molecular characterization of genes whose products allow Salmonella typhimurium to penetrate tissue culture cells. *Proceedings of the National Academy of Sciences of the United States of America* 86:6383-6387.

Galanis, E., D.M. Lo Fo Wong, M.E. Patrick, N. Binsztein, A. Cieslik, T. Chalermchikit, A. Aidara-Kane, A. Ellis, F.J. Angulo, H.C. Wegener, and S.-S. World Health Organization Global. 2006. Web-based surveillance and global Salmonella distribution, 2000-2002. *Emerging infectious diseases* 12:381-388.

Garcia Vescovi, E., F.C. Soncini, and E.A. Groisman. 1996. Mg2+ as an extracellular signal: environmental regulation of Salmonella virulence. *Cell* 84:165-174.

Gerlach, R.G., N. Claudio, M. Rohde, D. Jackel, C. Wagner, and M. Hensel. 2008. Cooperation of Salmonella pathogenicity islands 1 and 4 is required to breach epithelial barriers. *Cellular microbiology* 10:2364-2376.

Gerlach, R.G., D. Jackel, N. Geymeier, and M. Hensel. 2007. Salmonella pathogenicity island 4-mediated adhesion is coregulated with invasion genes in Salmonella enterica. *Infect Immun* 75:4697-4709.

Golding, I., J. Paulsson, S.M. Zawilski, and E.C. Cox. 2005. Real-time kinetics of gene activity in individual bacteria. *Cell* 123:1025-1036.

Gophna, U., E.Z. Ron, and D. Graur. 2003. Bacterial type III secretion systems are ancient and evolved by multiple horizontal-transfer events. *Gene* 312:151-163.

Gordon, M.A. 2008. Salmonella infections in immunocompromised adults. *The Journal of infection* 56:413-422.

Grassl, G.A., E. Bohn, Y. Muller, O.T. Buhler, and I.B. Autenrieth. 2003. Interaction of Yersinia enterocolitica with epithelial cells: invasin beyond invasion. *International journal of medical microbiology : IJMM* 293:41-54.

Griessl, M.H., B. Schmid, K. Kassler, C. Braunsmann, R. Ritter, B. Barlag, Y.D. Stierhof, K.U. Sturm, C. Danzer, C. Wagner, T.E. Schaffer, H. Sticht, M. Hensel, and Y.A. Muller. 2013. Structural insight into the giant Ca(2)(+)-binding adhesin SiiE: implications for the adhesion of Salmonella enterica to polarized epithelial cells. *Structure* 21:741-752.

Groisman, E.A., E. Chiao, C.J. Lipps, and F. Heffron. 1989. Salmonella typhimurium phoP virulence gene is a transcriptional regulator. *Proceedings of the National Academy of Sciences of the United States of America* 86:7077-7081.

Guzman, L.M., D. Belin, M.J. Carson, and J. Beckwith. 1995. Tight regulation, modulation, and high-level expression by vectors containing the arabinose PBAD promoter. *Journal of bacteriology* 177:4121-4130.

Haag, A.F., K.K. Myka, M.F. Arnold, P. Caro-Hernandez, and G.P. Ferguson. 2010. Importance of Lipopolysaccharide and Cyclic beta-1,2-Glucans in Brucella-Mammalian Infections. *International journal of microbiology* 2010:124509.

Hamburger, Z.A., M.S. Brown, R.R. Isberg, and P.J. Bjorkman. 1999. Crystal structure of invasin: a bacterial integrin-binding protein. *Science* 286:291-295.

Hapfelmeier, S., B. Stecher, M. Barthel, M. Kremer, A.J. Muller, M. Heikenwalder, T. Stallmach, M. Hensel, K. Pfeffer, S. Akira, and W.D. Hardt. 2005. The Salmonella pathogenicity island (SPI)-2 and SPI-1 type III secretion systems allow Salmonella serovar typhimurium to trigger colitis via MyD88-dependent and MyD88-independent mechanisms. *Journal of immunology* 174:1675-1685.

Hardt, W.D., L.M. Chen, K.E. Schuebel, X.R. Bustelo, and J.E. Galan. 1998a. S. typhimurium encodes an activator of Rho GTPases that induces membrane ruffling and nuclear responses in host cells. *Cell* 93:815-826.

Hardt, W.D., H. Urlaub, and J.E. Galan. 1998b. A substrate of the centisome 63 type III protein secretion system of Salmonella typhimurium is encoded by a cryptic bacteriophage. *Proceedings of the National Academy of Sciences of the United States of America* 95:2574-2579.

Hautefort, I., M.J. Proenca, and J.C.D. Hinton. 2003. Single-Copy Green Fluorescent Protein Gene Fusions Allow Accurate Measurement of Salmonella Gene Expression In Vitro and during Infection of Mammalian Cells. *Applied and environmental microbiology* 69:7480-7491.

Hautefort, I., A. Thompson, S. Eriksson-Ygberg, M.L. Parker, S. Lucchini, V. Danino, R.J. Bongaerts, N. Ahmad, M. Rhen, and J.C. Hinton. 2008. During infection of epithelial cells Salmonella enterica serovar Typhimurium undergoes a time-dependent transcriptional adaptation that results in simultaneous expression of three type 3 secretion systems. *Cellular microbiology* 10:958-984.

Henderson, I.R., F. Navarro-Garcia, M. Desvaux, R.C. Fernandez, and D. Ala'Aldeen. 2004. Type V protein secretion pathway: the autotransporter story. *Microbiology and molecular biology reviews : MMBR* 68:692-744.

Hensel, M. 2004. Evolution of pathogenicity islands of Salmonella enterica. *International journal of medical microbiology : IJMM* 294:95-102.

Heyndrickx, M., F. Pasmans, R. Ducatelle, A. Decostere, and F. Haesebrouck. 2005. Recent changes in Salmonella nomenclature: the need for clarification. *Veterinary journal* 170:275-277.

Hoelzer, S. 2010. Functional analysis of the type III secretion systems in Salmonella enterica. In Naturwissenschaftliche Fakultät. Friedrich-Alexander-Universität Erlangen-Nürnberg (FAU), Nürnberg.

Hoiseth, S.K., and B.A. Stocker. 1981. Aromatic-dependent Salmonella typhimurium are non-virulent and effective as live vaccines. *Nature* 291:238-239.

Hol, F.J., and C. Dekker. 2014. Zooming in to see the bigger picture: microfluidic and nanofabrication tools to study bacteria. *Science* 346:1251821.

Holzer, S.U., M.C. Schlumberger, D. Jackel, and M. Hensel. 2009. Effect of the O-antigen length of lipopolysaccharide on the functions of Type III secretion systems in Salmonella enterica. *Infect Immun* 77:5458-5470.

Hornef, M.W., K. Putsep, J. Karlsson, E. Refai, and M. Andersson. 2004. Increased diversity of intestinal antimicrobial peptides by covalent dimer formation. *Nature immunology* 5:836-843.

Humphrey, T. 2004. Salmonella, stress responses and food safety. *Nature reviews. Microbiology* 2:504-509.

Humphreys, S., G. Rowley, A. Stevenson, M.F. Anjum, M.J. Woodward, S. Gilbert, J. Kormanec, and M. Roberts. 2004. Role of the two-component regulator CpxAR in the virulence of Salmonella enterica serotype Typhimurium. *Infect Immun* 72:4654-4661.

Humphreys, S., A. Stevenson, A. Bacon, A.B. Weinhardt, and M. Roberts. 1999. The alternative sigma factor, sigmaE, is critically important for the virulence of Salmonella typhimurium. *Infect Immun* 67:1560-1568.

Hurley, D., M.P. McCusker, S. Fanning, and M. Martins. 2014. Salmonella-host interactions - modulation of the host innate immune system. *Frontiers in immunology* 5:481.

Ieva, R., and H.D. Bernstein. 2009. Interaction of an autotransporter passenger domain with BamA during its translocation across the bacterial outer membrane. *Proceedings of the National Academy of Sciences of the United States of America* 106:19120-19125.

Ilg, K., K. Endt, B. Misselwitz, B. Stecher, M. Aebi, and W.D. Hardt. 2009. O-antigen-negative Salmonella enterica serovar Typhimurium is attenuated in intestinal colonization but elicits colitis in streptomycin-treated mice. *Infect Immun* 77:2568-2575.

Isberg, R.R., D.L. Voorhis, and S. Falkow. 1987. Identification of invasin: a protein that allows enteric bacteria to penetrate cultured mammalian cells. *Cell* 50:769-778.

Issenhuth-Jeanjean, S., P. Roggentin, M. Mikoleit, M. Guibourdenche, E. de Pinna, S. Nair, P.I. Fields, and F.X. Weill. 2014. Supplement 2008-2010 (no. 48) to the White-Kauffmann-Le Minor scheme. *Research in microbiology* 165:526-530.

Johnson, T.L., J. Abendroth, W.G. Hol, and M. Sandkvist. 2006. Type II secretion: from structure to function. *FEMS microbiology letters* 255:175-186.

Jones, B.D., N. Ghori, and S. Falkow. 1994. Salmonella typhimurium initiates murine infection by penetrating and destroying the specialized epithelial M cells of the Peyer's patches. *The Journal of experimental medicine* 180:15-23.

Kaern, M., T.C. Elston, W.J. Blake, and J.J. Collins. 2005. Stochasticity in gene expression: from theories to phenotypes. *Nature reviews. Genetics* 6:451-464.

Kashiwagi, A., I. Urabe, K. Kaneko, and T. Yomo. 2006. Adaptive response of a gene network to environmental changes by fitness-induced attractor selection. *PloS one* 1:e49.

Kenyon, W.J., S.M. Thomas, E. Johnson, M.J. Pallen, and M.P. Spector. 2005. Shifts from glucose to certain secondary carbon-sources result in activation of the extracytoplasmic function sigma factor sigmaE in Salmonella enterica serovar Typhimurium. *Microbiology* 151:2373-2383.

Kiviet, D.J., P. Nghe, N. Walker, S. Boulineau, V. Sunderlikova, and S.J. Tans. 2014. Stochasticity of metabolism and growth at the single-cell level. *Nature* 514:376-379.

Klauser, T., J. Pohlner, and T.F. Meyer. 1993. The secretion pathway of IgA protease-type proteins in gram-negative bacteria. *BioEssays : news and reviews in molecular, cellular and developmental biology* 15:799-805.

Knowles, T.J., A. Scott-Tucker, M. Overduin, and I.R. Henderson. 2009. Membrane protein architects: the role of the BAM complex in outer membrane protein assembly. *Nature reviews. Microbiology* 7:206-214.

Kong, Q., J. Yang, Q. Liu, P. Alamuri, K.L. Roland, and R. Curtiss, 3rd. 2011. Effect of deletion of genes involved in lipopolysaccharide core and O-antigen synthesis on virulence and immunogenicity of Salmonella enterica serovar typhimurium. *Infect Immun* 79:4227-4239.

Kreibich, S., and W.D. Hardt. 2015. Experimental approaches to phenotypic diversity in infection. *Current opinion in microbiology* 27:25-36.

Kubori, T., Y. Matsushima, D. Nakamura, J. Uralil, M. Lara-Tejero, A. Sukhan, J.E. Galan, and S.I. Aizawa. 1998. Supramolecular structure of the Salmonella typhimurium type III protein secretion system. *Science* 280:602-605.

LaRock, D.L., A. Chaudhary, and S.I. Miller. 2015. Salmonellae interactions with host processes. *Nature reviews. Microbiology* 13:191-205.

Laughlin, R.C., L.A. Knodler, R. Barhoumi, H.R. Payne, J. Wu, G. Gomez, R. Pugh, S.D. Lawhon, A.J. Baumler, O. Steele-Mortimer, and L.G. Adams. 2014. Spatial segregation of virulence gene expression during acute enteric infection with Salmonella enterica serovar Typhimurium. *mBio* 5:e00946-00913.

Leblanc, S.K., C.W. Oates, and T.L. Raivio. 2011. Characterization of the induction and cellular role of the BaeSR two-component envelope stress response of Escherichia coli. *Journal of bacteriology* 193:3367-3375.

Lee, C.A., B.D. Jones, and S. Falkow. 1992. Identification of a Salmonella typhimurium invasion locus by selection for hyperinvasive mutants. *Proceedings of the National Academy of Sciences of the United States of America* 89:1847-1851.

Leo, J.C., I. Grin, and D. Linke. 2012. Type V secretion: mechanism(s) of autotransport through the bacterial outer membrane. *Philosophical transactions of the Royal Society of London. Series B, Biological sciences* 367:1088-1101.

Leo, J.C., P. Oberhettinger, M. Schütz, and D. Linke. 2015. The inverse autotransporter family: intimin, invasin and related proteins. *International journal of medical microbiology : IJMM* 305:276-282.

Leyton, D.L., A.E. Rossiter, and I.R. Henderson. 2012. From self sufficiency to dependence: mechanisms and factors important for autotransporter biogenesis. *Nature reviews. Microbiology* 10:213-225.

Li, X., B. Wang, L. Feng, H. Kang, Y. Qi, J. Wang, and Y. Shi. 2009. Cleavage of RseA by RseP requires a carboxyl-terminal hydrophobic amino acid following DegS cleavage. *Proceedings of the National Academy of Sciences of the United States of America* 106:14837-14842.

Liu, D., and P.R. Reeves. 1994. Escherichia coli K12 regains its O antigen. *Microbiology* 140 (Pt 1):49-57.

Lopez, C.A., S.E. Winter, F. Rivera-Chavez, M.N. Xavier, V. Poon, S.P. Nuccio, R.M. Tsolis, and A.J. Baumler. 2012. Phage-mediated acquisition of a type III secreted effector protein boosts growth of salmonella by nitrate respiration. *mBio* 3:

Lostroh, C.P., V. Bajaj, and C.A. Lee. 2000. The cis requirements for transcriptional activation by HilA, a virulence determinant encoded on SPI-1. *Molecular microbiology* 37:300-315.

Lostroh, C.P., and C.A. Lee. 2001. The HilA box and sequences outside it determine the magnitude of HilA-dependent activation of P(prgH) from Salmonella pathogenicity island 1. *Journal of bacteriology* 183:4876-4885.

Maamar, H., and D. Dubnau. 2005. Bistability in the Bacillus subtilis K-state (competence) system requires a positive feedback loop. *Molecular microbiology* 56:615-624.

Macnab, R.M. 2003. How bacteria assemble flagella. *Annual review of microbiology* 57:77-100.

Macnab, R.M., and D.E. Koshland, Jr. 1972. The gradient-sensing mechanism in bacterial chemotaxis. *Proceedings of the National Academy of Sciences of the United States of America* 69:2509-2512.

Maier, L., M. Barthel, B. Stecher, R.J. Maier, J.S. Gunn, and W.D. Hardt. 2014a. Salmonella Typhimurium strain ATCC14028 requires H2-hydrogenases for growth in the gut, but not at systemic sites. *PloS one* 9:e110187.

Maier, L., M. Diard, M.E. Sellin, E.S. Chouffane, K. Trautwein-Weidner, B. Periaswamy, E. Slack, T. Dolowschiak, B. Stecher, C. Loverdo, R.R. Regoes, and W.D. Hardt. 2014b. Granulocytes impose a tight bottleneck upon the gut luminal pathogen population during Salmonella typhimurium colitis. *PLoS pathogens* 10:e1004557.

Maier, L., R. Vyas, C.D. Cordova, H. Lindsay, T.S. Schmidt, S. Brugiroux, B. Periaswamy, R. Bauer, A. Sturm, F. Schreiber, C. von Mering, M.D. Robinson, B. Stecher, and W.D. Hardt. 2013. Microbiota-derived hydrogen fuels Salmonella typhimurium invasion of the gut ecosystem. *Cell host & microbe* 14:641-651.

Majdalani, N., M. Heck, V. Stout, and S. Gottesman. 2005. Role of RcsF in signaling to the Rcs phosphorelay pathway in Escherichia coli. *Journal of bacteriology* 187:6770-6778.

Marcus, S.L., J.H. Brumell, C.G. Pfeifer, and B.B. Finlay. 2000. Salmonella pathogenicity islands: big virulence in small packages. *Microbes and infection / Institut Pasteur* 2:145-156.

Martin, R.G., and J.L. Rosner. 2001. The AraC transcriptional activators. *Current opinion in microbiology* 4:132-137.

Martinez, L.C., H. Yakhnin, M.I. Camacho, D. Georgellis, P. Babitzke, J.L. Puente, and V.H. Bustamante. 2011. Integration of a complex regulatory cascade involving the SirA/BarA and Csr global regulatory systems that controls expression of the Salmonella SPI-1 and SPI-2 virulence regulons through HilD. *Molecular microbiology* 80:1637-1656.

McBroom, A.J., and M.J. Kuehn. 2007. Release of outer membrane vesicles by Gram-negative bacteria is a novel envelope stress response. *Molecular microbiology* 63:545-558.

McMeechan, A., M. Roberts, T.A. Cogan, F. Jorgensen, A. Stevenson, C. Lewis, G. Rowley, and T.J. Humphrey. 2007. Role of the alternative sigma factors sigmaE and sigmaS in survival of Salmonella enterica serovar Typhimurium during starvation, refrigeration and osmotic shock. *Microbiology* 153:263-269.

Mecsas, J., P.E. Rouviere, J.W. Erickson, T.J. Donohue, and C.A. Gross. 1993. The activity of sigma E, an Escherichia coli heat-inducible sigma-factor, is modulated by expression of outer membrane proteins. *Genes & development* 7:2618-2628.

Miller, S.I., A.M. Kukral, and J.J. Mekalanos. 1989. A two-component regulatory system (phoP phoQ) controls Salmonella typhimurium virulence. *Proceedings of the National Academy of Sciences of the United States of America* 86:5054-5058.

Mills, D.M., V. Bajaj, and C.A. Lee. 1995. A 40 kb chromosomal fragment encoding Salmonella typhimurium invasion genes is absent from the corresponding region of the Escherichia coli K-12 chromosome. *Molecular microbiology* 15:749-759.

Missiakas, D., M.P. Mayer, M. Lemaire, C. Georgopoulos, and S. Raina. 1997. Modulation of the Escherichia coli sigmaE (RpoE) heat-shock transcription-factor activity by the RseA, RseB and RseC proteins. *Molecular microbiology* 24:355-371.

Moest, T.P., and S. Meresse. 2013. Salmonella T3SSs: successful mission of the secret(ion) agents. *Current opinion in microbiology* 16:38-44.

Müller, Andreas J., P. Kaiser, Kurt E.J. Dittmar, Thomas C. Weber, S. Haueter, K. Endt, P. Songhet, C. Zellweger, M. Kremer, H.-J. Fehling, and W.-D. Hardt. 2012. Salmonella Gut Invasion Involves TTSS-2-Dependent Epithelial Traversal, Basolateral Exit, and Uptake by Epithelium-Sampling Lamina Propria Phagocytes. *Cell host & microbe* 11:19-32.

Murray, P.R., E.J. Baron, P.M. A., F.C. Tenover, and R.H. Yolken. 1999. Manual of clinical microbiology. ASM Press, Washington, DC.,

Navarre, W.W., S. Porwollik, Y. Wang, M. McClelland, H. Rosen, S.J. Libby, and F.C. Fang. 2006. Selective silencing of foreign DNA with low GC content by the H-NS protein in Salmonella. *Science* 313:236-238.

Neuenschwander, M. 2007. High-throughput assays for detecting enzymatic activities in living cells. In ETH Zurich, Zurich.

Novick, A., and M. Weiner. 1957. Enzyme Induction as an All-or-None Phenomenon. *Proceedings of the National Academy of Sciences of the United States of America* 43:553-566.

Oberhettinger, P., J.C. Leo, D. Linke, I.B. Autenrieth, and M.S. Schütz. 2015. The inverse autotransporter intimin exports its passenger domain via a hairpin intermediate. *The Journal of biological chemistry* 290:1837-1849.

Oberhettinger, P., M. Schütz, J.C. Leo, N. Heinz, J. Berger, I.B. Autenrieth, and D. Linke. 2012. Intimin and invasin export their C-terminus to the bacterial cell surface using an inverse mechanism compared to classical autotransport. *PloS one* 7:e47069.

Ochman, H., F.C. Soncini, F. Solomon, and E.A. Groisman. 1996. Identification of a pathogenicity island required for Salmonella survival in host cells. *Proceedings of the National Academy of Sciences of the United States of America* 93:7800-7804.

Olekhnovich, I.N., and R.J. Kadner. 2002. DNA-Binding Activities of the HilC and HilD Virulence Regulatory Proteins of Salmonella enterica Serovar Typhimurium. *Journal of bacteriology* 184:4148-4160.

Olekhnovich, I.N., and R.J. Kadner. 2006. Crucial roles of both flanking sequences in silencing of the hilA promoter in Salmonella enterica. *Journal of molecular biology* 357:373-386.

Osterberg, S., T. del Peso-Santos, and V. Shingler. 2011. Regulation of alternative sigma factor use. *Annual review of microbiology* 65:37-55.

Ozbudak, E.M., M. Thattai, I. Kurtser, A.D. Grossman, and A. van Oudenaarden. 2002. Regulation of noise in the expression of a single gene. *Nature genetics* 31:69-73.

Pegues, D.A., M.J. Hantman, I. Behlau, and S.I. Miller. 1995. PhoP/PhoQ transcriptional repression of Salmonella typhimurium invasion genes: evidence for a role in protein secretion. *Molecular microbiology* 17:169-181.

Pohlner, J., R. Halter, K. Beyreuther, and T.F. Meyer. 1987. Gene structure and extracellular secretion of Neisseria gonorrhoeae IgA protease. *Nature* 325:458-462.

Prouty, A.M., and J.S. Gunn. 2000. Salmonella enterica serovar typhimurium invasion is repressed in the presence of bile. *Infect Immun* 68:6763-6769.

Public Health Agency of Canada. 2011. Salmonella enterica spp. Pathogen safety data sheet - infectiuos substances. In.

Raffatellu, M., M.D. George, Y. Akiyama, M.J. Hornsby, S.P. Nuccio, T.A. Paixao, B.P. Butler, H. Chu, R.L. Santos, T. Berger, T.W. Mak, R.M. Tsolis, C.L. Bevins, J.V. Solnick, S. Dandekar,

and A.J. Baumler. 2009. Lipocalin-2 resistance confers an advantage to Salmonella enterica serotype Typhimurium for growth and survival in the inflamed intestine. *Cell host & microbe* 5:476-486.

Raj, A., and A. van Oudenaarden. 2008. Nature, nurture, or chance: stochastic gene expression and its consequences. *Cell* 135:216-226.

Ramos, H.C., M. Rumbo, and J.C. Sirard. 2004. Bacterial flagellins: mediators of pathogenicity and host immune responses in mucosa. *Trends in microbiology* 12:509-517.

Raser, J.M., and E.K. O'Shea. 2005. Noise in gene expression: origins, consequences, and control. *Science* 309:2010-2013.

Rescigno, M., M. Urbano, B. Valzasina, M. Francolini, G. Rotta, R. Bonasio, F. Granucci, J.P. Kraehenbuhl, and P. Ricciardi-Castagnoli. 2001. Dendritic cells express tight junction proteins and penetrate gut epithelial monolayers to sample bacteria. *Nature immunology* 2:361-367.

Romeo, T. 1998. Global regulation by the small RNA-binding protein CsrA and the non-coding RNA molecule CsrB. *Molecular microbiology* 29:1321-1330.

Rowley, G., H. Skovierova, A. Stevenson, B. Rezuchova, D. Homerova, C. Lewis, A. Sherry, J. Kormanec, and M. Roberts. 2011. The periplasmic chaperone Skp is required for successful Salmonella Typhimurium infection in a murine typhoid model. *Microbiology* 157:848-858.

Rowley, G., M. Spector, J. Kormanec, and M. Roberts. 2006. Pushing the envelope: extracytoplasmic stress responses in bacterial pathogens. *Nature reviews. Microbiology* 4:383-394.

Ruiz, N., D. Kahne, and T.J. Silhavy. 2006. Advances in understanding bacterial outer-membrane biogenesis. *Nature reviews. Microbiology* 4:57-66.

Ruiz, N., D. Kahne, and T.J. Silhavy. 2009. Transport of lipopolysaccharide across the cell envelope: the long road of discovery. *Nature reviews. Microbiology* 7:677-683.

Runkel, S., H.C. Wells, and G. Rowley. 2013. Living with Stress: A Lesson from the Enteric Pathogen Salmonella enterica. *Advances in applied microbiology* 83:87-144.

Saini, S., J.R. Ellermeier, J.M. Slauch, and C.V. Rao. 2010a. The role of coupled positive feedback in the expression of the SPI1 type three secretion system in Salmonella. *PLoS pathogens* 6:e1001025.

Saini, S., J.M. Slauch, P.D. Aldridge, and C.V. Rao. 2010b. Role of cross talk in regulating the dynamic expression of the flagellar Salmonella pathogenicity island 1 and type 1 fimbrial genes. *Journal of bacteriology* 192:5767-5777.

Salzman, N.H., D. Ghosh, K.M. Huttner, Y. Paterson, and C.L. Bevins. 2003. Protection against enteric salmonellosis in transgenic mice expressing a human intestinal defensin. *Nature* 422:522-526.

Sanchez-Vargas, F.M., M.A. Abu-El-Haija, and O.G. Gomez-Duarte. 2011. Salmonella infections: an update on epidemiology, management, and prevention. *Travel medicine and infectious disease* 9:263-277.

Santos, R.L., and A.J. Baumler. 2004. Cell tropism of Salmonella enterica. *International journal of medical microbiology : IJMM* 294:225-233.

Schechter, L.M., S.M. Damrauer, and C.A. Lee. 1999. Two AraC/XylS family members can independently counteract the effect of repressing sequences upstream of the hilA promoter. *Molecular microbiology* 32:629-642.

Schechter, L.M., S. Jain, S. Akbar, and C.A. Lee. 2003a. The small nucleoid-binding proteins H-NS, HU, and Fis affect hilA expression in Salmonella enterica serovar Typhimurium. *Infect Immun* 71:5432-5435.

Schechter, L.M., S. Jain, S. Akbar, and C.A. Lee. 2003b. The Small Nucleoid-Binding Proteins H-NS, HU, and Fis Affect hilA Expression in Salmonella enterica Serovar Typhimurium. *Infection and Immunity* 71:5432-5435.

Schechter, L.M., and C.A. Lee. 2001. AraC/XylS family members, HilC and HilD, directly bind and derepress the Salmonella typhimurium hilA promoter. *Molecular microbiology* 40:1289-1299.

Schlumberger, M.C., A.J. Muller, K. Ehrbar, B. Winnen, I. Duss, B. Stecher, and W.D. Hardt. 2005. Real-time imaging of type III secretion: Salmonella SipA injection into host cells. *Proceedings of the National Academy of Sciences of the United States of America* 102:12548-12553.

Schmidt, M.A. 2010. LEEways: tales of EPEC, ATEC and EHEC. *Cellular microbiology* 12:1544-1552.

Schneider, C.A., W.S. Rasband, and K.W. Eliceiri. 2012. NIH Image to ImageJ: 25 years of image analysis. *Nature methods* 9:671-675.

Scholz, O., A. Thiel, W. Hillen, and M. Niederweis. 2000. Quantitative analysis of gene expression with an improved green fluorescent protein. p6. *European journal of biochemistry / FEBS* 267:1565-1570.

Shelobolina, E.S., S.A. Sullivan, K.R. O'Neill, K.P. Nevin, and D.R. Lovley. 2004. Isolation, Characterization, and U(VI)-Reducing Potential of a Facultatively Anaerobic, Acid-Resistant Bacterium from Low-pH, Nitrate- and U(VI)-Contaminated Subsurface Sediment and Description of Salmonella subterranea sp. nov. *Applied and environmental microbiology* 70:2959-2965.

Simeone, R., D. Bottai, and R. Brosch. 2009. ESX/type VII secretion systems and their role in host-pathogen interaction. *Current opinion in microbiology* 12:4-10.

Skovierova, H., G. Rowley, B. Rezuchova, D. Homerova, C. Lewis, M. Roberts, and J. Kormanec. 2006. Identification of the sigmaE regulon of Salmonella enterica serovar Typhimurium. *Microbiology* 152:1347-1359.

Smits, W.K., O.P. Kuipers, and J.W. Veening. 2006a. Phenotypic variation in bacteria: the role of feedback regulation. *Nature reviews. Microbiology* 4:259-271.

Smits, W.K., J.W. Veening, and O.P. Kuipers. 2006b. Phenotypic variation and bistable switching in bacteria. Springer Berlin Heidelberg,

Stecher, B., S. Hapfelmeier, C. Muller, M. Kremer, T. Stallmach, and W.D. Hardt. 2004. Flagella and chemotaxis are required for efficient induction of Salmonella enterica serovar Typhimurium colitis in streptomycin-pretreated mice. *Infect Immun* 72:4138-4150.

Stecher, B., R. Robbiani, A.W. Walker, A.M. Westendorf, M. Barthel, M. Kremer, S. Chaffron, A.J. Macpherson, J. Buer, J. Parkhill, G. Dougan, C. von Mering, and W.D. Hardt. 2007. Salmonella enterica serovar typhimurium exploits inflammation to compete with the intestinal microbiota. *PLoS biology* 5:2177-2189.

Stender, S., A. Friebel, S. Linder, M. Rohde, S. Mirold, and W.D. Hardt. 2000. Identification of SopE2 from Salmonella typhimurium, a conserved guanine nucleotide exchange factor for Cdc42 of the host cell. *Molecular microbiology* 36:1206-1221.

Stewart, E.J., R. Madden, G. Paul, and F. Taddei. 2005. Aging and death in an organism that reproduces by morphologically symmetric division. *PLoS biology* 3:e45.

Stewart, P.S., and M.J. Franklin. 2008. Physiological heterogeneity in biofilms. *Nature reviews. Microbiology* 6:199-210.

Sturm, A., M. Heinemann, M. Arnoldini, A. Benecke, M. Ackermann, M. Benz, J. Dormann, and W.D. Hardt. 2011. The cost of virulence: retarded growth of Salmonella Typhimurium cells expressing type III secretion system 1. *PLoS pathogens* 7:e1002143.

Suel, G.M., J. Garcia-Ojalvo, L.M. Liberman, and M.B. Elowitz. 2006. An excitable gene regulatory circuit induces transient cellular differentiation. *Nature* 440:545-550.

Swain, P.S., M.B. Elowitz, and E.D. Siggia. 2002. Intrinsic and extrinsic contributions to stochasticity in gene expression. *Proceedings of the National Academy of Sciences of the United States of America* 99:12795-12800.

Takaya, A., T. Tomoyasu, A. Tokumitsu, M. Morioka, and T. Yamamoto. 2002. The ATP-Dependent Lon Protease of Salmonella enterica Serovar Typhimurium Regulates Invasion and Expression of Genes Carried on Salmonella Pathogenicity Island 1. *Journal of bacteriology* 184:224-232.

Takeuchi, A., and H. Sprinz. 1967. Electron-Microscope Studies of Experimental Salmonella Infection in the Preconditioned Guinea Pig: II. Response of the Intestinal Mucosa to the Invasion by Salmonella typhimurium. *The American journal of pathology* 51:137-161.

Temme, K., H. Salis, D. Tullman-Ercek, A. Levskaya, S.H. Hong, and C.A. Voigt. 2008. Induction and relaxation dynamics of the regulatory network controlling the type III secretion system encoded within Salmonella pathogenicity island 1. *Journal of molecular biology* 377:47-61.

Thanassi, D.G., C. Stathopoulos, A. Karkal, and H. Li. 2005. Protein secretion in the absence of ATP: the autotransporter, two-partner secretion and chaperone/usher pathways of gram-negative bacteria (review). *Molecular membrane biology* 22:63-72.

Thijs, I.M., S.C. De Keersmaecker, A. Fadda, K. Engelen, H. Zhao, M. McClelland, K. Marchal, and J. Vanderleyden. 2007. Delineation of the Salmonella enterica serovar Typhimurium HilA regulon through genome-wide location and transcript analysis. *Journal of bacteriology* 189:4587-4596.

Trent, M.S., C.M. Stead, A.X. Tran, and J.V. Hankins. 2006. Diversity of endotoxin and its impact on pathogenesis. *Journal of endotoxin research* 12:205-223.

Tsai, J.C., M.R. Yen, R. Castillo, D.L. Leyton, I.R. Henderson, and M.H. Saier, Jr. 2010. The bacterial intimins and invasins: a large and novel family of secreted proteins. *PloS one* 5:e14403.

Tucker, S.C., and J.E. Galan. 2000. Complex function for SicA, a Salmonella enterica serovar typhimurium type III secretion-associated chaperone. *Journal of bacteriology* 182:2262-2268.

Veening, J.W., W.K. Smits, and O.P. Kuipers. 2008. Bistability, epigenetics, and bet-hedging in bacteria. *Annual review of microbiology* 62:193-210.

Wallden, K., A. Rivera-Calzada, and G. Waksman. 2010. Type IV secretion systems: versatility and diversity in function. *Cellular microbiology* 12:1203-1212.

Wang, P., L. Robert, J. Pelletier, W.L. Dang, F. Taddei, A. Wright, and S. Jun. 2010. Robust growth of Escherichia coli. *Current biology : CB* 20:1099-1103.

Wendland, M., and D. Bumann. 2002. Optimization of GFP levels for analyzing Salmonella gene expression during an infection. *FEBS letters* 521:105-108.

West, N.P., P. Sansonetti, J. Mounier, R.M. Exley, C. Parsot, S. Guadagnini, M.C. Prevost, A. Prochnicka-Chalufour, M. Delepierre, M. Tanguy, and C.M. Tang. 2005. Optimization of virulence functions through glucosylation of Shigella LPS. *Science* 307:1313-1317.

Winter, S.E., P. Thiennimitr, M.G. Winter, B.P. Butler, D.L. Huseby, R.W. Crawford, J.M. Russell, C.L. Bevins, L.G. Adams, R.M. Tsolis, J.R. Roth, and A.J. Baumler. 2010. Gut inflammation provides a respiratory electron acceptor for Salmonella. *Nature* 467:426-429.

Yu, J., J. Xiao, X. Ren, K. Lao, and X.S. Xie. 2006. Probing gene expression in live cells, one protein molecule at a time. *Science* 311:1600-1603.

Zhou, D., M.S. Mooseker, and J.E. Galan. 1999. Role of the S. typhimurium actin-binding protein SipA in bacterial internalization. *Science* 283:2092-2095.

6 Acknowledgements

In this final part, I would like to thank all people that were involved in this work the last years. First and foremost I would like to thank Wolf-Dietrich Hardt. He offered me a second opportunity to do a PhD after an unsuccessful start in another group. From the beginning, Wolf was supportive by giving feedback, criticism and valuable input. I really appreciate his way of keeping an eye on everyone, but still letting enough freedom to work independently and try out own ideas.

I would also like to acknowledge the members of my thesis committee, Martin Ackermann, Manfred Claassen and Hans-Martin Fischer. With their valuable input during our meetings, they significantly contributed to the progress of my work.

I am grateful to the support of all of my collaborators who were always doing their best in trying to solve problems during my work. Markus Arnoldini, Ima Avalos Vizcarra, Daniel Kiviet, Peter Kaiser and Markus Schlumberger were essential at different stages of my work with the microfluidics microscopy setup. I would also like to thank my collaborator Eirini Arvaniti for her programming efforts to analyze my data. My cloning buddies Bidong Nguyen and Silke Reiter always knew solutions and offered new strategies for cloning. Furthermore, a big "thank you" to Alexander Sturm and Nicolas Studer, whom I worked with intensely for the RpoE/RseP project. I would also like to thank Tsuyoshi Miki for his collaboration.

I would like to show my gratitude to all the members of the Hardt lab. It was a joy to be surrounded by all these people and work in a collaborative and supportive atmosphere. I would especially like to thank Alexander Sturm, who introduced me into my project and showed me everything during the first stages of my PhD. Médéric Diard was my source of knowledge and inspiration and always had time for interesting discussions. Thank you for that! I would also like to thank Tamas Dolowschiak, Mikael Sellin, Saskia Kreibich and Emma Wetter Slack for numerous scientific discussions. My incredible office mates Daniel Andritschke, Manja Barthel Scherrer and Saskia Kreibich in G411 were great. I will remember numerous hilarious moments that we spent together. A big "thank you" also goes to my G422 lab mates, Médéric Diard, Saskia Kreibich, Pascale Vonaesch, Nicolas Studer, Romina Sigrist. It was very enjoyable and funny to share the lab with them. I am happy to have shared numerous sportive

moments with my pilates crew Anna Müller and Boas Felmy. I would also like to thank Markus Furter, Annika Hausmann, Kathrin Moor, Sandra Wotzka and Rebekka Bauer. I would also like to thank my student Barbara Müller, who inspired and challenged me.

I am very grateful to the institute staff, Susanne Soo Jin Jäger, Ilka Riedel and Markus Schlumberger, Palmira da Silva Duarte and Daniel Zogg. A big thank you to the IT staff, Aurel Schwitter, Patrice Sutter, Arian Zuta and Jacques Laville. Without the efforts, working at the Microbiology institute would be much more complicated.

My gratitude also goes to all my friends, especially the "Mädls-Runde" with Jenny, Clodi, Susi, Resa and Bine. I would like to acknowledge the great time spent with all members of the LSZYSN. It was a great to share all efforts, work, discussions and success we had with them. A big thanks goes also to my brother Elmir, his wife Yasmin and my little nephew Adin. Lastly, I would like to thank Elvis for his support, advice, inspiration and encouragement throughout the last years.

Finally, I would like to dedicate this thesis to my parents. They have always supported me in all possible ways. I am very happy that they enabled me all the chances that I had during my life that they did not have.